



Istituto Universitario  
di Studi Superiori



Università degli  
Studi di Pavia

EUROPEAN SCHOOL FOR ADVANCED STUDIES IN  
REDUCTION OF SEISMIC RISK

**ROSE SCHOOL**

**A DISPLACEMENT-BASED DESIGN APPROACH FOR  
SEISMIC RETROFITTING OF RC FRAMES WITH STEEL BRACES**

A Dissertation Submitted in Partial Fulfilment of the  
Requirements for the Master Degree in

**EARTHQUAKE ENGINEERING**

by

**Romain Ribeiro de Sousa**

Supervisors:

**Dr Miguel Castro and Dr Rui Pinho**

April, 2010

The dissertation entitled “A Displacement-Based Design Approach for Seismic Retrofitting of RC Frames with Steel Braces”, by Romain Ribeiro de Sousa, has been approved in partial fulfilment of the requirements for the Master Degree in Earthquake Engineering.

Miguel Castro \_\_\_\_\_

Rui Pinho \_\_\_\_\_



## **ABSTRACT**

The introduction in Europe of the new regulation for seismic design will impose stricter performance requirements for building structures. This will result in a significant number of existing reinforced concrete structures having inadequate seismic resistance and therefore requiring intervention. One of the possible retrofitting options is the application of steel braces. However, this approach is not widely used due to the lack of seismic regulation in this field. The main goal of this work is the development of a fast and reliable design method that can promote the retrofitting of reinforced concrete frames with steel braces. In the last years, the scientific community has demonstrated that seismic design based in displacements is more adequate and rigorous than the traditional based in forces. Focused in obtaining the fundamental parameters for the application of this new method, it has been realized static and dynamic non-linear analysis in reinforced concrete structures strengthened with concentric steel braces. The results enable the definition of parameters such as displacement profiles, yielding displacements and target displacements among others. Based on the obtained results, it is proposed a displacement based method that enable, in a simple way, to design the retrofitting system so that the hybrid structure presents adequate seismic behaviour.

Keywords: seismic retrofitting, reinforced concrete frames, steel braces, displacement-based design, design method.

## ACKNOWLEDGEMENTS

I would like to thank to all the persons that, in one way or the other, helped me to overcome all the difficulties during the Masters program.

First of all I would like to thank Prof. Humberto Varum and Prof. Rui Pinho for the support and confidence that they always given to me, and specially, for the motivation and friendship during the last years. Without them, this work would never be possible.

To Dr. Miguel Castro for the knowledge, motivation and close supervision that was always present during the months I worked on this thesis.

To my real friends, João, Mario, Ricardo, António, Kent, Melissa, Andrea, Henrique, Sanja and Gary, you were the joy in my live for the time I was away from Portugal.

To my girlfriend Fatima for the support, friendship and specially love that I always felt, especially in the hardest hours.

Last but not the least, to my family, and in particular to my parents for the financial support, motivation, love and, furthermore, to make me the person I am today.

### Poem on the Lisbon Disaster

*“UNHAPPY mortals! Dark and mourning earth!  
Affrighted gathering of human kind!  
Eternal lingering of useless pain!  
Come, ye philosophers, who cry, "All's well,"  
And contemplate this ruin of a world.  
Behold these shreds and cinders of your race,  
This child and mother heaped in common wreck,  
These scattered limbs beneath the marble shafts—  
A hundred thousand whom the earth devours,  
Who, torn and bloody, palpitating yet,  
Entombed beneath their hospitable roofs,  
In racking torment end their stricken lives.”*

*(...)*

Voltaire (1756)

## TABLE OF CONTENTS

Abstract .....	i
Acknowledgements .....	ii
Table of Contents .....	iv
List of Figures.....	vii
List of Tables.....	xi
1. Introduction .....	1
1.1. Historical Background .....	1
1.2. Objectives.....	4
1.3. Layout of the Thesis .....	5
2. Reinforced Concrete Steel Braced Frames .....	6
2.1. Overview .....	6
2.2. Bracing Layout.....	7
2.3. Advantages and Disadvantages of Steel Bracing .....	8
2.4. Behaviour of Hybrid RC-Steel System .....	10
2.5. Innovative Bracing Systems.....	11
2.6. Experimental Tests .....	14
2.7. Analytical Studies .....	18
2.8. Concluding Remarks.....	21
3. Seismic Design of Hybrid Systems .....	22
3.1. Lack of Regulations.....	22
3.2. Force-Based Design of Hybrid Structures.....	23

## TABLE OF CONTENTS

---

3.3.	Displacement-Based Design .....	28
3.4.	Seismic Assessment.....	31
3.5.	Rehabilitation Approaches .....	32
3.6.	Concluding Remarks.....	34
4.	Behaviour of Steel Braced RC Systems .....	35
4.1.	Introduction .....	35
4.2.	Behaviour of Steel Braces.....	35
4.3.	Behaviour of RC members.....	37
4.4.	Interaction between braces and RC frame .....	39
4.5.	Lateral Displacement Profiles.....	42
4.5.1.	Geometrical and Material Properties .....	42
4.5.2.	Numerical Modelling.....	44
4.5.3.	Materials .....	45
4.5.4.	Record Selection for Time-History Analysis .....	47
4.5.5.	Discussion of Results .....	50
4.5.6.	Comparison of Obtained Profiles with Existing Expressions.....	52
4.6.	Concluding Remarks.....	55
5.	Proposal of a Design Method for Steel Braced RC Frames.....	56
5.1.	Introduction .....	56
5.2.	Basis of the Method .....	56
5.3.	Input Parameters.....	58
5.3.1.	Yield Displacement ( $\Delta_y$ ) .....	58
5.3.2.	Ultimate Displacement ( $\Delta_u$ ).....	61
5.3.2.1.	Parameters for the Calculation of the Ultimate Displacement.....	62
5.3.2.2.	Column Deformation Capacity.....	62
5.3.3.	Lateral Strength ( $V_y$ ) .....	65
5.3.4.	Equivalent Viscous Damping (EVD) .....	65



## TABLE OF CONTENTS

---

5.3.5. Earthquake Demand.....	66
5.4. Retrofitting Solution.....	66
5.5. Alternative Process.....	68
5.6. Concluding Remarks.....	68
6. Validation of the Proposed Method .....	70
6.1. Introduction .....	70
6.2. Structure Characterization and Seismic Vulnerability.....	70
6.3. Seismic Assessment.....	71
6.4. Retrofitting Design .....	73
6.5. Verification of the Obtained Results .....	80
6.6. Concluding Remarks.....	82
7. Conclusion.....	83
7.1. Final Remarks .....	83
7.2. Future Developments.....	84
References .....	85

---

## LIST OF FIGURES

Figure 1.1 - Typical strengthening methods (adapted from Sugano (1996)).....	2
Figure 1.2 - Exterior diagonal bracing applied in tall buildings (John Hancock Building).....	3
Figure 1.3 - Seismic retrofitting of RC buildings with steel braces.....	4
Figure 2.1 - Bracing configuration .....	7
Figure 2.2 - Bracing patterns .....	7
Figure 2.3 - RC building retrofitted with steel braces (Tokyo Institute of Technology) .....	9
Figure 2.4 - Connection solutions for RC bracing systems .....	10
Figure 2.5 - Typical unbonded brace: layout and response curve (adapted from Di Sarno and Elnashai, 2008) .....	12
Figure 2.6 - K-Bracing with shear links layout .....	12
Figure 2.7 - Example of a dissipative device applied in BRB .....	13
Figure 2.8 - Domiziano Viola school (Potenza, Italy), retrofit with energy dissipating braces in 2002 .....	13
Figure 2.9 - Detail of the X-bracing system and its connection to the RC frame .....	14
Figure 2.10 - Comparison between the analytical force-displacement curves of the unbraced frame, X-bracing and the X-braced frame .....	14
Figure 2.11 - Test setup of brace system (adapted from Youssef <i>et al.</i> , (2006)) .....	15
Figure 2.12 - Lateral load-drift curve of the RC frame (left) and Braced frame (right) (adapted from Youssef <i>et al.</i> , (2006)) .....	16
Figure 2.13 - Variation of the energie dissipation with lateral drift.....	16
Figure 2.14 - Strain variation of column transverse reinforcement, beam-column joint transversal reinforcement and top beam reinforcement (from left to right) of RC frame (top) and braced frame (bottom) .....	17

---

Figure 2.15 - Details of connections constructed for experimental investigation.....	17
Figure 2.16 - Relationship between the PGA and the mean storey drift ratio for the existing and rehabilitation cases.....	19
Figure 2.17 - Bracing system in the central bay: device details and general layout [Varum (2003)] .....	20
Figure 2.18 - Bracing system in the shorter-external bay: device details and general layout [Varum (2003)] .....	20
Figure 3.1 - Shape of the elastic response spectrum defined in EC8 [CEN, 2005] .....	23
Figure 3.2 - Relationship between ductility and force reduction factor (adapted from Pauley <i>et al.</i> , 1992) .....	24
Figure 3.3 - Displacement spectra for different levels of damping (adapted from Priestley, 2003).....	24
Figure 3.4 - Concept of behaviour factor .....	25
Figure 3.5 - Effect of number of storeys on the R value of X-braced frames .....	26
Figure 3.6 - Effect of brace share of base shear on R value of X-braced frames (adapted from Maheri <i>et al.</i> , 2003).....	26
Figure 3.7 - Initial and secant stiffness characterization of hysteretic response (adapted from Priestley <i>et al.</i> , 2007) .....	28
Figure 3.8 - Fundamentals of direct displacement-based design .....	29
Figure 3.9 - Capacity spectrum method (adapted from ATC-40 by Varum (2003)).....	31
Figure 3.10 - Preliminary calculation for retrofit using strengthening and stiffening .....	32
Figure 3.11 - Global modification of the structural system (adapted from Moehle, 2000).....	33
Figure 3.12 - Local modification of structural components (adapted from Moehle, 2000).....	33
Figure 4.1 - Behaviour of steel braces (adapted from Longo <i>et al.</i> , 2008).....	36
Figure 4.2 - Axial load-moment interaction diagram (adapted from Collins <i>et al.</i> , 1997).....	37
Figure 4.3 - Influence of axial load on moment-curvature response (Adapted from Collins <i>et al.</i> , 1997) .....	38
Figure 4.4 - Example of an axial load-shear interaction diagram.....	38
Figure 4.5 - Deformation of hybrid system .....	39

---

Figure 4.6 - Forces path of hybrid system .....	39
Figure 4.7 - Independent systems contributing for global base shear (adapted from Queirós <i>et al.</i> , 2009) .....	40
Figure 4.8 - Variation in axial load in the compressed RC column .....	41
Figure 4.9 - Schematic response of braced structure (adapted from Della Corte <i>et al.</i> , 2008) .....	41
Figure 4.10 - layout of RC frame and elements details .....	43
Figure 4.11 - Stress-Strain relationship for reinforcement (left) and steel braces (right) .....	45
Figure 4.12 - Stress-Strain relationship for poorly confined concrete .....	45
Figure 4.13 - Stress-strain relationship for concrete proposed by Mander <i>et al.</i> [1988]. .....	46
Figure 4.14 - Discretization adopted for the RC braced frame .....	46
Figure 4.15 - Comparison of experimental and analytical response of steel braces .....	46
Figure 4.16 – Acceleration time series of the records selected for time-history analysis .....	49
Figure 4.17 - 1 <sup>st</sup> mode shape of the original and the two braced braces analyzed .....	51
Figure 4.18 - Displacement profiles at yielding .....	51
Figure 4.19 - Displacement profiles at failure .....	52
Figure 4.20 - Comparison of displacement profiles from different frames at different stages .....	53
Figure 4.21 - Comparison of displacement profiles obtained with the one resulting from the generalized expressions .....	54
Figure 4.22 - Comparison of analysis results with new expression .....	55
Figure 5.1 - Preliminary calculation for retrofit using strengthening and stiffening .....	57
Figure 5.2 - Identification of yield displacement on steel braced RC frames .....	58
Figure 5.3 - Brace frame model: a) forces; b) lateral deformation; c) vertical deformation (adapted from Moon <i>et al.</i> , 2007) .....	59
Figure 5.4 - Influence of frame rotation in braces behaviour .....	60
Figure 5.5 - Contribution of displacement components to total lateral displacement (adapted from Sozen <i>et al.</i> , 2004) .....	63

Figure 5.6 - Evolution of moments: a) bare frame, b) braced frame .....	63
Figure 5.7 - Moments evolution in RC columns with and without bracing system .....	64
Figure 5.8 - Comparison of an RC column capacity considering different contra- flexure lengths.....	64
Figure 5.9 - M-N interaction plot (adapted from RESPONSE-2000 Program) .....	65
Figure 5.10 - Illustration of a base shear-target displacement plot for different brace properties .....	66
Figure 5.11 - Evaluation of the seismic behaviour for two different solutions: a) unsatisfactory seismic behaviour; b) satisfactory behaviour .....	67
Figure 6.1 – RC frame .....	71
Figure 6.2 – Beam and column cross-sections .....	71
Figure 6.4 - Capacity curve of the MDOF .....	72
Figure 6.5 - Bilinear curve of the SDOF .....	72
Figure 6.6 - Application of the CSM procedure .....	73
Figure 6.7 - History of axial loads in the pushover analyze .....	73
Figure 6.8 - M-N interaction diagram (adapted from RESPONSE-2000) .....	74
Figure 6.9 - Solution 1.....	75
Figure 6.10 - Solution 2.....	76
Figure 6.11 - Solution 3.....	76
Figure 6.12 - Comparison of the design displacements for all studied solutions .....	78
Figure 6.13 - Superposition of response spectra with the performance points of braces 5 and 4 .....	79
Figure 6.14 - Superposition of response spectra with the performance points of braces 3 and 2 .....	80
Figure 6.15 - Superposition of response spectra with the performance points of brace 1 .....	80
Figure 6.16 - Comparison of the calculated target point with the capacity curve of the braced structure.....	81
Figure 6.17 - Representation of the Capacity curve with the corresponding bilinear representation.....	82

## LIST OF TABLES

Table 2.1 - Values of the parameter $\gamma$ for existing and rehabilitated frames R1 to R6.....	19
Table 3.1 - Tentative values of R factor for steel-braced, RC frame dual systems .....	26
Table 3.2 - q values obtained for different RC frames and steel braces [Queirós <i>et al.</i> , (2009)] .....	27
Table 4.1 - Properties of the braces adopted in the analysis.....	43
Table 4.2 - Earthquake records used in the analysis.....	47
Table 4.3 - Resume of scale factors obtained in dynamic analysis .....	50
Table 4.4 - Fundamental periods of vibration of the analyzed frames .....	50
Table 6.1 - Basic properties of selected steel braces .....	74
Table 6.2 – Global yield displacement of the frame for different braces .....	75
Table 6.3 - Maximum compressive axial load in the RC column for different brace properties .....	76
Table 6.4 - Minimum compressive axial load in the RC column for different brace properties .....	76
Table 6.5 - Maximum deformation capacity for each RC column in solution 1.....	77
Table 6.6 - Maximum deformation capacity for each RC column in solution 2.....	77
Table 6.7 - Maximum deformation capacity for each RC column in solution 3.....	77
Table 6.8 - DBD parameters for all solutions studied .....	78
Table 6.9 - Values of ductility and equivalent viscous damping for all studies solutions .....	79
Table 6.10 - Fundamental period of vibration of the original and retrofitted structure .....	81

# 1. INTRODUCTION

*“The first and most important thing to be done (...) is to learn thoroughly what it is that I have undertaken”*

Frontinus  
(Curator Aquarum of ancient Rome)

## 1.1. HISTORICAL BACKGROUND

Recent seismic events such as the 1985 Mexico, the 1994 Northridge, the 1995 Kobe and the 1999 Kocaeli earthquakes induced severe damage to non-ductile reinforced concrete (RC) buildings proving that many constructions located in seismic zones are unable to withstand moderate to severe earthquakes and therefore observe significant damage and contribute to significant loss of lives.

After big earthquake events such as those mentioned above, the scientific community focused their attention to better understand the phenomenon. As a result, the design codes have experienced significant developments over the years. At the same time researchers have also concentrated to studying various strengthening techniques to enhance the seismic performance of existing buildings.

Framed systems are extensively used for building structures in earthquake-prone regions because of their potential for good seismic performance. Many existing RC structures worldwide were designed for gravity load only, with inadequate lateral load resistance, lateral stiffness and poor detailing of the reinforcement.

Wyllie (1983) defined seismic retrofitting as the “judicious modification of the structural properties of an existing building in order to improve its performance in futures earthquakes”.

The two main approaches for structural rehabilitation consist of: i) adding new structural elements such as walls and steel braces, and ii) strengthening of structural elements by encasing with steel, FRP or RC jackets. In recent years, some new trends, which are called passive energy dissipating devices, have appeared to enhance the seismic behaviour of existing structures [Aydin *et al.*, 2008]. Sugano (1996) summarized the most common strengthening methods in a flowchart, as shown in Figure 1.1:

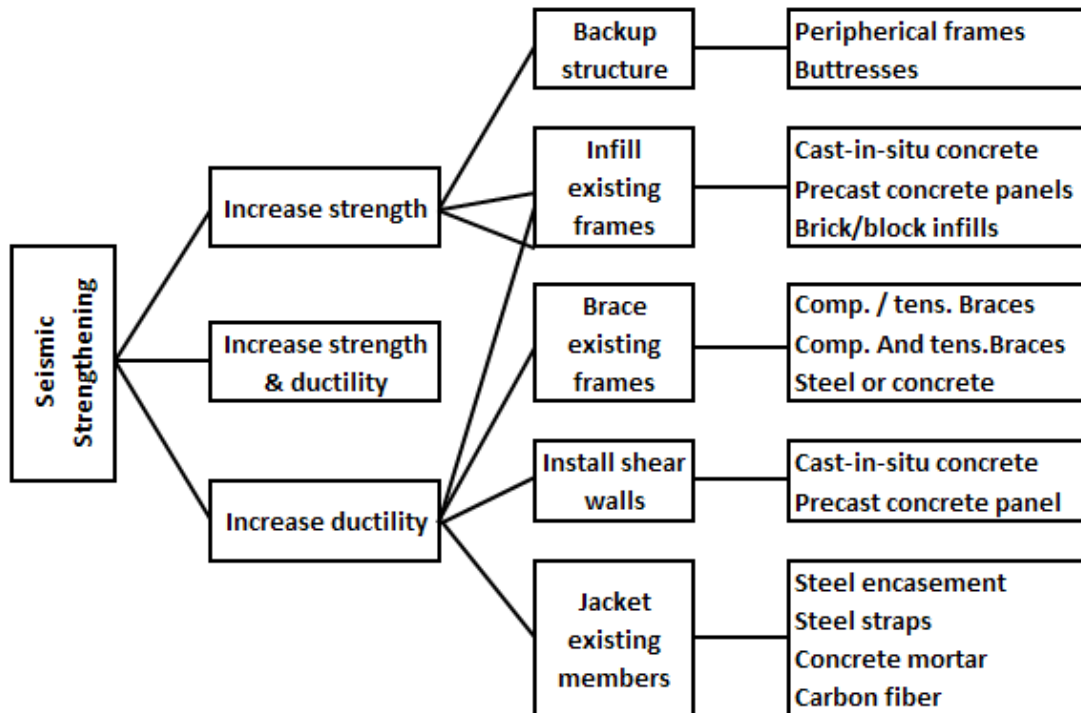


Figure 1.1 - Typical strengthening methods (adapted from Sugano (1996))

Global intervention methods may represent a more cost-effective strategy than upgrading of the existing components, especially if the disruption of occupancy and the demolition and replacement of partitions, architectural finishes and other non-structural components are considered [Fardis, 1998]. This is particularly true for structures where no horizontal load-path is available, or in the case of all structural members being extremely flexible. In such cases the methods described below may indeed provide an optimum solution [Pinho, 2000].

While many of these techniques can effectively improve the lateral stiffness and strength of the structure, adequate seismic behaviour will be obtained only if the retrofitted structure can satisfy the strength and ductility imposed by the earthquake [Pincheira *et al.*, 1995]. Independently of the retrofitting scheme, besides the increment in stiffness or strength of the existing structure, not every retrofitted structure performs adequately under any seismic event considered [Jordan, 1990].

Traditionally, steel bracing systems have been used to increase the lateral load resistance of steel structures. In the past two decades, a number of reports have also indicated the



effective use of steel bracing in RC frames [Youssef *et al.*, 2007; Badoux *et al.*, 1990]. Steel bracing of RC buildings started as a retrofitting measure to strengthen earthquake-damaged buildings or to increase the load resisting capacity of existing buildings [Maheri *et al.*, 2003].

The bracing techniques adopted in the past fall into two main categories, namely (i) external bracing and (ii) internal bracing [Maheri *et al.*, 2003].

However, while the structural efficiency provided by diagonal braces was well recognized, their aesthetic potential was not entirely appreciated. Thus, diagonals were generally embedded within the building cores which were usually located in the interior of the building [Moon *et al.*, 2007].

A major departure from this design approach occurred when braced tubular structures were introduced in the late 1960s. In the 100-storey tall John Hancock Building in Chicago, the diagonals were located along the entire exterior perimeter frames (Figure 1.2) of the building in order to maximize their structural effectiveness and capitalize on the aesthetic innovation.



Figure 1.2 - Exterior diagonal bracing applied in tall buildings (John Hancock Building)

Others examples of this retrofitting scheme can be found for example in Mexico City and California (Figure 1.3). According to Moon *et al.* (2007) this strategy is much more effective than confining diagonals to narrower building cores.

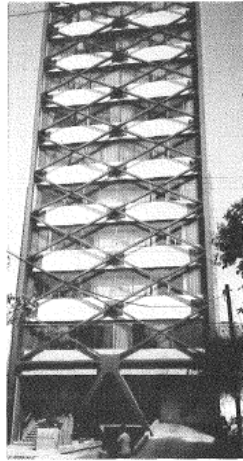


Figure 1.3 - Seismic retrofitting of RC buildings with steel braces

Increased architectural flexibility, reduced weight of the structure, easy and speed of construction and the ability to choose more ductile systems can be considered as the main advantages of steel bracing in comparison with strengthening based on the inclusion of RC shear walls [Maheri *et al.*, 2008].

Despite the several experimental and analytical studies conducted [Maheri *et al.*, 1997; Badoux *et al.*, 1990] in the last years trying to understand the behaviour of this type of hybrid structures, the fact is that only a few have resulted in proposal of values for the so call behaviour factor to be use in the design process. Moreover, due to the discrepancy of the results, the values obtained in past works do not provide enough confidence to the designer. In fact, as it will be discussed herein, some authors support that a force-based design approach is not entirely suitable for this type of structures.

## 1.2. OBJECTIVES

The aim of the present work is to develop a displacement-based design procedure for the seismic retrofitting of RC frames with steel braces that overcomes the limitations identified with traditional force-based design procedures. The methodology to be proposed should be simple and easy to apply by the designer but should conduct to reliable structural solutions. Moreover, it should take into account the complex interaction between the steel braces and the RC elements. In addition to this main objective, the research also intends to describe the lateral behaviour of steel braced RC frames, particularly in terms of the lateral deformation characteristics of this type of structural systems.

### **1.3. LAYOUT OF THE THESIS**

The dissertation is organized in seven chapters. This chapter (Chapter 1) provides a general introduction to the topic along with the main objectives expected from the research. Chapter 2 reviews past experimental, numerical and analytical studies performed on steel braced RC frames. The current situation regarding the seismic design of this type of structures is discussed in Chapter 3. The limitations associated with the application of traditional force-based procedures in the seismic design of steel RC braced frames are highlighted. In Chapter 4 the results from numerical studies are used in order to describe the behaviour of steel RC hybrid systems, particularly the interaction between the steel braces and the RC elements. A parametric study is also described which aimed at the characterisation of the lateral deformation mode shapes of this type of structural systems. In Chapter 5 a new displacement-based design method for hybrid systems is proposed which aims at producing retrofitted solutions with better and more predictable seismic performance. The new design method is applied in Chapter 6 to design the bracing system of a regular RC structure that is found to have inadequate strength to resist a given design earthquake. Several solutions are tested comprising different bracing layouts and brace cross-sections. The accuracy of the method is confirmed through a non-linear static analysis of the adopted solution. In Chapter 7 the main conclusions of the research are summarised along with some suggestions for future research on this topic.

## 2. REINFORCED CONCRETE STEEL BRACED FRAMES

*“To find the answer, you must know the answer”*

The third principle of engineering (1939)

### 2.1. OVERVIEW

To resist lateral earthquake loads, shear walls are commonly used in RC framed buildings, whereas steel bracing is most often used in steel structures. In the past two decades, a number of reports [Maheri *et al.*, 1997; Badoux *et al.*, 1990] have indicated the effective use of steel bracing in RC frames. Steel bracing of RC buildings started as a retrofitting measure to strengthen earthquake-damaged buildings and/or to increase the lateral load resistance of existing buildings. The steel system technique was firstly used to rehabilitate an existing RC structure in Japan during the 80's [Badoux *et al.*, 1990].

The bracing methods adopted in the past fall into two main categories, namely (i) external bracing and (ii) internal bracing. In the external bracing system, existing buildings are retrofitted by attaching a local or global steel bracing system to the exterior frames. Architectural concerns and difficulties in providing appropriate connections between the steel bracing and RC frames are two of the shortcomings of this method. In the internal bracing method, the buildings are retrofitted by incorporating a bracing system inside the individual bays of the RC frames. The bracing may be attached to the RC frame either direct or indirectly.

In the indirect internal bracing, a braced steel frame is positioned inside the RC frame. The indirect internal bracing method can be an expensive solution resulting from the difficulties resulting from the fixation of the braced frame to the RC frame. Another limitation of this method is that the retrofitted frame is susceptible to dynamic effects due

to interaction between the steel frame and the concrete frame. To overcome the shortcomings of the indirect internal bracing, Maheri and Sahebi proposed a direct connection between the steel bracing and RC frame without the need for an intermediary steel frame [Maheri *et al.*, 2003].

## 2.2. BRACING LAYOUT

The definition of an appropriate bracing layout is important because the effect of retrofitting on the flow of the forces through the structures should be as simple as possible, in order to avoid load concentration or potential weak zones. From a structural point of view, it may be desirable to brace as many bays as possible, so that increases in strength and stiffness are uniformly distributed within the existing RC structure.

However, it is often preferable not to brace the end bays due to two main reasons. Firstly, because the end bays may be shorter than intermediate bays, making bracing geometry difficult. Secondly, because a typical interior column can resist overturning forces better than an exterior (end) one [Badoux *et al.*, 1990].

In the Figure 2.1 and Figure 2.2, it is possible to observe some configurations and patterns for bracing systems proposed by Badoux *et al.* (1990).

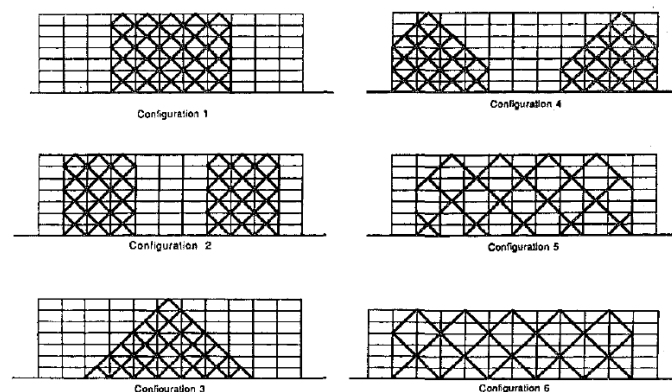


Figure 2.1 - Bracing configuration

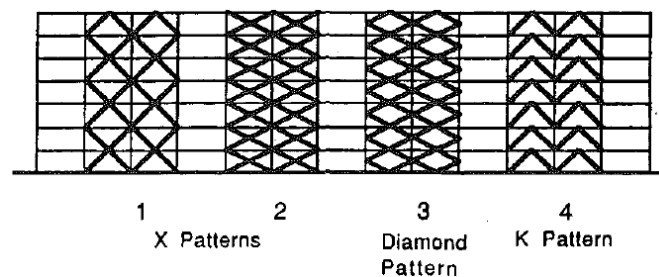


Figure 2.2 - Bracing patterns

### 2.3. ADVANTAGES AND DISADVANTAGES OF STEEL BRACING

When an engineer is faced with an assessment and retrofitting problem, he must decide the strategy based on many factors such as: aesthetics of steel bracing, speed of constructing, economy, occupancy of the building, efficiency...

Each retrofitting technique has its advantages and disadvantages. Regarding the use of steel bracing systems, one of the advantages is the fact that most of the construction work can be performed on the exterior of the building in order to speed erection and to minimize disruption of the occupants and comprise the possibility of including openings.

This can be a very effective method for global strengthening of the building. Concentric or eccentric bracing schemes may be used in selected bays of an RC frame to provide a significant increase of the lateral capacity of the structure. Normally, no intervention to foundations is required and its installation is not as disruptive as that of shear walls [Pinho, 2000]. However, in some cases it might be necessary to verify if the additional loads imposed by the braces will not affect the capacity of the foundations.

At the same time the erecting of the braces in the perimeter will increase the capacity of the building to resist to torsional forces during the earthquake. The loss of space and accessibility in the retrofitted building and the cost of interior remodelling are minimized as well. These may be a significant advantages compared to other retrofitting schemes.

Another advantage is the small increment in the mass comparatively with the existing building or with that of adding new RC walls, specially comparing with the increase in stiffness [Abou-Elfath *et al.*, 2000; Badoux *et al.*, 1990].

Finally it must be pointed out that one of the most critical aspects found in buildings with low seismic resistance is the potential for the formation of soft-storeys particularly when there are no infill walls in the ground storey. In such cases, bracing the bare bays may result in a fast, economical and efficient way to avoid this undesirable collapse mechanism.

On the other hand, steel braces have also some drawbacks, namely the aesthetical changes caused to the original structure. The structure shown in Figure 2.3 is a good example of harmony between the retrofitting scheme and the architectural issues.



Figure 2.3 - RC building retrofitted with steel braces (Tokyo Institute of Technology)

Another important issue that can be seen as a disadvantage is the connection between the bracing system and the RC frame [Maheri *et al.*, 2008]. This link between the two systems is responsible for the transmission of the loads carried by the braces to the structure and plays a fundamental role on the success of the strengthening intervention [Youssef *et al.*, 2006].

The advantage of connecting the steel bracing system directly to the RC frame is that the connection is generally easy to execute and therefore inexpensive. However, the connection should be strong enough to safely transfer the loads between the braces and the RC frame.

Maheri *et al.* (1997) investigated the behaviour of various connection schemes. The connections shown in Figure 2.4 represented different arrangements for existing frames and were found to have an adequate behaviour. Moreover, experimental investigation indicated that the connections can be designed successfully by combining the current guidelines and the provisions set by codes of practice for designing brace/steel frame connections and base plate/RC member connections [Maheri *et al.*, 2003].

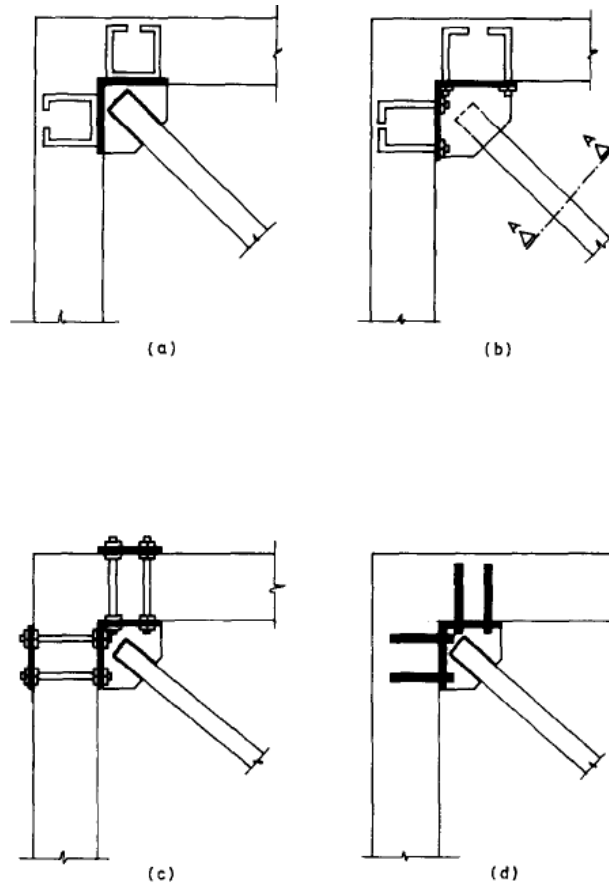


Figure 2.4 - Connection solutions for RC bracing systems

Finally, the lack of design models can be seen as the main disadvantage in the application of this retrofitting method.

## 2.4. BEHAVIOUR OF HYBRID RC-STEEL SYSTEM

Several studies demonstrated that in a steel-braced RC frame deforming laterally, the bracing system and the RC frame can be considered as coupled independent systems adding their lateral strength and stiffness [Badoux *et al.*, 1990; Di Sarno *et al.*, 2009]. Some authors like Di Sarno and Manfredi (2009) stated that the new bracing system should absorb and dissipate large amount of hysteretic energy under earthquake ground motion, at the same time that the original system is capable to withstand the vertical loads and respond elastically under earthquakes loads [Di Sarno *et al.*, 2009]. In the present study however, for economical and structural reasons, it is believed that the original RC system should still be allowed to undergo inelastic deformations.

The bracing system can compensate for inadequate frame strength and/or stiffness, but cannot change the frame's failure mode. As explained subsequently, increasing the capacity of the braces will increase the axial forces in the columns and this will lead to a possible reduction in the deformation capacity. It is possible that the solution adopted for



the braces could lead to a premature failure of the column. For these cases, a complementary solution may be adopted or even adopt a completely different retrofitting solution.

In some investigations, bracing was applied to the concrete frame indirectly through a steel-frame, itself confined in the concrete frame. This rather elaborated “indirect bracing system” can be costly and economically non-viable [Maheri *et al.*, 1997], but in order to avoid the problems referred above, it may represent in some cases a good solution.

## 2.5. INNOVATIVE BRACING SYSTEMS

In recent decades many studies were developed as an attempt to improve the original steel bracing systems. Many of these innovating systems have arisen to overcome possible inconveniences identified previously. This chapter intends to summarize some of the “upgrades” introduced in the steel bracing systems.

- **Buckling Restrained Braces**

One of the disadvantages of traditional braced systems may be overcome whether the occurrence of buckling for the metallic braces in compression is inhibited by using unbonded braces (UB) or buckling-restrained braces (BRB). These system exhibits large and stable hysteretic dissipation (Figure 2.5). The UBs are braces where the core is placed within a hollow section member, filled with either mortar or concrete [Di Sarno *et al.*, 2009].

BRBs are an efficient solution to the problem of the limited ductility of classical concentric bracing, thanks to the avoidance of global compression buckling. Experimental and numerical simulations prove that the energy dissipating capacity of BRBs is extremely high [Di Sarno *et al.*, 2009]. They are basically made of very slender steel plates, forming the core of the BRB, which are allowed to yield both in tension and compression. The slender plates are inserted inside steel rectangular or square hollow section profiles, which provide the restraining effect against lateral buckling. In the most classical form, the restraining tube is filled with concrete and an unbonding layer is placed at the contact surface between the core plates and the filling concrete, thus the name ‘unbonded brace’ of this version [Mazzolani, 2007].

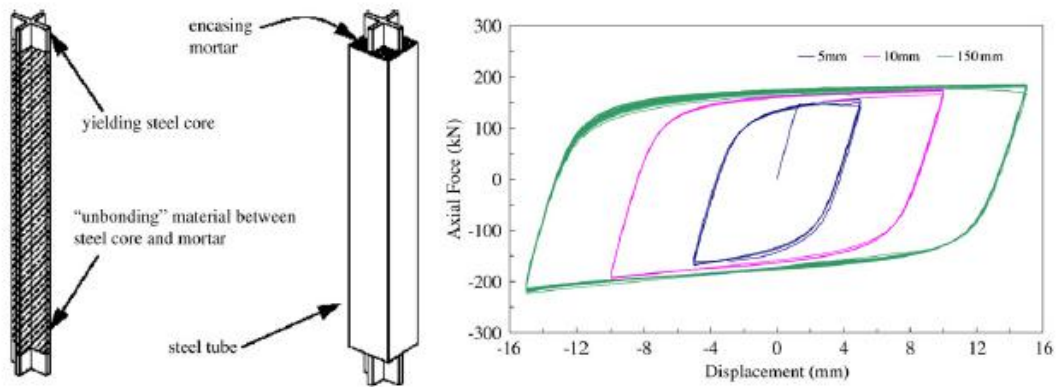


Figure 2.5 - Typical unbonded brace: layout and response curve (adapted from Di Sarno and Elnashai, 2008)

- **K – Bracing with shear links**

The K-bracing with shear-link system consist of an eccentrically braced steel assembly with a vertical shear-link located at mid-span of either the upper or bottom floor beam (Figure 2.6).

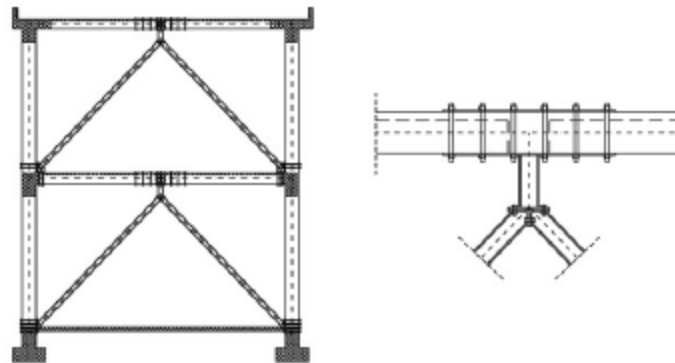


Figure 2.6 - K-Bracing with shear links layout

Comparing this system with the traditional X-bracing scheme, this will have a lateral load resistance similar to the initial resistance but with a significant increased energy dissipating capacity. Hence, the risk of overloading the foundation can be significantly reduced [Bouwkamp *et al*, 2000].

- **Bracing System with Dissipative Devices**

In the dissipative brace (Figure 2.7), the energy dissipation is concentrated in the brace itself or in one opposite element (dissipator) in a way to avoid damage in the main structural elements (beams and columns) [Antonucci *et al.*, 2009]. The device can increase both the stiffness and damping of the overall system, consequently leading to a reduction of the deformation demand.



Figure 2.7 - Example of a dissipative device applied in BRB

Passive energy dissipation devices or shear links may also be used in conjunction with the bracing to efficiently increase dynamic damping. However, if the bracing system increases the stiffness of the frame considerably, the efficiency of the damping mechanism is compromised since these normally require large levels of deformation to be cost-effective [Fardis, 1998]. Figure 2.8 illustrates one example of application of bracing systems with dissipative devices.



Figure 2.8 - Domiziano Viola school (Potenza, Italy), retrofit with energy dissipating braces in 2002

- **Post Tensioned Braces**

In recent years, it has been shown that the seismic performance of existing buildings can be enhanced considerably by bracing with post-tensioned rods or cables [Pinho, 2000]. This upgrading technique has several advantages, which include architectural versatility, low cost and fast construction. Furthermore, it does not add a significant mass to the existing building.

This system involves the addition of post-tensioned rods that will yield for small levels of deformation, allowing energy dissipation at an early stage of a large seismic event.

However, the initial brace prestressing induces additional forces in the structure modifying the internal force distribution. This needs to be considered, especially for serviceability limit states [Pinho, 2000].

## 2.6. EXPERIMENTAL TESTS

Maheri, *et al.* (2003) carried out monotonic tests on reduced scaled steel X-Braced RC frames. The objective of the study was to examine several response and design parameters, namely load capacity, stiffness, ductility and behaviour factor (R).

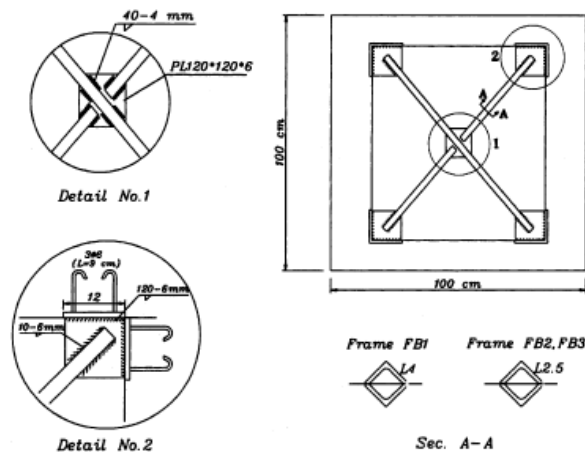


Figure 2.9 - Detail of the X-bracing system and its connection to the RC frame

Test results showed that the load capacity of an existing ductile frame can be increased to the desired level by directly adding a bracing system to the frame, without the need for prior strengthening of the existing frame (Figure 2.10).

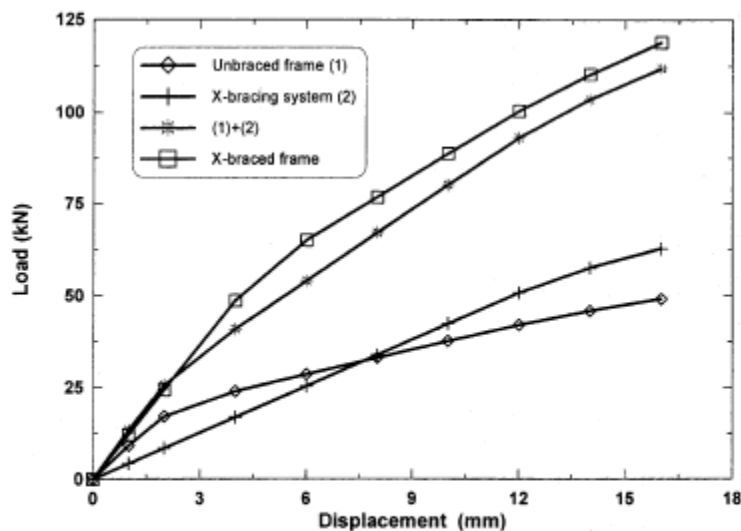


Figure 2.10 - Comparison between the analytical force-displacement curves of the unbraced frame, X-bracing and the X-braced frame

The study demonstrated that load capacities of the braced frames are higher than the summation of the capacities of the unbraced frame and the bracing system. Two factors can be attributed to the increase in the strength of the RC frame. Firstly, in the braced frame, because of the bracing system, the formation of the first plastic hinge in the RC beams occurs at higher loads. In other words, the bracing system increases the yield capacity of the RC frame members. Secondly, the rigid connections between the brace and the frame add to the strength of the frame mainly by reducing the effective lengths in beams and columns.

The test results led the authors to conclude that X-bracing is more suitable for a strength-based design. However, the relatively small post-yield capacity and the somewhat brittle failure mode of the X-braced frame make this system unfavourable for a ductile design. It was found that steel bracing reduced the ductility and the performance factor (R) of a ductile RC frame. The ductility capacity was reduced from 4.19 to 2.71. Similarly, the R factor was reduced from 12.1 to 4.3.

Youssef *et al.*, (2006) conducted experimental tests that proved the brace system as a good retrofitting solution.



Figure 2.11 - Test setup of brace system (adapted from Youssef *et al.*, (2006))

The results presented in Figure 2.12 showed that in the braced system, the pinching was less significant, indicating an overall better seismic performance. It was also observed that the lateral load capacity was significantly increased and the ultimate drift was slight reduced.

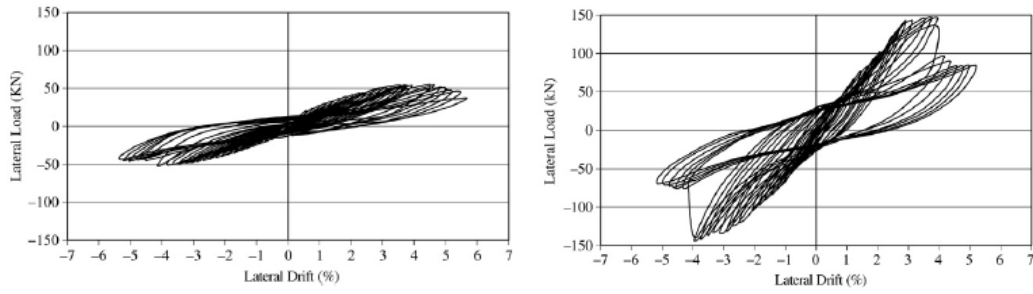


Figure 2.12 - Lateral load-drift curve of the RC frame (left) and Braced frame (right) (adapted from Youssef *et al.*, (2006))

Furthermore it was observed that at low drift levels, the energy dissipated by the braced system was lower than that dissipated by the RC frame. This was mainly attributed to the initial high stiffness of the braced frame. At higher levels of drift, the authors of the study found that the energy dissipated by the braced frame was much higher than that dissipated by the RC frame.

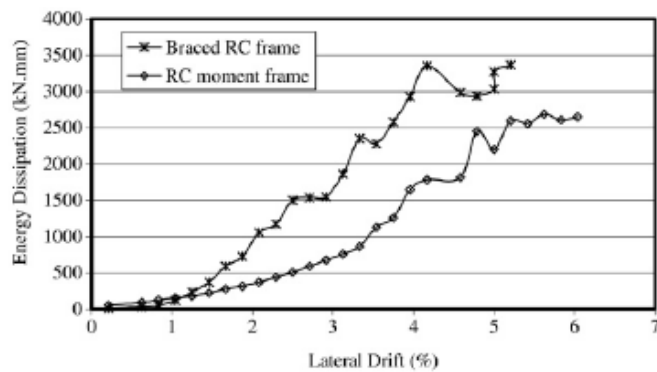


Figure 2.13 - Variation of the energie dissipation with lateral drift (adapted from Youssef *et al.*, (2006))

The analysis of the reinforcement revealed that strains reduced significantly when steel braces were applied to the RC frames (Figure 2.14). This observation allowed the authors to conclude that the forces in the braced members were mainly transferred to the RC beams and columns as axial forces and hence indicating that shear failure should not be expected.

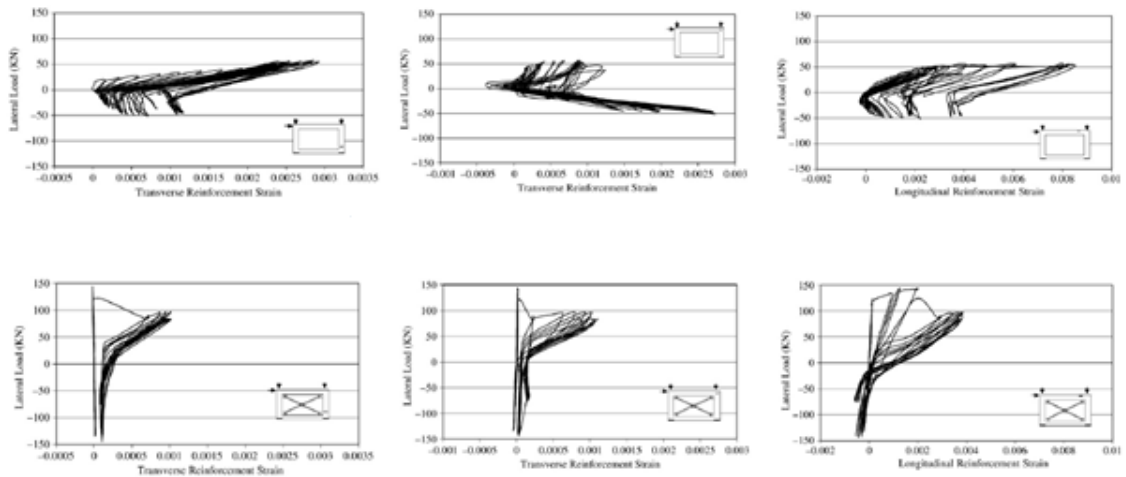


Figure 2.14 - Strain variation of column transverse reinforcement, beam-column joint transversal reinforcement and top beam reinforcement (from left to right) of RC frame (top) and braced frame (bottom)

Recognized as one of the issues to address in the retrofitting process of RC frames, some authors (e.g., Maheri and Hadjipour (2003)), carried out experimental investigations on the connection between steel braces and RC frames.

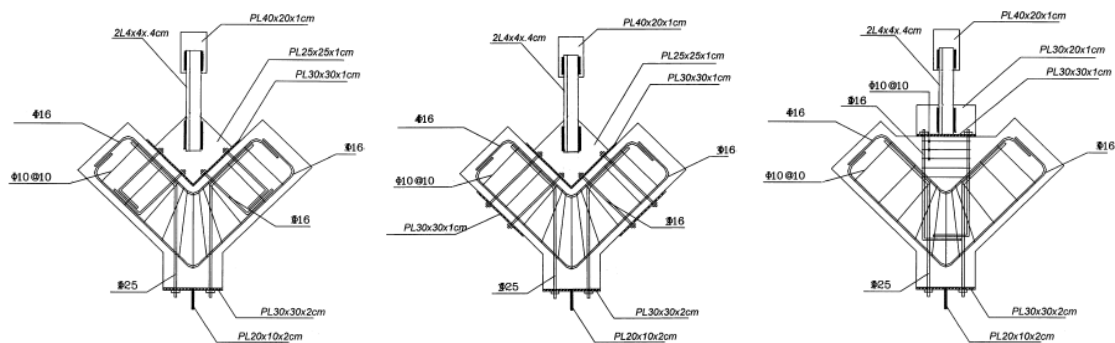


Figure 2.15 - Details of connections constructed for experimental investigation

The study indicated that these connections could be designed successfully by combining guidelines and provisions set out by codes of practice for designing brace/steel frame connections and base plate/RC member connections [Maheri *et al.*, 2003].

Experimental tests, conducted in 2006 allowed to conclude that connections could be designed using a similar procedure to that for braces in steel structures. In that study, brace member connections, including welds and head studs, exhibited adequate behaviour [Youssef *et al.*, 2007].

Di Sarno and Manfredi (2009) performed *in situ* tests on full scale RC frames retrofitted with Buckling Restrained Braces. The results obtained from an energy analysis were found to be useful to quantify the contribution of the braces and the bare RC frame to the global hysteretic response.

## 2.7. ANALYTICAL STUDIES

Analytical studies performed in the past provided insights into the effectiveness of various global retrofitting schemes. For example, Pincheira and Jirsa (1995) carried out inelastic static and dynamic analysis of three prototype buildings. Retrofit schemes included the post-tensioned bracing, structural steel bracing, and infill walls of reinforced concrete frames. The buildings selected for study were 3-, 7- and 12-storey high frames of reinforced concrete. The prototype designs contain typical reinforcement details of older frames and represent low and medium rise construction in regions of high seismicity in US. The authors of the study also evaluate the displacements capacity of the mentioned structures for different earthquakes and different retrofitted solutions.

The study concluded that there is not a unique solution and that several different retrofit schemes can be designed to provide effective seismic resistance. Satisfactory response was obtained only for schemes that adequately controlled interstorey lateral drifts to levels that did not cause significant damage to the existing structure. For bracing systems that resulted in controlled lateral drifts, the level of axial forces induced by steel braces would adversely affect the lateral strength of the existing reinforced concrete member or, in some cases, exceed the axial capacity of the member.

Abou-Elfath and Ghobarah (2000) conducted analysis in different configurations and distribution of steel braces in a nonductile RC building. The following six different frames were tested, where the parameter  $\Gamma$  indicates the brace distribution per floor of the frame.

The first parameters evaluated were the lateral load capacity and variation in drift ratios over the height. To do that, the parameter  $\gamma$  is introduced to measure the variation in the storey drift ratios from the average storey drift:

$$\gamma = \frac{\left( \sum_{i=1}^n \left| \frac{S_i}{S_{avg}} - 1.0 \right| \right)}{2 \times (n-1)} \quad (1)$$

Where  $S_i$  is the storey drift ratio of the  $i$ th storey,  $S_{avg}$  is the average storey drift ratio and  $n$  is the total number of stories. The value of  $\gamma$  equal to 0 represents equal storey drift ratio for all the building stories. The value of  $\gamma$  equal to 1 indicates that one given storey is the only source of overall building deformation (soft storey).

This parameter was useful for comparing the plastic mechanism of buildings with different heights or different rehabilitation options. Moreover, this parameter was also useful in



evaluating the distribution of braces over the height of the building [Abou-Elfath *et al.*, 2000].

Table 2.1 - Values of the parameter  $\gamma$  for existing and rehabilitated frames R1 to R6

Case	Parameter $\gamma$
Existing	0.43
R <sub>1</sub>	0.60
R <sub>2</sub>	0.25
R <sub>3</sub>	0.68
R <sub>4</sub>	0.74

The second rehabilitation case with the lowest value of  $\gamma$  exhibited the best performance of all the rehabilitation cases, while the fourth rehabilitation case with the largest value of  $\gamma$  exhibited the poorest performance.

The following figure represents the variation of the mean storey drift ratio of the analyses using 12 earthquakes. The results in the figures show that there is a direct correlation between the building seismic performance and the level of the parameter  $\gamma$  (listed in table above).

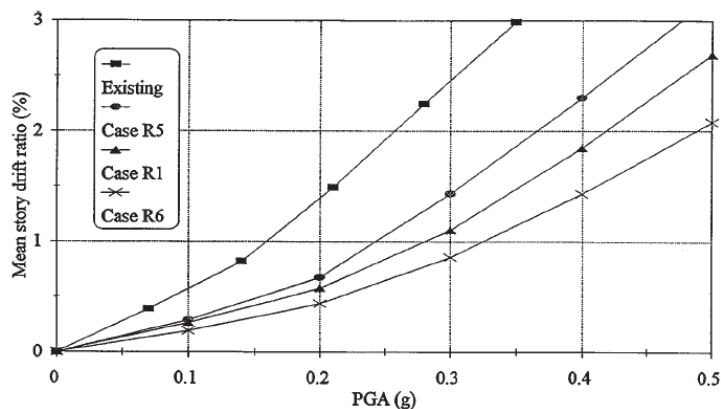


Figure 2.16 - Relationship between the PGA and the mean storey drift ratio for the existing and rehabilitation cases

Tests conducted by Abou-Elfath and Ghobarah (2000) in structures with different bracing configuration and with changing the braces capacity over the height, showed that adding steel bracing uniformly distributed over the height may not represent the optimum solution. It is possible to improve the plastic mechanism of the rehabilitated building by special arrangement of the lateral strength distribution along the frame height to force most of the members to contribute to the building overall deformation. This can be also achieved by increasing the number of braced bays.

The degree of improvement in the seismic performance of the rehabilitated building depends significantly on the level of increase of the load carrying capacity as well as on the change in seismic demand that results from the associated stiffness increase. In general the improvement in the building capacity is superior to the increase in seismic demand. At

the same time, increasing too much the braces capacity may lead to expensive solutions and axial loads in the concrete columns that may not be accepted. By increasing the number of braced bays the loads on the reinforced concrete columns decrease and column failure may be avoided [Abou-Elfath *et al.*, 2000].

In some of the analytical studies available the results may not represent real structural scenarios. In many of the studies, the retrofitted schemes exhibited large deformation capacity and large ductility in comparison with the original structures. That was mainly due to the use of models that neglected important factors such as P-Δ effects and the interaction of the axial force with both moment and deformation capacities of the RC member [Abou-Elfath *et al.*, 2000].

Varum (2003) investigated several strengthening techniques on existing buildings. Amongst others, he studied the application of X- and K-bracing with dissipative devices. The layouts and device details of the structures investigated are plotted in Figure 2.17 and Figure 2.18.

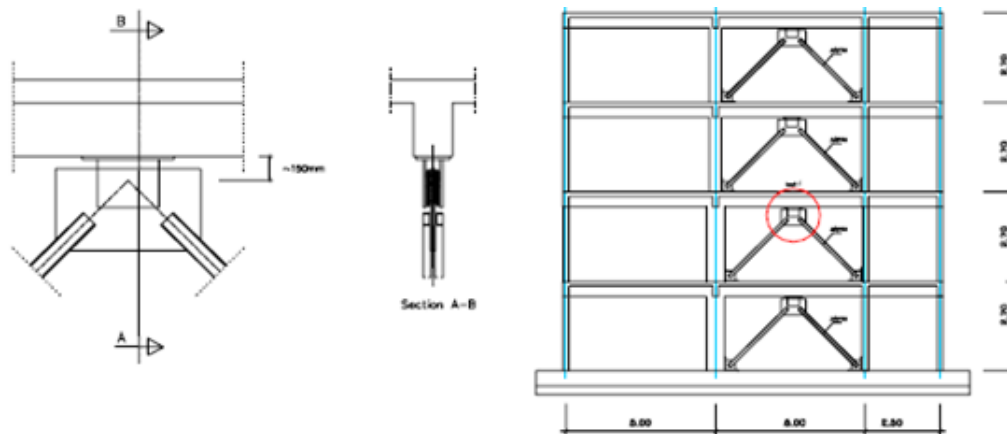


Figure 2.17 - Bracing system in the central bay: device details and general layout [Varum (2003)]

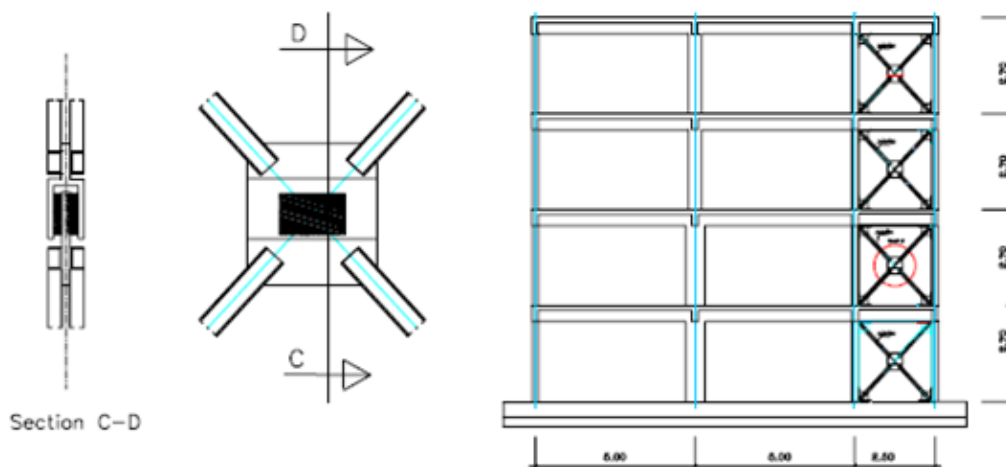


Figure 2.18 - Bracing system in the shorter-external bay: device details and general layout [Varum (2003)]

Seismic vulnerability functions were calculated to investigate the behaviour of the retrofitted solutions. Seismic vulnerability functions of structural systems are expressions that relate earthquake intensities with quantitative measures of their probable consequences on the performance of those systems.

The numerical analysis for the retrofitted frame case (K- and X-bracing with rubber dissipator) allowed the author to conclude that the light retrofitting solution appeared to be effective for low, medium and high seismic intensities, but not particularly effective for very high intensities when infill panels exist. This retrofitting system was designed for the bare frame and it was very effective for that case. However, according to the author of the study, a more accurate design should consider the infill panels. Additionally, the retrofitting system led only to a small increase of the storey shear forces. Finally, an important increase on the energy dissipation capacity was observed. The contribution of the RC frame, of the infill panels and of the retrofitting devices to the total energy dissipation was approximately equal.

## **2.8. CONCLUDING REMARKS**

In this chapter an overview of steel braced RC frames was presented. Several experimental and analytical studies performed on this topic were reviewed. The main conclusions resulting from past studies are summarised below:

1. Both experimental and analytical studies indicated that the adoption of steel braces to retrofit existing RC buildings is a good strategy and that, in some situations, that solution may be more suitable in comparison with other more traditional retrofitting solutions.
2. The lateral resistance and stiffness of RC frames significantly increases when steel braces are added to the structure. The improvements are visible even when "light" braces are considered.
3. Besides the loss of local ductility observed in the RC column elements, previous research demonstrated an increase in the ductility capacity of the global structure.
4. A good performance of the connections between the two systems is expected if traditional guidelines and provisions set out by codes of practice are applied.

Despite the many advantages of retrofitting RC frames with steel braces, an important factor can limit the use of this technique. In effect there is not yet available a simple and accurate design method that can be used by practitioners. In the next chapter the current situation concerning the seismic design of RC frames retrofitted with steel braces will be discussed.

### 3. SEISMIC DESIGN OF HYBRID SYSTEMS

*“The truth is, the science of Nature has been already too long made only a work of the brain and the fancy: It is now high time that it should return to the plainness and soundness of observations on material and obvious things.”*

Robert Hooke (1635 - 1703)

#### 3.1. LACK OF REGULATIONS

Traditionally, structural seismic design has been based primarily on forces. The reasons for this are largely historical, and started to how we design for other actions, such as dead and live load [Priestley *et al.*, 2007]. This is mainly the reason why, seismic design is currently codified by structural codes and standards of practice, using the so-called “force-based” design (FBD). In this design, the earthquake action is considered as equivalent static forces with different intensity and distribution over the height of the structure as a function of the earthquake shaking intensity at the site of interest and the structural type.

In the preceding chapter several studies, involving the behaviour of steel braces and RC braced structures, were presented in order to better understand the behaviour of this type of structures and its main advantages and disadvantages. Despite the good seismic behaviour of the retrofitted structures [Badoux *et al.* in 1990] there is still a lack of design rules for hybrid structures in seismic codes.

In order to overcome this situation, several researchers conducted studies to find important parameters such as behaviour factor ( $q$ ), also known as response modification factor ( $R$ ), associated to this type of structures so that they might be adopted in FBD methodologies. A brief summary of FBD is presented in the next section.

### 3.2. FORCE-BASED DESIGN OF HYBRID STRUCTURES

Seismic design arises historically as an extension of the design for static loads. Despite the evolution in the seismic engineering field over the past decades, particularly the development of performance-based design concepts, in general the codes of practice are still based on forces. In simple terms, Force-Based Design (FRD) consists of the calculation of a design base shear which is a function of the fundamental period of the structure, of a behaviour factor that takes into account the ductility expected to develop within the structure and also a function of an acceleration response spectrum (Figure 3.1). The base shear is then applied to the structure as set of equivalent static forces which are adequately distributed over the height of the structure. Section and member design checks are then carried out along with some simple lateral deformation checks.

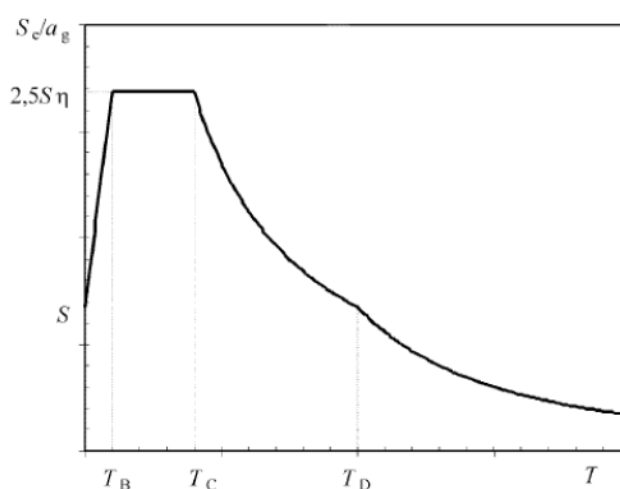


Figure 3.1 - Shape of the elastic response spectrum defined in EC8 [CEN, 2005]

The base shear is calculated by multiplying the total mass of the building by the design spectral acceleration. The design acceleration is calculated by dividing the spectral acceleration by the behaviour factor ( $q$ ).

$$F_b = S_d(T) \times M \quad (2)$$

In order to estimate the actions on the structure the base shear is distributed over the height of the building, typically according to the shape of the fundamental mode.

It is accepted that damage can be related to material strains, and that material strains can be related to maximum response displacements, but not to response accelerations. It would thus seem important for design procedures to emphasize the importance of estimating peak displacement response. In fact, the situation pertaining ten years ago was characterized by uncertainty in the estimation of deformations of inelastic systems. The normal approach involves modification of the displacements of the corresponding elastic system of equal initial stiffness and unlimited strength. The most common assumption was the equal displacement approximation, which states that the displacement of the inelastic

systems is the same as that of the equivalent system with the same elastic stiffness, and unlimited strength. The equal displacement approximation is known to be non-conservative for short-period structures. As a consequence, some design codes apply the equal energy approximation when determining peak displacements.

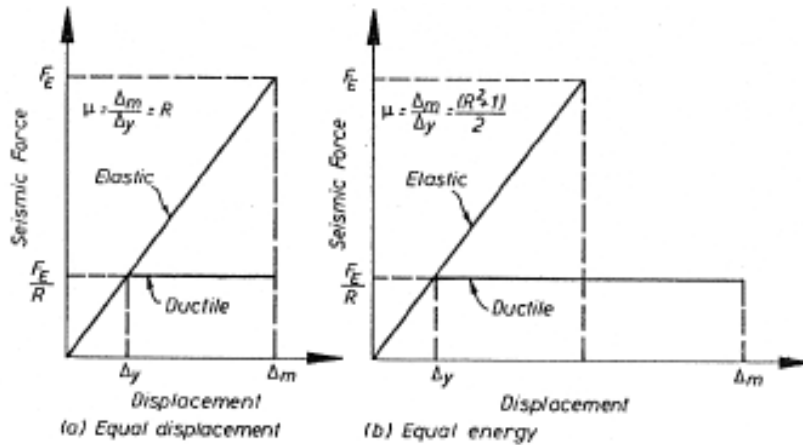


Figure 3.2 - Relationship between ductility and force reduction factor (adapted from Pauley *et al.*, 1992)

It would appear that it should be a comparatively simple matter to determine, on the basis of inelastic time-history analysis, which rule is correct. Unfortunately, it was found that all are correct at some part of the period range of structural response, and all are wrong at other periods. This is pointed out in the Figure 3.3.

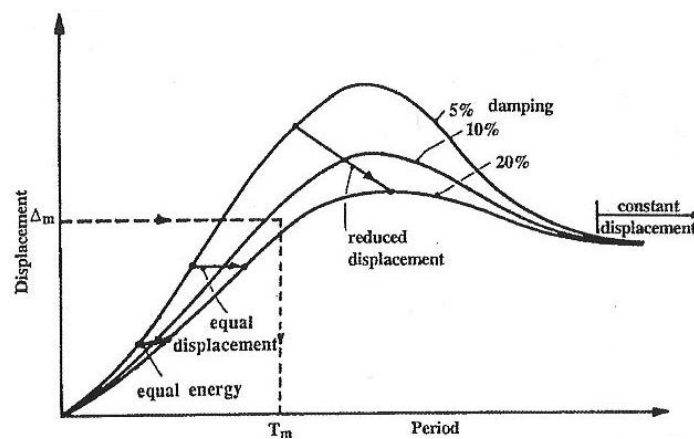


Figure 3.3 - Displacement spectra for different levels of damping (adapted from Priestley, 2003)

Based on the above principles, ( $q$ ) or ( $R$ ), is a force reduction factor used to reduce the linear elastic response spectra to the inelastic response spectra. In other words, it is the ratio of the strength required to maintain the structure elastic to the inelastic design strength of the structure expected to observe a pre-defined displacement ductility demand. The behaviour factor, therefore, accounts for the inherent ductility and overstrength of a structure and the difference in the level of stresses considered in its design.

In Figure 3.4 is represented a typical lateral response curve of a ductile structure.  $V_{el}$  represents the base shear if the structure were to respond elastically,  $V_y$  represents the maximum base shear of the ductile structure and, finally,  $V_{1y}$  represents the base shear at the formation of the first plastic hinge. The horizontal axis refers to the displacements for the corresponding loading level referred previously.

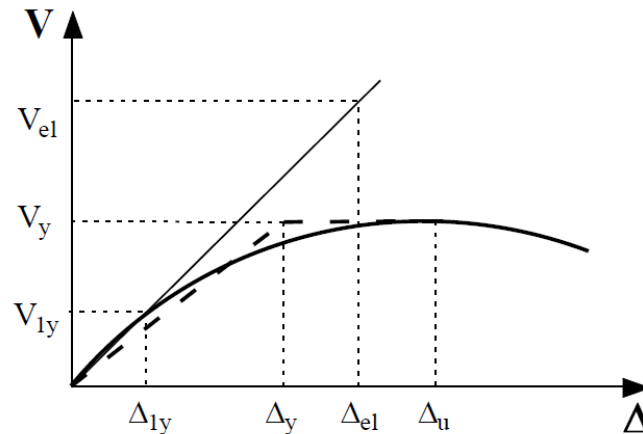


Figure 3.4 - Concept of behaviour factor

Based on the figure, the behaviour factor ( $q$  or  $R$ ) can be defined as:

$$q = \frac{V_{el}}{V_y} \times \frac{V_y}{V_{1y}} = \frac{V_{el}}{V_{1y}} \quad (3)$$

Di Sarno and Manfredi (2009) found values for the behaviour factor for BRBs between 4.5 and 6.5, that are in agreement with those estimated for steel framed structures [Di Sarno *et al.*, 2009].

In 2003, Maheri and Akbari investigated the variation of behaviour factor ( $R$ ) by doing numerical tests on RC buildings with 4-, 8- and 12-storeys and in each one of these, they changed the bracing layout in a way such that the braces could carry 0%, 50% and 100% of the total base shear. The tests were conducted for X braces and Knee braces. In Figure 3.5 it can be seen that the number of storey appear to be the predominant variable affecting the  $R$  factor in comparison with the type of bracing system and the share of bracing from the applied load.

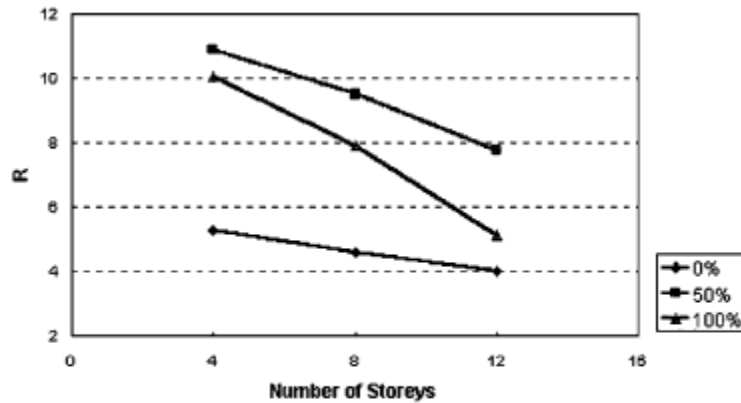


Figure 3.5 - Effect of number of storeys on the R value of X-braced frames (adapted from Maheri *et al.*, 2003)

However, the Figure 3.6 indicates that the bracing system adopted plays an important role. This factor is somehow expected since the characteristics of the braces, namely the strength capacity in tension and in compression, will govern both the yielding and ultimate capacity of the existing structure, and this way, the level of ductility capacity.

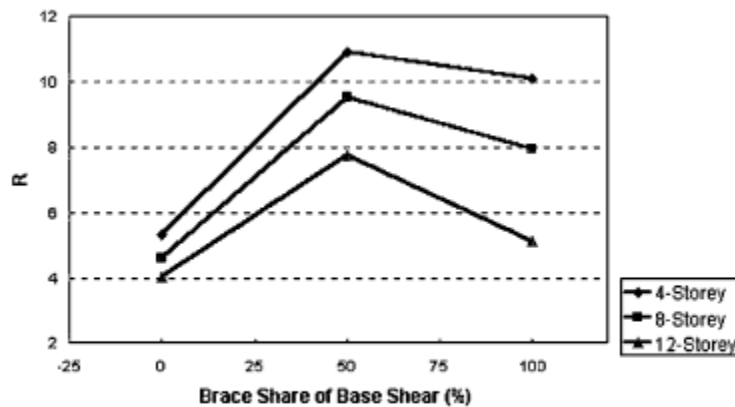


Figure 3.6 - Effect of brace share of base shear on R value of X-braced frames (adapted from Maheri *et al.*, 2003)

Tentative R values for steel-braced RC frames with intermediate ductility are presented in Table 3.1.

Table 3.1 - Tentative values of R factor for steel-braced, RC frame dual systems

Ductility demand	$\mu = 2$	$\mu = 3$	$\mu = 4$	$\mu = 5$
R	5.0	7.0	9.0	12.0

A relationship between the R factor determined and the shear strength contribution for the columns to resist lateral seismic loads was observed. The greater the shear strength contribution of the RC columns, the less the overstrength developed. Such an effect is



more notorious in low-rise buildings than in medium-rise buildings. In general, differences were observed between the assessed values and the proposed values, especially for models where columns resist less than 50% of the seismic shear force and nominal strength was considered. Godinez-Dominguez *et al.* (2010) concluded that these differences were greater for low-rise models than for medium-rise systems.

As a building becomes taller, an increase in the number of braces is required. This way, the axial load transmitted to the columns increase significantly. However, for the same building, the base shear does not change since the brace contribution is defined only by the braces at the first floor. So, in general, as the building becomes taller, a reduction in the R factor is expected.

Queirós *et al.* (2009) also investigated the evolution of  $q$ . They conducted numerical analysis in 1-storey and 3-storey frames with three different bracing systems. The braces were selected according to its non-dimensional slenderness ( $\bar{\lambda}$ ) as defined in EC3 [CEN, 2003]

Table 3.2 -  $q$  values obtained for different RC frames and steel braces [Queirós *et al.*, (2009)]

	$\bar{\lambda}$		
	2.5	2	1.5
1 storey	1.4	1.6	0.7
3 storey	3	2.7	1.5

The analyses confirmed that, in general, as the strength of the steel bracing system increased, the behaviour factor decreased. There was an exception however in the 1-storey frame. A possible reason for that may have been a particular case where the lateral deformation capacity of the RC columns was increased for an axial load similar to that induced by the brace. Another important observation made by the authors was that the values of  $q$ , almost doubled from the 1-storey frame to the 3-storey frame.

The most interesting value found in the study by Queirós *et al.* (2009) was the behaviour factor of 0.7 for the 1-storey frame retrofitted with the stronger braces. That value indicated that the ultimate capacity of the structure was higher than the elastic seismic demand and that the structure was expected to respond elastically to the design earthquake.

Due to strong changes in the global structural behaviour, the improvement of the seismic behaviour may not be, for certain types of braces, proportional to the increase of lateral strength of the structure. For this reason, the seismic design of this type of structures should be done in a perspective of deformation control and not in a methodology based on the utilization of behaviour factors.

### 3.3. DISPLACEMENT-BASED DESIGN

Deficiencies inherent to force-based seismic design, some of which have been outlined in the previous section, have been recognized for some time [Priestley *et al.*, 2007]. Based on those limitations, it has been recognised by the scientific community that seismic design should be based on deformation control, rather than based on strength control.

It would seem obvious that structural characteristics that represent performance at maximum response might be better predictors of performance at maximum response than the initial values of stiffness and damping.

It must be pointed out that the elastic cracked-section stiffness of concrete is a function of the axial load ratio and for columns or frame structure can vary by as much as +/- 50% or more during seismic response. As a consequence, according to Priestley (2003), modal analysis based on specified and constant stiffness is unable to provide accurate estimates of seismic forces, even within the elastic range of response. Calculated elastic periods are likely to be in error, and more importantly, the distribution of forces through the structure, which depends on relative stiffness of members, can be grossly in error.

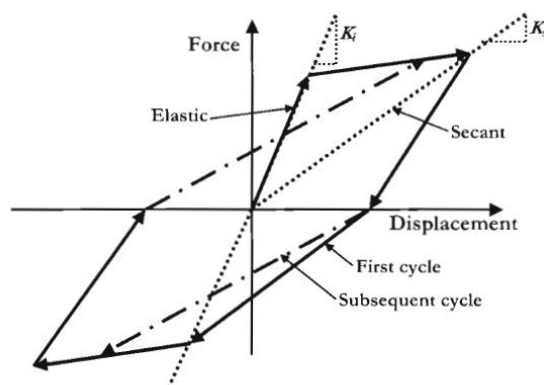


Figure 3.7 - Initial and secant stiffness characterization of hysteretic response (adapted from Priestley *et al.*, 2007)

Earthquakes induce forces and displacements in structures. For elastic systems these are directly related by system stiffness, but for structures responding inelastically, the relationship is complex, being dependent on both the current displacement, and in the history of displacements during seismic response.

The assumption that the elastic characterization of the structure is the best indicator of inelastic performance, as implied by force-based design is in itself clearly of doubtful validity. With RC structures, the initial elastic stiffness will never be valid after yield occurs, since stiffness degrades due to crushing of concrete, Bauschinger softening of reinforcing steel and damage on crack surfaces.

In recent years, researchers developed expressions to substitute real multi-storey buildings to a single degree of freedom based on the approximation that the first mode of vibration is dominant. Based on this observation, Priestley *et al.* (2007) proposed a direct displacement-based design (DDBD) procedure which aimed at an explicit definition of the base shear strength required to achieve a selected seismic performance objective.

The main steps involved in the direct displacement-based design procedure are represented in Figure 3.8.

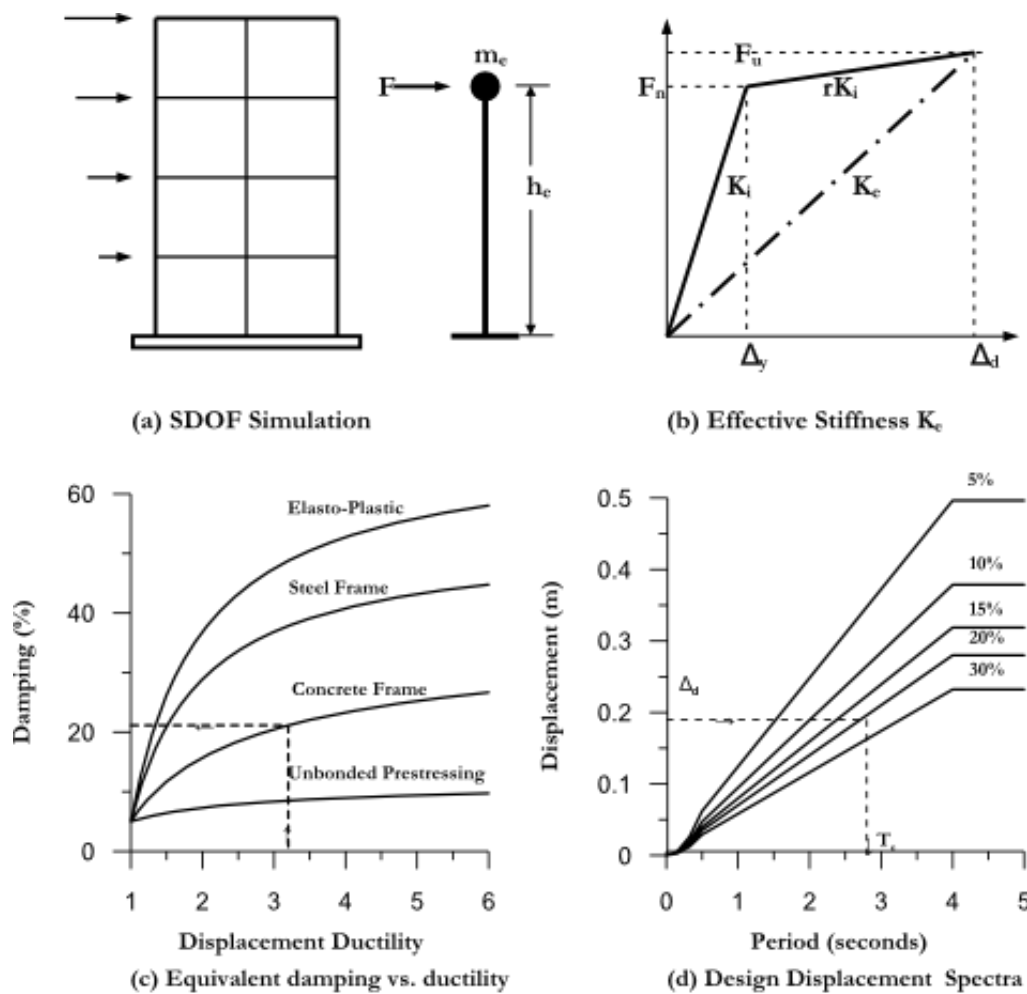


Figure 3.8 - Fundamentals of direct displacement-based design

In this design procedure, some parameters related to the structure need to be quantified. Firstly, it is necessary to substitute the multi-degree-of-freedom (MDOF) structure to an equivalent single-degree-of-freedom (SDOF) structure. In this process it is necessary to know the mass ( $m_i$ ) and the lateral displacement ( $\Delta_i$ ) of the structure at each DOF. As a consequence, the definition of the inelastic displacement profile is required. These parameters enable the calculation of the equivalent SDOF system design displacement ( $\Delta_d$ ) and equivalent mass ( $m_e$ ):

$$\Delta_d = \frac{\sum_{i=1}^n (m_i \times \Delta_i^2)}{\sum_{i=1}^n (m_i \times \Delta_i)} \quad (4)$$

$$m_e = \frac{\sum_{i=1}^n (m_i \times \Delta_i)}{\Delta_d} \quad (5)$$

In order to calculate the displacement ductility ( $\mu$ ), it is necessary to calculate the displacement of the SDOF when first significant yielding occurs ( $\Delta_y$ ). The Equation (4) can also be applied, but this time the displacement characterization should be that corresponding to first yielding.

By knowing the design displacement and the yielding displacement, the displacement ductility is then calculated:

$$\mu = \frac{\Delta_d}{\Delta_y} \quad (6)$$

In order to estimate the equivalent viscous damping (EVD) from the ductility of the system at the maximum response, Priestley *et al.* (2007) proposed expressions representing the combined effects of elastic and hysteretic energy dissipation within the system.

At this stage, by introducing the design displacement in the inelastic design displacement spectra, the period of the structure is identified and consequently the effective stiffness ( $K_e$ ) of the equivalent SDOF at maximum displacement.

$$K_e = \frac{4 \times \pi^2 \times m_e}{T_e^2} \quad (7)$$

Where  $K_e$  is the effective stiffness and  $m_e$  is the effective mass,  $T_e$  is the effective period. The design lateral force, which is also the design base shear force is thus:

$$V_{base} = K_e \times \Delta_d \quad (8)$$

Where  $V_{base}$  is the design base shear and  $\Delta_d$  is the equivalent SDOF system design displacement.

The base shear is then distributed over the high of the structure as lateral inertia forces, and the structure is analyzed under these forces to determine the design moments at locations of potential plastic hinges [Priestley *et al.* 2007].

### 3.4. SEISMIC ASSESSMENT

One of the most widespread procedures for the assessment of building behaviour due to the action of earthquakes is the Capacity Spectrum Method (CSM). The CSM was firstly introduced in the 1970s as a rapid evaluation procedure in a pilot project for assessing seismic vulnerability of buildings at the Puget Sound Naval Shipyard (Freeman *et al.*, 1975).

The CSM is a nonlinear static analysis method, which compares the global force-displacement capacity curve of a structure (pushover) with an earthquake response spectrum in a graphical shape (Freeman, 1998). For this, both the capacity curve and the response spectra have to be converted into a spectral acceleration  $S_a$  vs spectral displacement  $S_d$  graph. Due to this transformation, the structure is reduced to an equivalent SDOF-structure, responding in its fundamental mode. In this way, supply (pushover curve) can be directly compared to the seismic demand (capacity spectra).

In the scope of this procedure the capacity curve, which describes the ability of a building to resist an earthquake, will be superimposed with a response spectra, which represents the demand of an earthquake. Considering the ductility of the building, an intersection point can be determined and the response of the building, in terms of spectral displacement, can be evaluated.

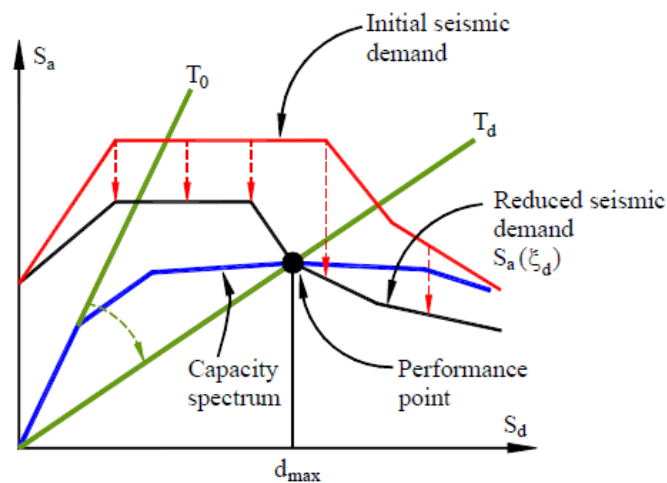


Figure 3.9 - Capacity spectrum method (adapted from ATC-40 by Varum (2003))

By determining the performance point, where this capacity spectrum “breaks through” the earthquake demand, engineers can develop an estimate of the spectral acceleration, displacement, and damage that may occur for specific structure responding to a given earthquake.

The Figure 3.10 shows how the addition of brace systems can improve the behaviour of a structure. In this case the original structure has a performance point close to the ultimate

capacity. In a more severe case, the capacity curve may not intersect the reduced demand spectra. For those cases, the structure will not withstand the earthquake demand.

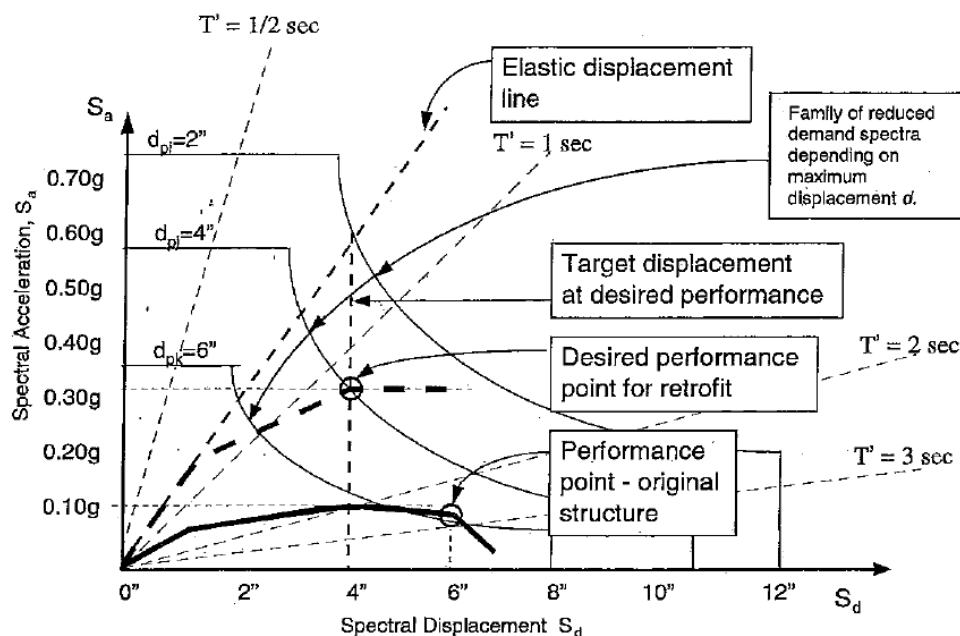


Figure 3.10 - Preliminary calculation for retrofit using strengthening and stiffening

By strengthening and stiffening the structure it is possible to shift the performance point to a desirable limit state. Once again, this point is defined by the intersection of the capacity curve with the corresponding inelastic spectra which is reduced from the elastic spectra to take into consideration the corresponding ductility imposed to the structure.

### 3.5. REHABILITATION APPROACHES

Two general approaches are usually considered for seismic retrofitting. The first approach, which is illustrated in Figure 3.11, involves global modification of the structural system. In this approach, the modifications to the structural system are designed so that the seismic demands, often denoted by a target displacement, on the existing structural and non-structural components are lower than the capacity available.

As a logical extension, a strengthening intervention is easier to design if it is considered as a means to reduce the global seismic displacement demands on the existing members to levels below the corresponding deformation capacities. In other words, the detailing of old members does not need to be upgraded to the level required by modern standards for new members on ductility grounds, provided that the demands imposed on them are not beyond their ultimate deformation capacity and do not impair their resistance against gravity loads [Fardis, 1998].

Common approaches include addition of structural walls, steel braces, or base isolators (Figure 3.11). Passive energy dissipation schemes are not common for reinforced concrete frames because the displacements required for them to be effective often are beyond the displacement capacities of the existing components. Active control is rarely used.

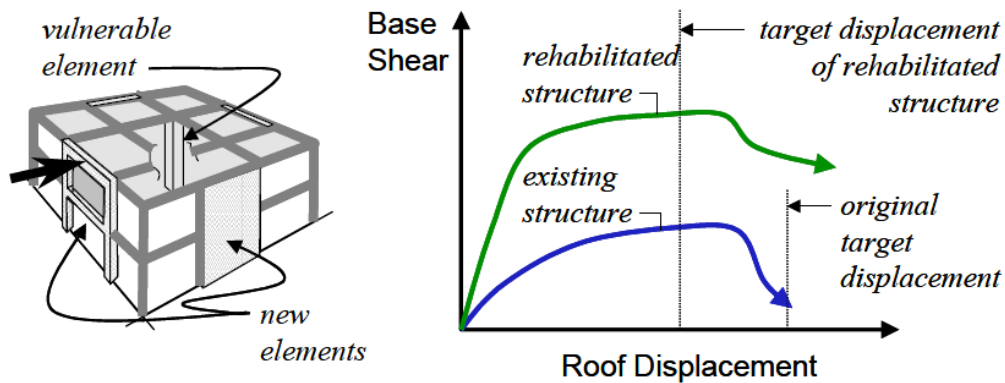


Figure 3.11 - Global modification of the structural system (adapted from Moehle, 2000)

The same retrofitting approach, which is illustrated in Figure 3.12, involves local modification of isolated components of the structural and nonstructural system. In this approach, the objective is to increase the deformation capacity of the weak components so that they will not reach their specified limit state as the building responds at the design level. Common approaches include addition of concrete, steel, or fibre reinforced polymer composite (FRPC) jackets [Moehle, 2000].

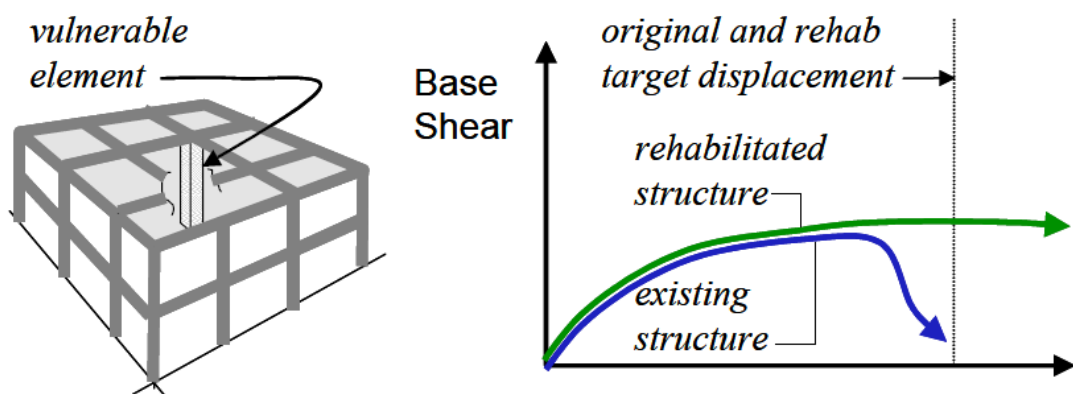


Figure 3.12 - Local modification of structural components (adapted from Moehle, 2000)

It must be pointed out that, in principle the local modification of structural elements will improve the behaviour of the structural elements, on the other hand, when global intervention is adopted this is not always true. In fact, steel braces, besides increasing the

lateral strength of the building, will transfer higher levels of axial loads (compression and tension) toward the columns. This change in the axial loads will affect the behaviour of the columns and consequently the behaviour of the structure during a seismic event. Further discussion on this topic will be presented in subsequent chapters.

### **3.6. CONCLUDING REMARKS**

In this chapter the currently available seismic design procedures were reviewed. The main assumptions and limitations associated with force-based design were presented and discussed. The studies that focused on the characterization of behaviour factor for steel braced RC frames were reviewed. The main conclusions from those studies revealed that the behaviour of hybrid structures is very sensitive to the strength of the applied braces, and hence that the use of a force-based design methodology appears to be inadequate. In effect, the wide range of behaviour factors obtained by different researchers indicates that the application of a FBD procedure is not recommended.

Due to the limitations associated with force-based design, and taking into account the behavioural characteristics of steel braced RC frames which will be discussed in the next chapter, it is clear that there are several advantages of adopting a displacement-based approach for the design of these structural systems.



## 4. BEHAVIOUR OF STEEL BRACED RC SYSTEMS

*“Analysis should be as simple as possible, but no simpler.”*

Albert Einstein (1879 - 1955)

### 4.1. INTRODUCTION

This chapter focus on the behaviour of hybrid steel-RC structures and discusses the interaction between the independent systems. In the last section, a numerical study aimed at the characterisation of the lateral deformation of steel braced RC frames is presented. The study provides a useful insight into the behaviour of steel-RC hybrid systems as well as important data to support the development of the displacement-based design procedure proposed in Chapter 5.

### 4.2. BEHAVIOUR OF STEEL BRACES

Steel braces can be employed with different layouts. The most common types of braced systems comprise the concentric and eccentric braced frames. In this work only the concentric X-braced systems with unrestrained braces will be considered.

Figure 4.1 illustrates the cyclic behaviour of an unrestrained brace. Under tension the brace reaches its yield capacity ( $P_y$ ). However, due to its slenderness, the brace buckles when subjected to compression. This is reflected in a lower capacity in compression ( $P_u < P_y$ ).

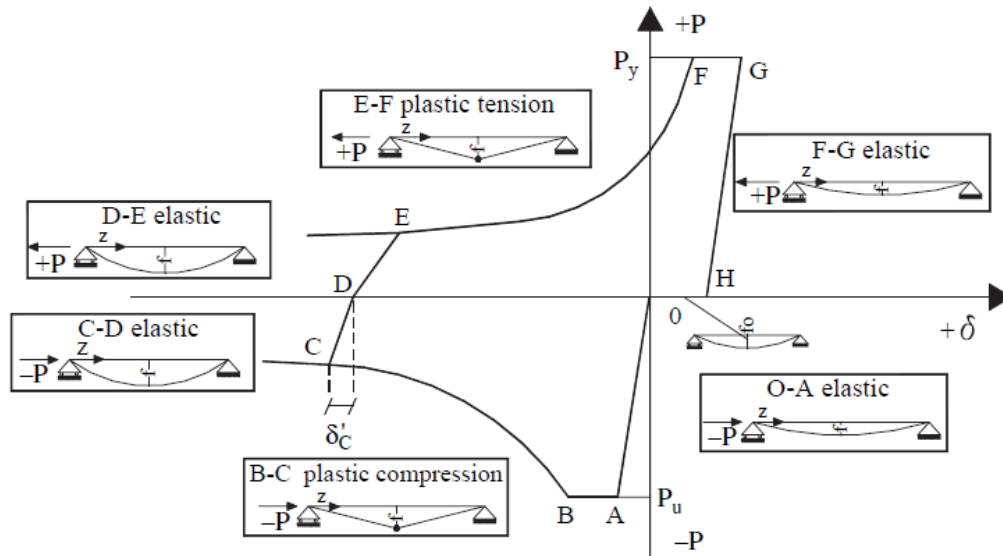


Figure 4.1 - Behaviour of steel braces (adapted from Longo *et al*, 2008)

Focusing on Figure 4.1, and assuming that the brace is initially subjected to compression, its elastic behaviour can be defined by means of a linear branch [OA] where point A corresponds to the attainment of the buckling load ( $P_u$ ). In the most stressed cross-section (at the mid-span) a plastic hinge occurs. The complete development of this plastic hinge is represented by the plateau [AB] leading (point B) to the formation of a kinematic mechanism whose equilibrium curve [BC] represents the brace post-buckling behaviour. The following branch [CD] corresponds to the elastic unloading. When the brace is completely unloaded, a residual plastic axial deformation can be observed which is related to the residual mid-span deflection. The following branches correspond to the straightening process of the brace member in tension. In the [DE] branch of the straightening process, the brace behaviour is elastic up to point E which corresponds again to the development of a kinematic mechanism due to the yielding of the mid-span cross-section subjected to tension combined with bending. Following the mechanism curve [EF], the brace becomes more and more straightened, so that the mid-span bending moment reduces and a new yielding condition is attained in pure tension (point F) when the brace is completely straightened [Longo *et al.*, 2008].

Analytically, the theoretical ultimate capacities of the brace in tension and compression according to Eurocode 3 [CEN, 2003] are given by:

- Tension 
$$N_{pl,Rd} = \frac{A \times f_y}{\gamma_{M0}} \quad (9)$$

- Compression 
$$N_{b,Rd} = \frac{\chi \times A \times f_y}{\gamma_{M1}} \quad (10)$$

Where  $\chi$  is the buckling coefficient that depends on the slenderness of the member and on the buckling curve defined in the code.

### 4.3. BEHAVIOUR OF RC MEMBERS

It is well known that axial load plays an important role in RC members subjected to flexure. For a given cross section, the calculated values of axial load ( $N$ ) and the moment ( $M$ ), for a particular combination of strains on the top and bottom faces of the section, could be plotted as a point on a diagram such that shown in the Figure 4.2.

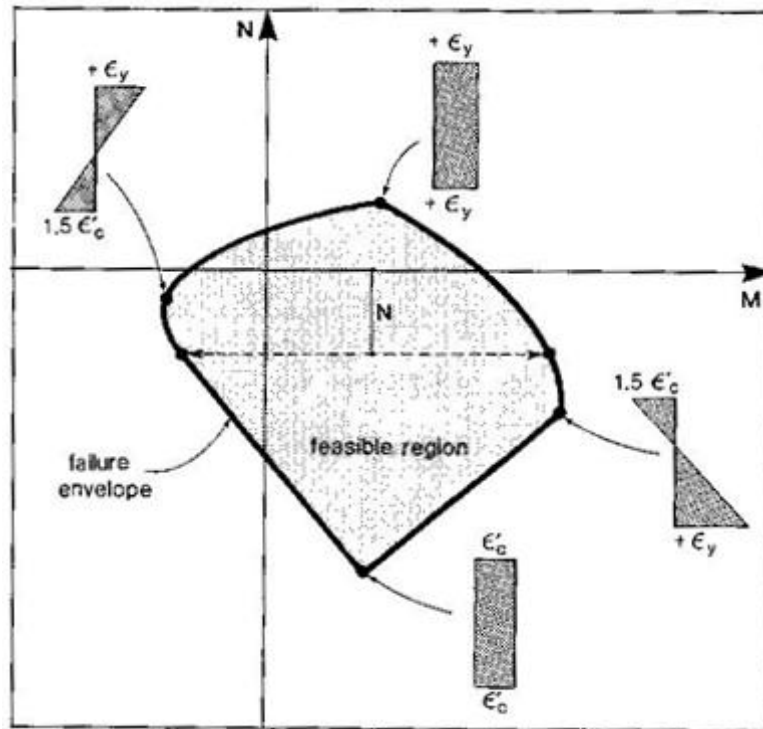


Figure 4.2 - Axial load-moment interaction diagram (adapted from Collins *et al.*, 1997)

Repeating the calculations for many different values of strains, would then define the "feasible region" of possible combinations of  $N$  and  $M$ . The boundary of this region can be called "failure envelope" or the "interaction curve". Values of  $N$  and  $M$ , which lie outside the failure envelope, cannot be resisted by the cross section being considered. That is, such loads will cause the failure of the section [Collins *et al.*, 1997].

Some interesting conclusions can be extracted from Figure 4.3 in which the influence of the level of axial load on the moment-curvature relationship of a RC cross-section is plotted. The maximum flexural capacity occurs when some compression load is present. Another important observation is that for high levels of compressive loads or in tension, the flexural capacity decreases substantially.

In addition to determine the range of axial loads and moments that can be resisted by a given section, sometimes it is need to find out the load-deformation response of members subjected to axial load and moment. Thus we may wish to determine how the moment-curvature response of a section changes as the axial load changes [Collins *et al.*, 1997].

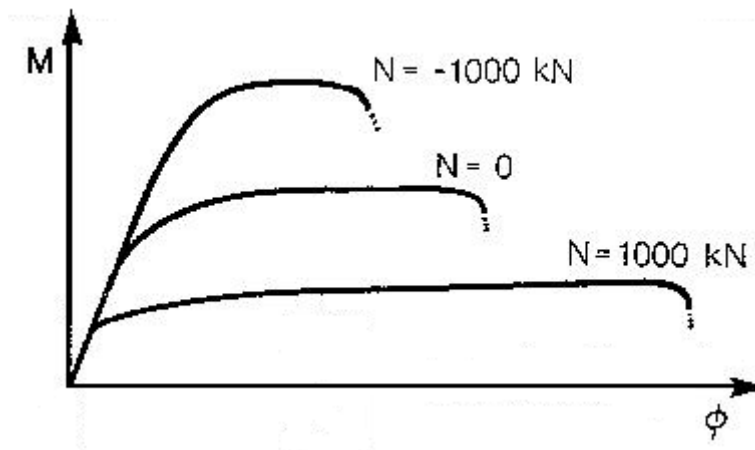


Figure 4.3 - Influence of axial load on moment-curvature response (Adapted from Collins *et al.*, 1997)

It can clearly be seen that the axial load increases in the column, the moment capacity also increases. On the opposite side, the increased axial load reduces the curvature capacity, and consequently the deformation capacity of the RC column.

On the other hand, as the axial load goes from high compression to high tension, the shear capacity decreases almost linearly:

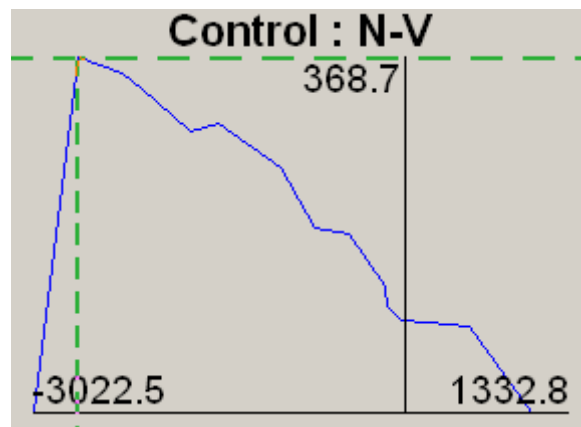


Figure 4.4 - Example of an axial load-shear interaction diagram (Adapted from [RESPONSE-2000])

#### 4.4. INTERACTION BETWEEN BRACES AND RC FRAME

To study hybrid systems, and in particular RC braced systems, it is essential to understand of each of the two systems and also the interaction between them. Figure 4.5 illustrates the force path and the displacements experienced by a two-storey hybrid structure under lateral loading.

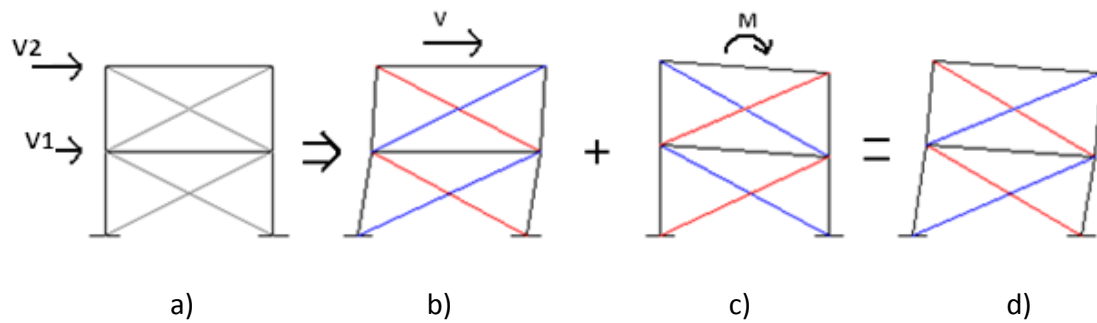


Figure 4.5 - Deformation of hybrid system

In the simple 1-bay, 2-storey building represented before, the first figure represents the initial RC steel braced frame. By imposing a lateral force it is easy to understand that the braces represented in blue will be in tension. On the other hand, the braces represented in red suffer shortening and consequently are in compression. The third figure illustrates the rotation of the frame due to overturning moments. The columns on the right observe compression and the columns on the left experience tension. The forces on the braces in Figure 4.5 b) are opposite signal from those developing under overturning. Since the level of forces due to lateral deformation is higher than due to overturning, the sign of the forces in the braces at the final stage can be defined by those in stage b).

Taking into account the previous figure, it is now easy to draw the force paths in the frame:

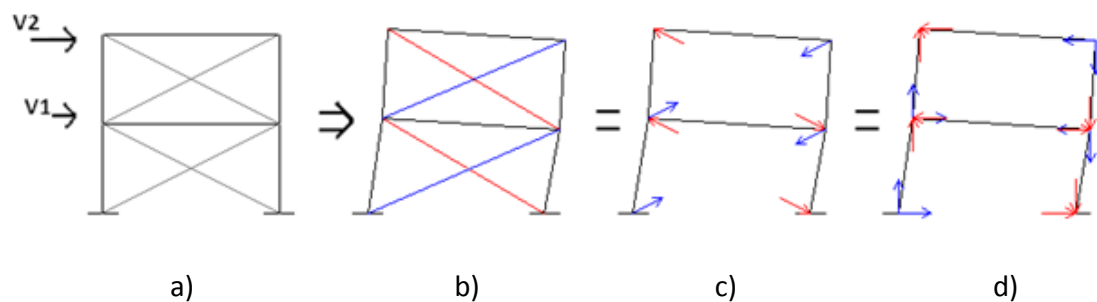


Figure 4.6 - Forces path of hybrid system

Queirós *et al.* (2009) analyzed the individual and global behaviour of steel braced RC frames. In Figure 4.7 two main conclusions can be observed:

1. The increment of base shear given by the steel braces in the RC hybrid frame is given by the summation of the horizontal components from the forces installed in the two braces of the first storey.

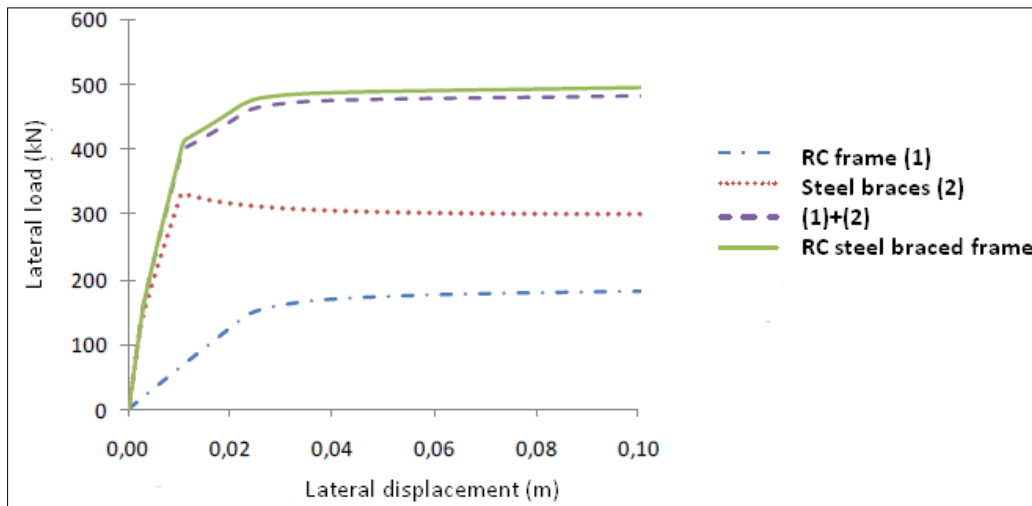


Figure 4.7 - Independent systems contributing for global base shear (adapted from Queirós *et al.*, 2009)

It can be verified that an individual summation of the lateral load capacity from both initial RC frame and steel bracing system produces a good approximation to the values obtained when both systems are tested together as a hybrid system.

2. The vertical components of all braces have the same signed for each side of the braced frame. This means that the column on the right suffer an increment in compression equal to the vertical components of the forces present in the braces. On the other hand, the column on the left will experience, now in tension, the same force due to vertical component of the braces.

Figure 4.8 indicates the variation on axial load in one RC column during a pushover analysis of a bare and braced frame. The line in blue is the variation on axial load of the bare frame. The line in green stands for the vertical component of the braces forces connected to the same column. And finally the red line represents the values of the axial loads in the column of the braced frame. The small difference between the purple and the red line are the demonstration of the assumption made in point 2.

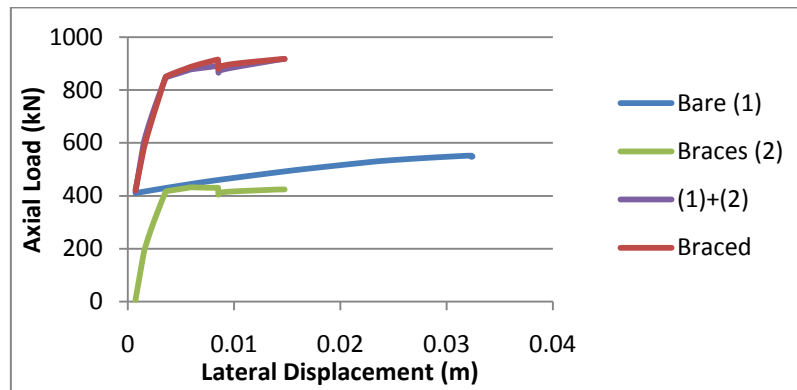


Figure 4.8 - Variation in axial load in the compressed RC column

The examples showed before help to understand that the hybrid system can be considered as two independent systems (steel braces and RC frame) associated in parallel. That means that the stiffness and strength of the hybrid system can be estimated by the addition of the two individual systems.

After identify the properties and investigate the behaviour of both initial RC elements and steel braces, we are now in position to investigate the performance and identify important limits when both systems are coupled together.

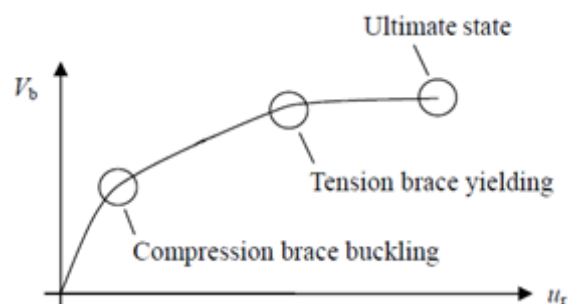


Figure 4.9 - Schematic response of braced structure (adapted from Della Corte *et al.*, 2008)

As expected, due to the high slenderness of the braces compared with the RC elements, the first yielding occurs in the brace in compression. In fact buckling occurs in the initial phase of lateral excitation. It can be seen that the tension brace yield before the RC column.

Regarding the ultimate state, Queirós *et al.* (2009) concluded that despite the significant increase in terms of lateral capacity of the hybrid structure when the brace strength is increased, it was observed that the deformation capacity of the RC columns decreased significantly when “stronger” braces were considered. That was due to the high levels of axial load induced by the braces on the RC columns.

From this analysis, two main ideas should be preserved:

1. Except in the cases where very stiff braces and very weak column are present, it is expected that the first significant yield occurs when the brace in compression buckles. Moreover, the lateral displacement corresponding to the global yield of the frame can be reasonably well predicted by relating it to the lateral displacement of the steel brace under tension.
2. The ultimate displacement of the structure is governed by the RC column capacity. Therefore, it is of critical importance to relate the deformation capacity of the RC columns with the level of axial load.

## **4.5. LATERAL DISPLACEMENT PROFILES**

As described in Section 3.3 the first stage of the DDBD process consists of the conversion of the MDOF structure into an equivalent SDOF structure. The conversion is carried out based in an initial estimation of the lateral deformation mode of the structure.

From previous analytical studies on hybrid RC-steel structures, namely by Pincheira and Jirsa (1995), it was possible to verify that the displacement shapes of the structures were very stable and that the drifts varied smoothly over the height of the buildings.

In the following sections a parametric study will be conducted in order to derive lateral displacement profiles to adapt in DDBD of hybrid structures.

### **4.5.1. Geometrical and Material Properties**

The displacement profiles of a 1-bay, 3-storey RC frame using two different steel braces is evaluated. It must be pointed out that the decision to consider a frame with just one bay was taken because the process of deriving lateral displacement profiles was extremely time consuming. Moreover, the existing expressions for RC structures (e.g. Priestley (2007)) are only dependent on the number of floors, indicating that the numbers of bays are unrelated with the deformation shape.

To better adapt this study to a real situation, the RC frame presented in Figure 4.10 was designed only for gravity loads only based on Eurocode 1 (EC1) and Eurocode 2 (EC2). To take into account the self weight of the structure other than that of the beams and columns a value of  $9\text{kN/m}^2$  was used. The imposed load was taken equal to  $5\text{kN/m}^2$ . The elements were designed adopting strength classes of S500 and C25/30 for steel reinforcement and concrete, respectively. The inertial effects of the design seismic action shall be evaluated by taking into account the presence of the masses associated with all gravity loads appearing in the following combination of actions:



$$\sum G_{k,j} + \sum \psi_{E,i} \times Q_{k,i} \quad (11)$$

Where,  $\psi_{E,i}$  is the combination coefficient for variable action i as defined in Eurocode 0.

The RC frame and cross sections adopted are presented in Figure 4.10:

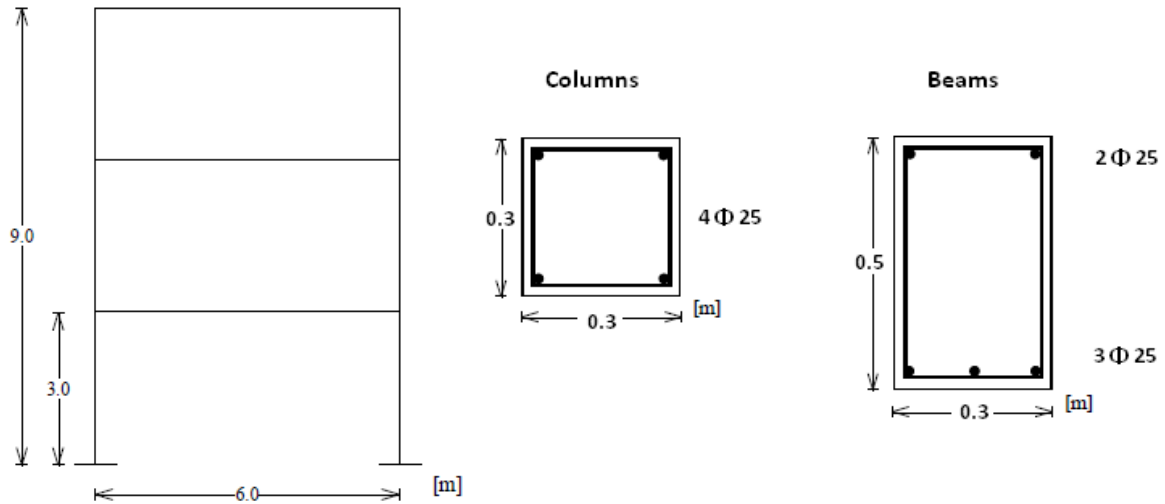


Figure 4.10 - layout of RC frame and elements details

The braces used in the analysis were hot finished circular hollow sections made of steel S275 with the following properties:

Table 4.1 - Properties of the braces adopted in the analysis

Slenderness	Outside diameter	Thickness	Mass	Sectional area	Moment of inertia	Radius of gyration	Elastic modulus	Plastic modulus	Torcional constants	Superficial area/m	Approx. Length/tonne	
$\bar{\lambda}$	D (mm)	T (mm)	M (kg/m)	A (cm <sup>2</sup> )	I (cm <sup>4</sup> )	i (cm)	W <sub>el</sub> (cm <sup>3</sup> )	W <sub>pl</sub> (cm <sup>3</sup> )	I <sub>t</sub> (cm <sup>4</sup> )	C <sub>t</sub> (cm <sup>3</sup> )	A <sub>s</sub> (m <sup>2</sup> /m)	(m/t)
3	76.1	3.2	5.75	7.33	48.8	2.58	12.8	17	97.6	25.6	0.239	17.4
2	114.3	3.2	8.77	11.2	172	3.93	30.2	39.5	345	60.4	0.359	114

According to section 6.7.3 from Eurocode 8 – Part 1, in steel frames with concentric braced frames, the non-dimensional slenderness should be limited to:  $1.3 < \bar{\lambda} \leq 2.0$ . However, in structures of up to two storeys, no limitation applies.

$$\bar{\lambda} = \sqrt{\frac{N_{el}}{N_{cr}}} = \sqrt{\frac{A \times f_y}{\pi^2 \times E \times I}} \quad (12)$$

The limit of 1.3 is defined to prevent overloading of the columns in the pre-buckling stage (when both compression and tension diagonals are active). It must be referred that this limit is associated to steel structures and, therefore, is just an indicative value for RC steel

bracing frames. In the structure considered in the study, one of the braces has a non-dimensional slenderness of 3. This is justified by the extremely high axial capacity of braces with lower slenderness. For small structures, in particular buildings that do not have been designed to account for the incremental axial load in the RC columns induced by the steel braces, the use of low non-dimensional slenderness braces may lead to extremely high axial loads in the columns which are likely to exceed the available capacity.

#### **4.5.2. Numerical Modelling**

The analysis of the structures was carried out with the Nonlinear Finite Element software OpenSees [PEER, 2006]. This software is being developed in the Pacific Earthquake Engineering (PEER) Center.

In this study, force-based elements with distributed elasticity were used to represent all structural members (beams, columns and braces). The force-based formulation has many advantages compared with the displacement-based formulation such as providing the exact solution, regardless of the material behaviour, even if it is highly non-linear [Calabrese *et al.*, 2010]. According to the recommendations for RC frames, one element per member should be used with at least 6 integration points per element. In the analysis, 8 integration points were used per element, and one element per member for the RC structure.

On the other hand, in the steel elements, 4 elements per member were adopted. This reveals to be important because with fewer elements, the program was not capable to capture the compressive behaviour of the braces after the peak force. A small transverse load was applied in the middle of the member to represent the imperfections. Both columns and brace elements were defined to take into account second-order effects.

The connection between the brace and the concrete elements was represented with the aid of “zero-length” elements, in which the nodes of different elements have the same coordinates. In this way, it was possible to impose a pin end at the end of each brace.

Following the recommendations of Calabrese *et al.*, (2010), the use of force based elements were adopted.

### 4.5.3. Materials

For the steel members the command Steel01 was used. This consists of a uniaxial bilinear material with kinematic hardening (Figure 4.11).

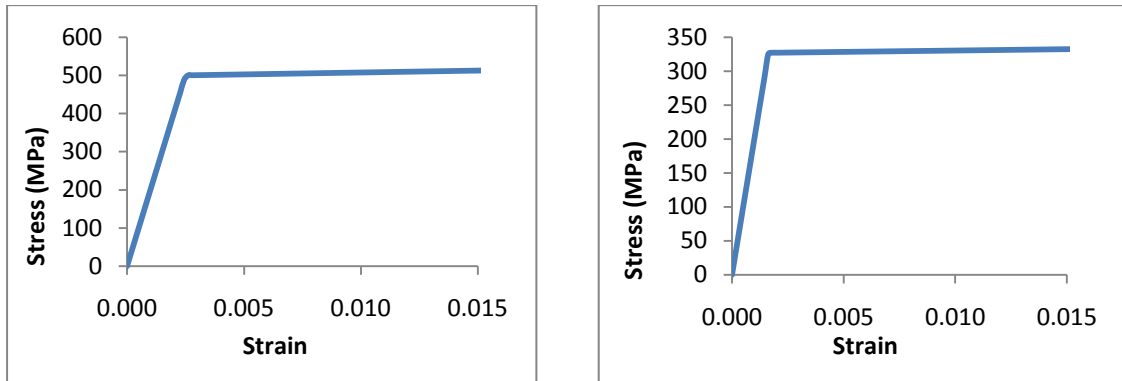


Figure 4.11 - Stress-Strain relationship for reinforcement (left) and steel braces (right)

On the other hand, the concrete was defined with the Concrete01 constitutive model which consists of the uniaxial Kent-Scott-Park concrete model with degraded linear unloading/reloading stiffness according to the work of Karsan-Jirsa (1969) and no tensile strength (Figure 4.12).

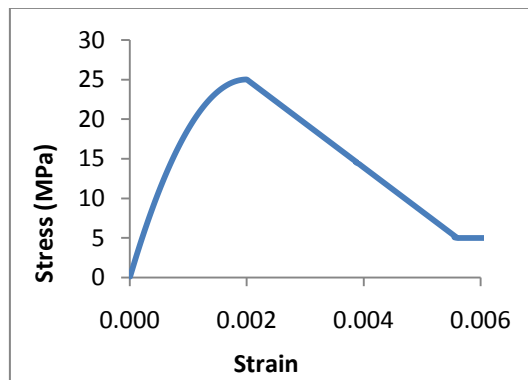


Figure 4.12 - Stress-Strain relationship for poorly confined concrete

It must be pointed out that since the goal was to model an existing structure that was not seismically designed, the concrete was defined with a sharp post peak softening branch, representing in this way a poorly confined concrete.

The concrete stress-strain properties were calculated based on the model proposed by Mander *et al.* (1988) (Figure 4.13)

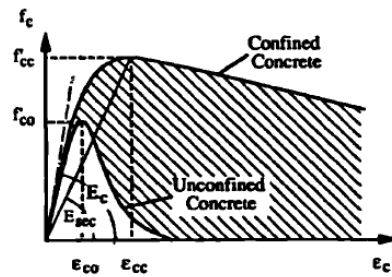


Figure 4.13 - Stress-strain relationship for concrete proposed by Mander *et al.* (1988)

The OpenSees model is illustrated in Figure 4.14.

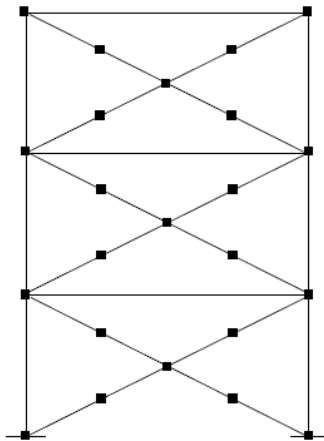


Figure 4.14 - Discretization adopted for the RC braced frame

In order to assess if the assumed discretization was able to reproduce the braces, a preliminary validation was performed by modelling the experimental test performed by the experimental work developed by Black *et al.* (1980). The results from OpenSees are compared with the test results in Figure 4.15.

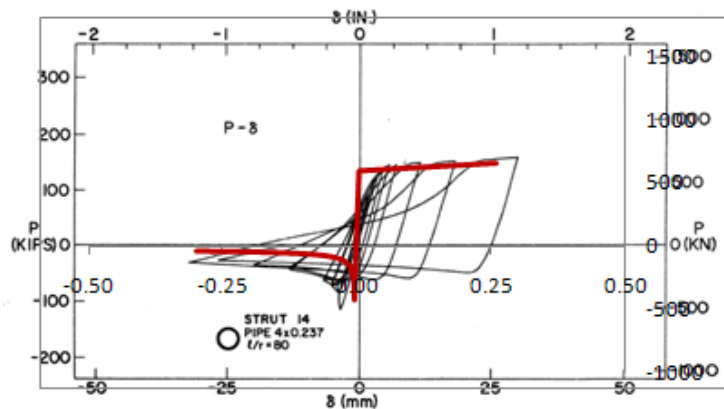


Figure 4.15 - Comparison of experimental and analytical response of steel braces

Despite the difference in terms of initial stiffness (it must be referred that it was not possible to find the modulus of elasticity of the steel used in the experiment; in the analytical work it was used a value of 200GPa), the results provide sufficient confidence to proceed with the analysis of the frames. In fact the peak strength values obtained are in line with the experimental ones.

#### 4.5.4. Record Selection for Time-History Analysis

In the past years numerous studies have been conducted to study the influence of structural properties and ground motion characteristics on the inelastic displacement demands of SDF systems. Considering the fact that the earthquake ground motion comprises various frequency components, it is important to find out a single parameter that represents the frequency content of ground motion.

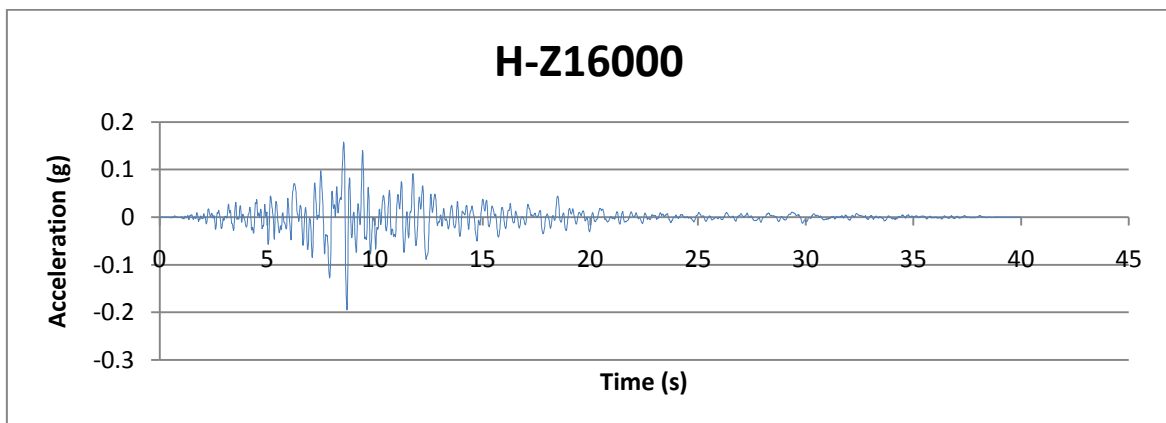
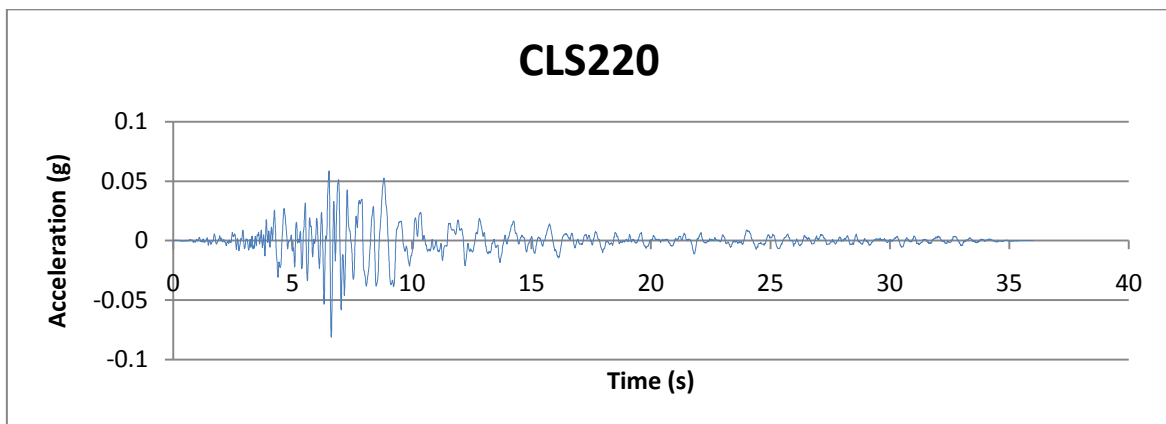
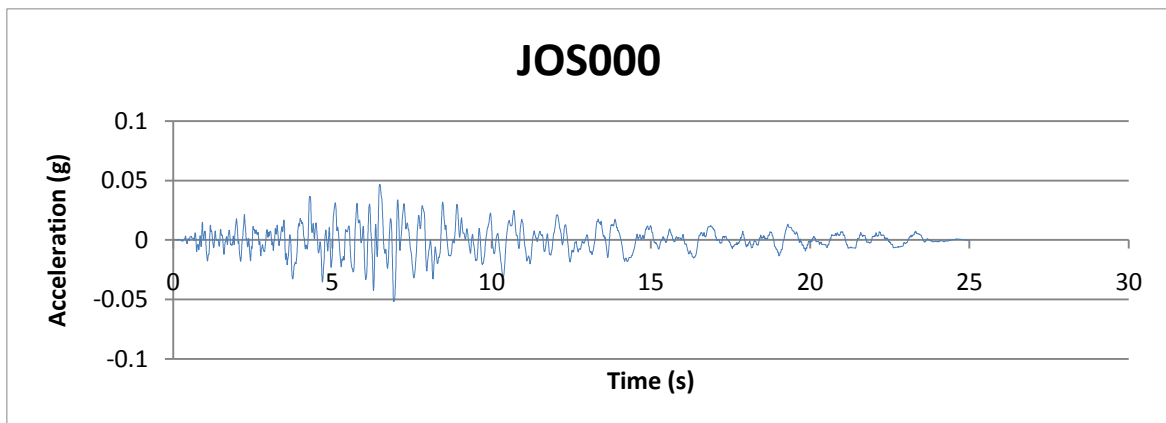
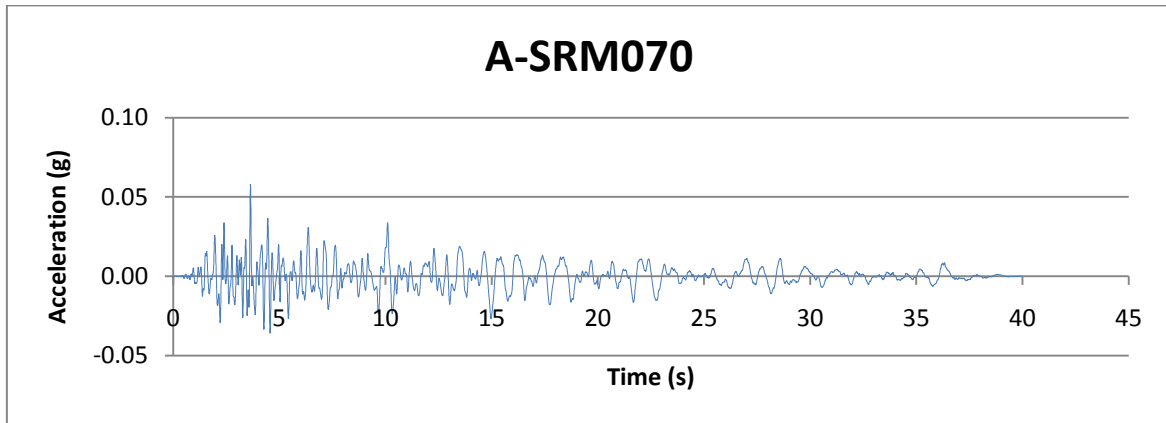
Rathjee *et al.* (2004) concluded that the ground motions can be categorized with respect to the mean period ( $T_m$ ) to achieve better prediction of inelastic demands on structures.  $T_m$  represents the mean of the periods of the Fourier Amplitude Spectrum (FAS) in a specified frequency ranges, where the weights are assigned based on the Fourier amplitudes.

An assessment of the effects of the mean period of ground motion on SDOF and MDOF systems carried out by Kumar *et al.* (2010) showed that the mean period ( $T_m$ ) appears to be an ideal parameter for representing the influence frequency content on structural response since this parameter is related to magnitude, distance and site conditions. A total of eight records were selected from the NGA database to be used in the time-history analysis. For consistency, the ground motions for the analysis have  $T_m$  values between 0.5 and 0.6s, representative of the intermediate group considering the work of Kumar *et al.* (2010).

A Summary of the record properties is provided in Table 4.2. The acceleration time series are depicted in Figure 4.16.

Table 4.2 - Earthquake records used in the analysis

number	Record ID	Earthquake Name	M	R (kM)	Site Class	$T_m$ (s)
1	A-SRM070	Livermore-01 1980-01-24	5.8	20.53	D	0.59
2	JOS000	N. Palm Springs 1986-07-08	6.06	26.88	C	0.55
3	CLS220	Morgan Hill 1984-04-24	6.19	23.24	C	0.53
4	H-Z16000	Coalinga-01 1983-05-02	6.36	27.67	D	0.51
5	H-E13140	Imperial Valley-06 1979-10-15	6.53	21.98	D	0.58
6	H-NIL090	Imperial Valley-06 1979-10-15	6.53	36.92	D	0.55
7	FRE000	Loma Prieta 1989-10-18	6.93	39.51	C	0.53
8	HWB 220	Loma Prieta 1989-10-18	6.93	54.15	C	0.53



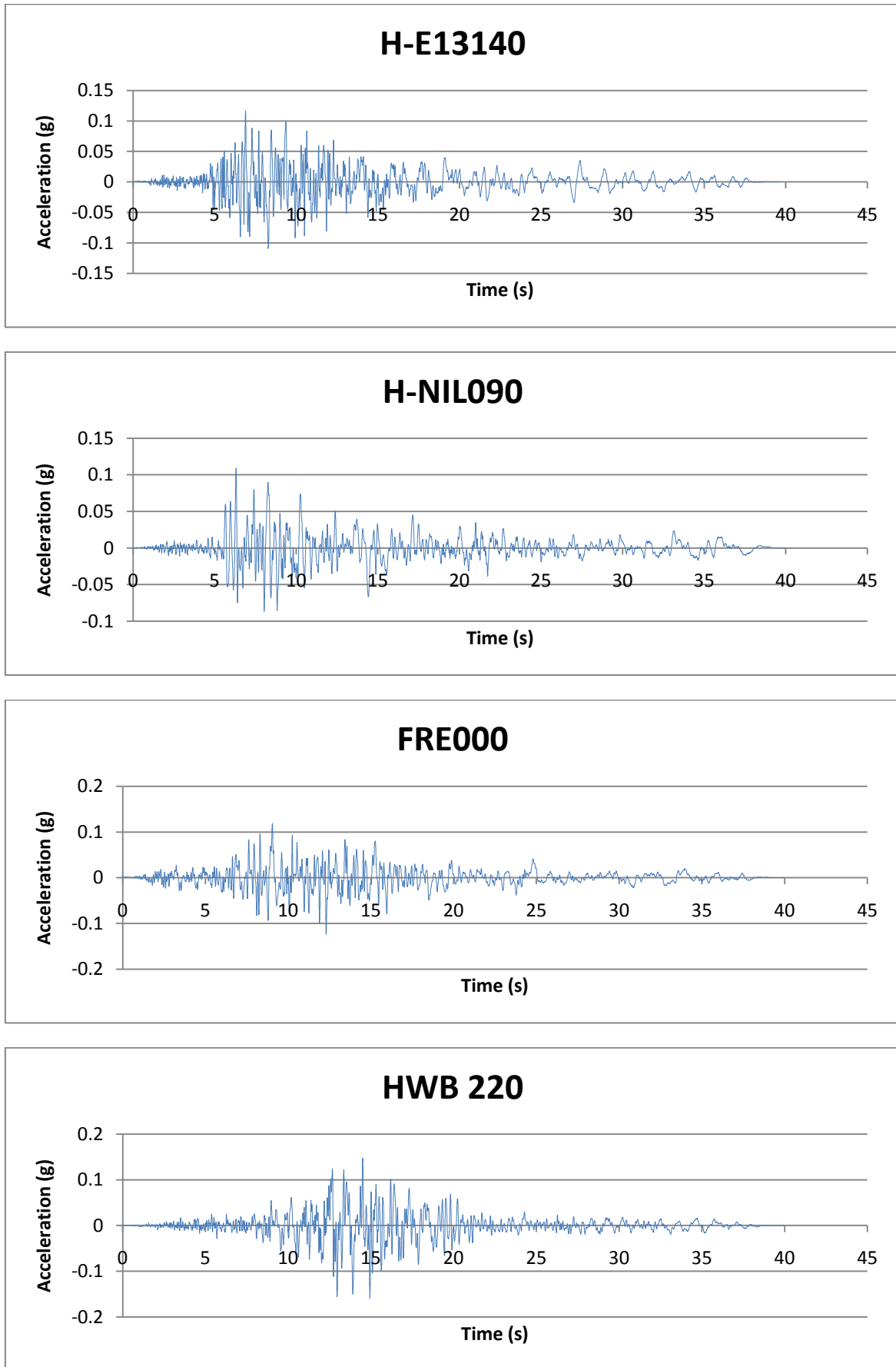


Figure 4.16 – Acceleration time series of the records selected for time-history analysis

The deformed shape of the two proposed frames was evaluated for two different deformed levels: i) first significant yielding, corresponding to the buckling of the compressive brace, ii) incipient failure of the structure, corresponding to the maximum capacity of the RC column. More details regarding the definition of failure of the RC members are provided in Section 4.3. In all analyses, the history of accelerations for all the records were scaled iteratively such that at the end of the each dynamic analysis, the maximum drift obtained was the one corresponding to the yielding and ultimate limit stage.

The scaling factors adopted are listed Table 4.3.

Table 4.3 - Resume of scale factors obtained in dynamic analysis

number	Earthquake Name	Slenderness, $\lambda$			
		2		3	
		1 <sup>st</sup> yielding	ultimate	1 <sup>st</sup> yielding	ultimate
1	Livermore-01 1980-01-24	3.8	7.34	1.1	6.95
2	N. Palm Springs 1986-07-08	2.2	5.8	0.9	6.5
3	Morgan Hill 1984-04-24	1.8	4.64	0.7	2.6
4	Coalinga-01 1983-05-02	0.8	2.3	0.35	1.5
5	Imperial Valley-06 1979-10-15	1.4	4	0.5	2.8
6	Imperial Valley-06 1979-10-15	0.9	2.9	0.45	2.5
7	Loma Prieta 1989-10-18	1.1	2.55	0.5	2.3
8	Loma Prieta 1989-10-18	1.5	3.8	0.55	2.6

#### 4.5.5. Discussion of Results

The dynamic characteristics of the three considered were evaluated based in modal analysis. The values obtained in the first three vibration modes are listed in Table 4.4.

Table 4.4 - Fundamental periods of vibration of the analyzed frames

	Structure		
	Original	$\bar{\lambda} = 3$	$\bar{\lambda} = 2$
T (s)	0.672	0.352	0.302

It can be seen from the table that the fundamental period of the retrofitted structures are around half of the original bare RC structure. Since the mass of the structure remains almost the same of the original structure, this means that the initial stiffness of the structure increases significantly. On the other hand, the fundamental period of the two braced frames does not change significantly.



Figure 4.17 shows that the 1<sup>st</sup> mode shape does not change significantly with the introduction of the steel braces. This might be justified by the fact that the braces are uniformly distributed over the height of the building.

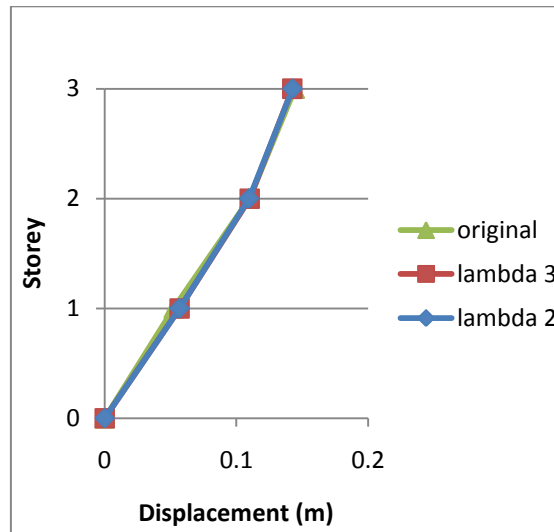


Figure 4.17 - 1<sup>st</sup> mode shape of the original and the two braced frames analyzed

The lateral deformation modes obtained for the two retrofitted frames and for the two limit stages considered (brace buckling and RC column failure) are depicted in Figure 4.18 and Figure 4.19.

The median mode shape is also plotted in the figures.

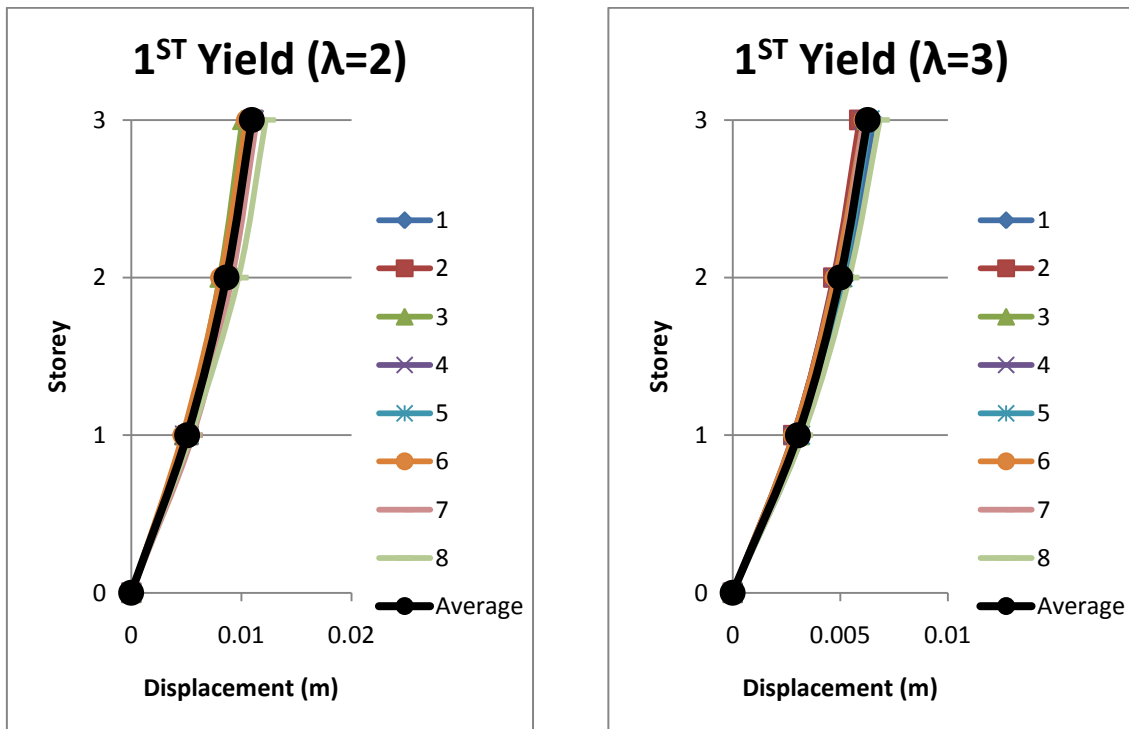


Figure 4.18 - Displacement profiles at yielding

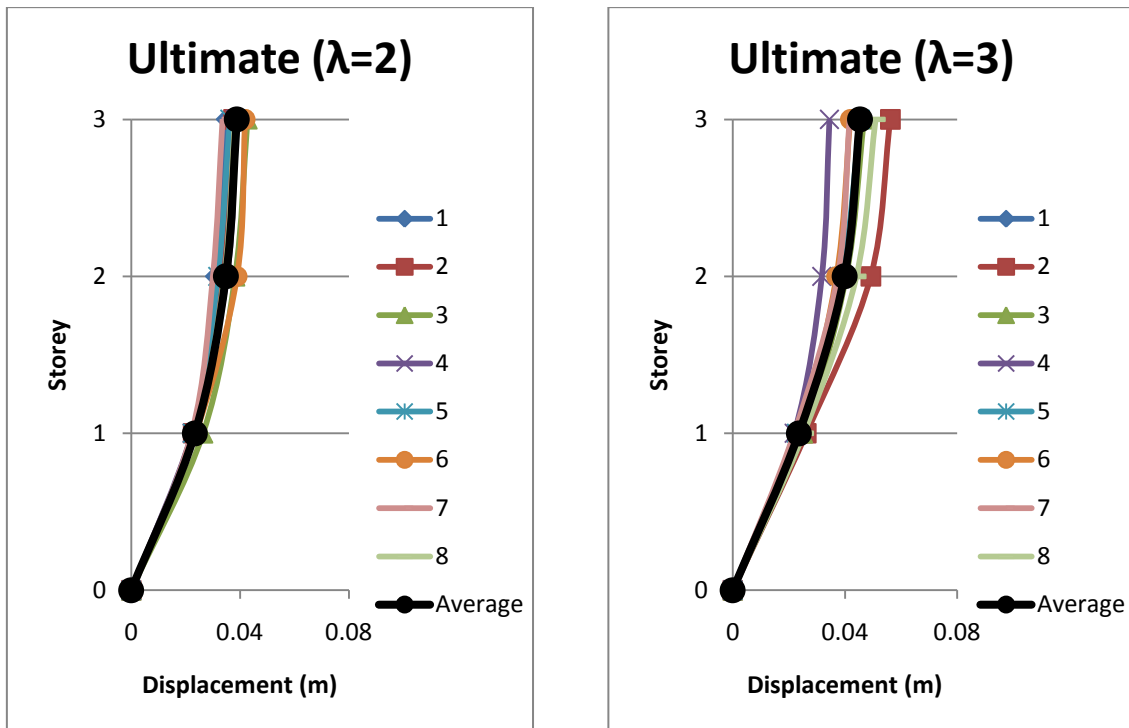


Figure 4.19 - Displacement profiles at failure

Figure 4.18 and Figure 4.19 clearly shows that for both frames, the lateral displacements at the moment of brace buckling are very similar and close to the ones corresponding to the 1<sup>st</sup> mode shape. As the intensity of the record is increased, the structure appears to behave almost the same way, with just a slight concentration of the damage at the first floor of the frame with lighter braces. This prove that even close to collapse, the behaviour of the structure is relatively stable, proving that the use of steel braces can control the damage over the height of the buildings as concluded in previous studies.

#### **4.5.6. Comparison of Obtained Profiles with Existing Expressions**

As mentioned previously, the design displacement profile of a MDOF system at maximum response is fundamental to characterize the equivalent SDOF system required to apply DDBD procedure. Pettinga and Priestley (2005) developed empirical expressions for displacement profiles of RC frames function of structural height and number of stories. They concluded that the displacement profiles have no dependence on the level of seismic response making no distinction between elastic and inelastic displacement shapes.

For regular frame buildings, the following equations have been shown to be adequate for design purposes:

Number of storeys ( $n$ )  $\leq 4$

$$\delta_i = \frac{H_i}{H_n} \quad (13)$$

Number of storeys ( $n$ )  $> 4$

$$\delta_i = \frac{4}{3} \times \left( \frac{H_i}{H_n} \right) \times \left( 1 - \frac{H_i}{4 \times H_n} \right) \quad (14)$$

Where  $H_i$  and  $H_n$  are the heights of level  $i$ , and the roof (level  $n$ ) respectively.

At this stage, it is important to compare the results obtained for RC braced frames with the previously recommended expressions for regular RC frames. Firstly, it is important to confirm if the elastic and inelastic displacement shapes obtained are similar as it was referred in the definition of existing expressions. To do that, all the displacements obtained in the analysis were divided by the displacement corresponding to the 1<sup>st</sup> storey in order to normalize all the displacements (relative interstorey drift).

Figure 4.20 shows that there is no significant difference between the displacements at yielding and at the ultimate state for both frames investigated. This observation is in line with those made in the past for regular RC frames and hence enables the conversion of the MDOF structure to an equivalent SDOF using the same displacement profile independently of the level of deformation of the system.

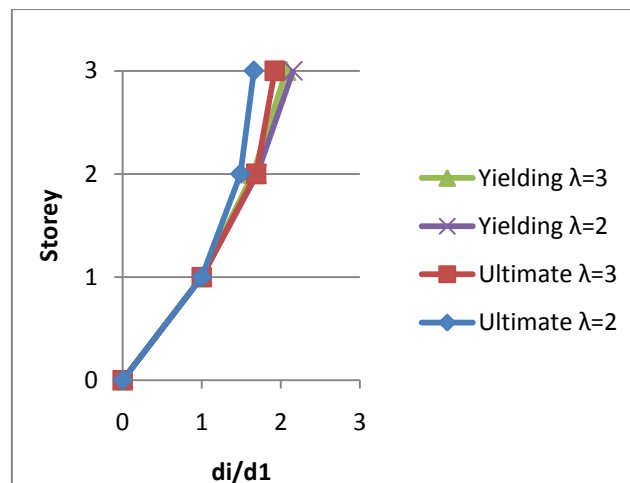


Figure 4.20 - Comparison of displacement profiles from different frames at different stages

In order to investigate if the recommended expressions for RC frames can be used for hybrid frames, Equations (13) and (14) were plotted against the results obtained in this work. Since the deformed shape obtained for the two different frames and for different deformation levels are very similar, in order to compare the results with the expressions, it

was decided to represent all the result to its average. It was found that the linear approximation do not satisfy the displacements profiles obtained since these follow a quadratic function. As a result, the second expression, corresponding to frames with more than 4 storeys was also compared.

It can be seen in Figure 4.21 that even compared with the second equation, the displacement shape of the braced frames is substantially different. It is clear that by using steel braces the displacements over the height of the building are more controlled. This proves that the general equations are not valid for this type of structural system, and, this way, cannot be adopted in the DDBD of RC steel braced frames.

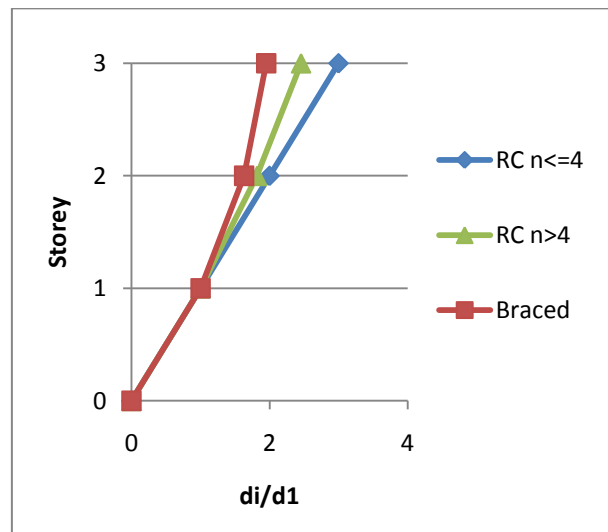


Figure 4.21 - Comparison of displacement profiles obtained with the one resulting from the generalized expressions

To overcome this limitation, a new expression for displacement mode shape is proposed.

$$\delta_i = \frac{4}{3} \times \left( \frac{H_i}{H_n} \right) \times \left( 1 - \frac{H_i}{2.25 \times H_n} \right) \quad (15)$$

It must be emphasized that the expression was validated only with the results obtained for the two frames considered in this study and hence there is a need to conduct more analysis with different braces (layout and/or strength) and in taller system.

The error on the results obtained with the proposed equation and the results from analytical analysis is negligible (less than 1%) as shown in Figure 4.22.

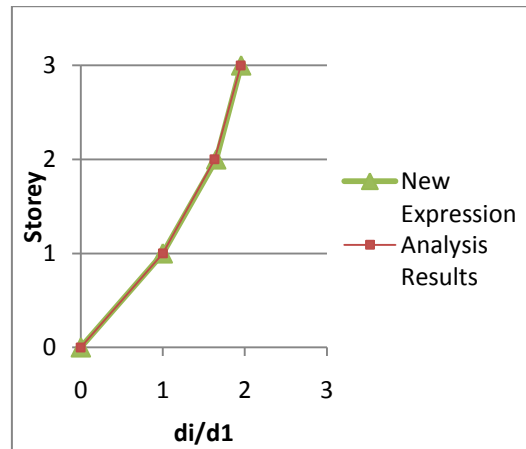


Figure 4.22 - Comparison of analysis results with new expression

#### 4.6. CONCLUDING REMARKS

This chapter provided a discussion on the behaviour of steel braced RC frames. The interaction of the two systems was analysed through results from numerical analysis. It was concluded that despite the fact that the application of steel braces is reflected in substantial increases in terms of lateral capacity, the axial loads induced in the RC columns by the braces can lead to significant reductions of the lateral deformation capacity of the hybrid system. The chapter concluded with a numerical study that aimed to examine the lateral deformation characteristics of hybrid systems. A new expression for the lateral deformation shape was proposed.

In the next chapter a new design method for the seismic retrofitting of RC frames with steel braces will be proposed.

## 5. PROPOSAL OF A DESIGN METHOD FOR STEEL BRACED RC FRAMES

*“Strength is essential, but otherwise unimportant”*

Hardy Cross (1885 - 1959)

### 5.1. INTRODUCTION

It has been demonstrated earlier in this work that steel braces can be successfully employed to improve the seismic behaviour of existing and new RC buildings. Moreover, a few attempts have been made to find reliable values for the behaviour factor so that force-based design can be applied. However, the values proposed by different researchers are not entirely consistent due to the relatively complex interaction between the RC members and steel braces. This situation points out to the need for the development of an alternative design procedures for this type of structural systems.

In recent years displacement-based design methodologies have suffered many developments, particularly in terms of their application to traditional RC schemes [Priestley *et al.*, 2007]. However, there were no developments of DBD methods for the type of hybrid schemes studied in this work.

### 5.2. BASIS OF THE METHOD

It has been demonstrated that the introduction of steel braced members in RC structures will imply the modification of the behaviour of the original RC frame, namely in terms of lateral strength and deformation capacity.

Due to the complex interaction between the two systems it is important that the displacement-based methodology that will be proposed accounts for response modification of the structure during lateral excitation. To this end, a strategy based on the fundamentals of the Capacity Spectrum Method (CSM) appears to be the more rational approach for the development of method.

As described in more detail in Section 3.4, the CSM is a graphical procedure that compares the global force-displacement capacity curve of a structure (pushover) with a given seismic demand which is defined in terms of a response spectrum [Freeman, 1998]. Figure 5.1 illustrates a schematic representation of the CSM applied to a framed structure.

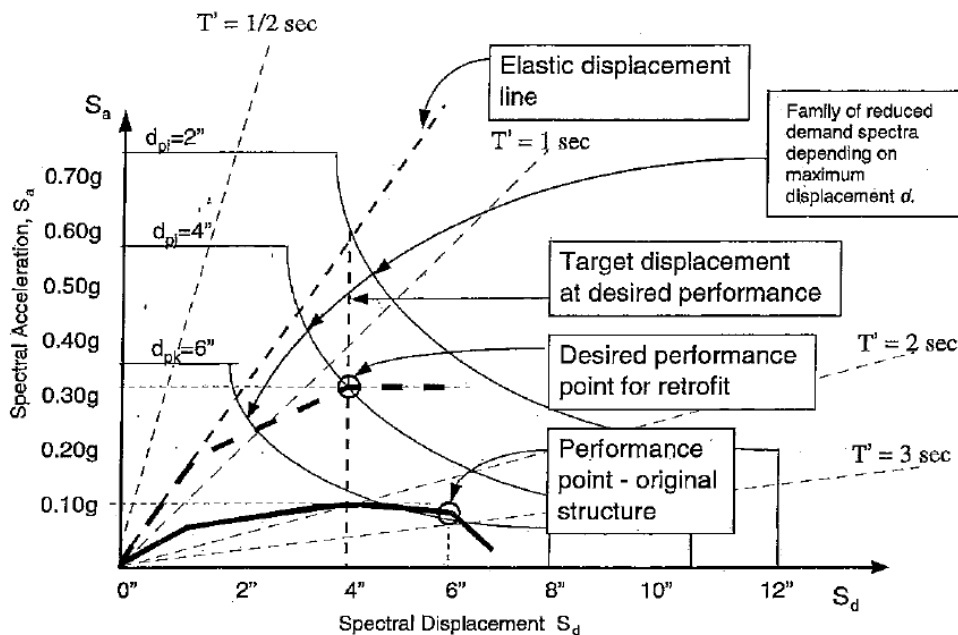


Figure 5.1 - Preliminary calculation for retrofit using strengthening and stiffening

In order to apply this methodology, five input parameters are required:

- Yield Displacement
- Lateral Strength
- Ultimate Displacement
- Equivalent Viscous Damping
- Earthquake Demand

In addition to these requirements, the successful application of the CSM depends on the estimate of the lateral deformation mode of the structure. In the previous chapter a study was conducted in order to define an analytical expression for the lateral deformation mode of hybrid structures.

The objective of the proposed method that is to be applied to existing RC structures with unsatisfactory seismic behaviour is to estimate the steel bracing system required such that the final hybrid system exhibits adequate seismic performance.

In this section two different methods based on displacements are proposed. The first one, and in the authors opinion preferable, is a non-iterative procedure based on the CSM. The second method, on the other hand, is an extension of the DDBD to steel braced RC structures. Since both the proposals follow a displacement-based philosophy and due to the fact that there are no significant differences between them, the non-iterative method will be described in more detail. Additional information will be given at the end of this chapter in order to explain the main differences between the two methods.

### 5.3. INPUT PARAMETERS

In this chapter a clarification on the definition of the different parameter for the application of the proposed method is evaluated.

#### 5.3.1. Yield Displacement ( $\Delta_y$ )

As explained before, the first yielding will take place when the braces in the first storey buckle. It must be referred that when buckling restrained braces are applied, this limit does not occur since buckling is prevented. For these cases, yielding is expected to happen when the braces reach their tensile capacity.

However, and as already discussed in Section 4.4, despite the first yielding occurs when the brace in compression buckles, analytical studies performed in the past, namely by Queirós *et al.*, (2009) indicated that buckling of the braces occurs in a very preliminary stage. Figure 5.2 illustrates the variation of the axial load in the braces during a pushover analysis. It is clear that the global yield displacement of the hybrid structure occurs when the 1<sup>st</sup> storey brace yields in tension.

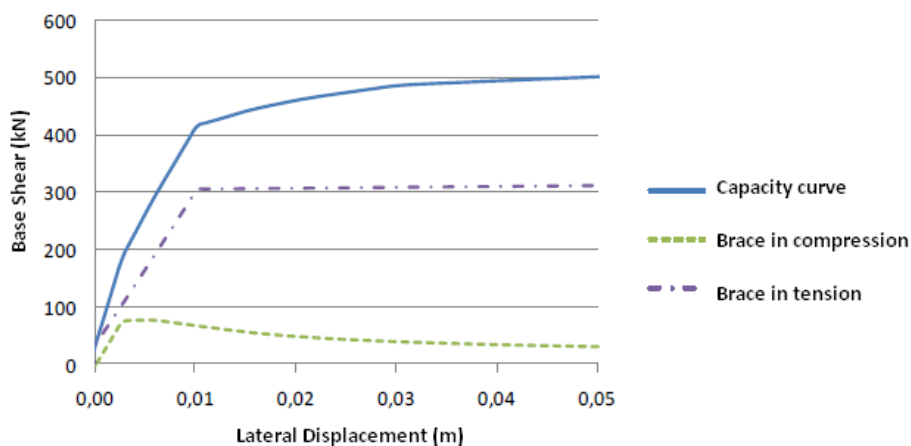


Figure 5.2 - Identification of yield displacement on steel braced RC frames



Based on the above observation, the force required to yield the steel brace in tension is given by:

$$N_{pl,Rd} = \frac{A \times f_y}{\gamma_{M0}} \quad (16)$$

Where  $A$  is the cross section of the steel brace,  $f_y$  is the yield strength of the steel brace and  $\gamma_{M0}$  is the partial factor for resistance.

Based on elastic principles, it is possible to relate the applied axial force ( $N_{pl,rd}$ ) to the axial deformation ( $\Delta_{yb}$ ) of the brace and hence to find the deformation at yielding:

$$\Delta_{yb} = \frac{N_{pl,Rd} \times L}{E \times A} \quad (17)$$

Where  $E$  refer to the Young modulus of the material.

Focusing now on the deformation parameters calculated for the braces, and taking into account the bay length, it is simple, by using geometric relations, to identify the displacement of the first floor required to impose yielding to the brace.

In Figure 5.3 it is represented an element of a braced frame and the two possible deformation modes. It is worth noting that the tensile brace (in red) observes a small compression due to vertical deformation associated with the rotation of the frame.

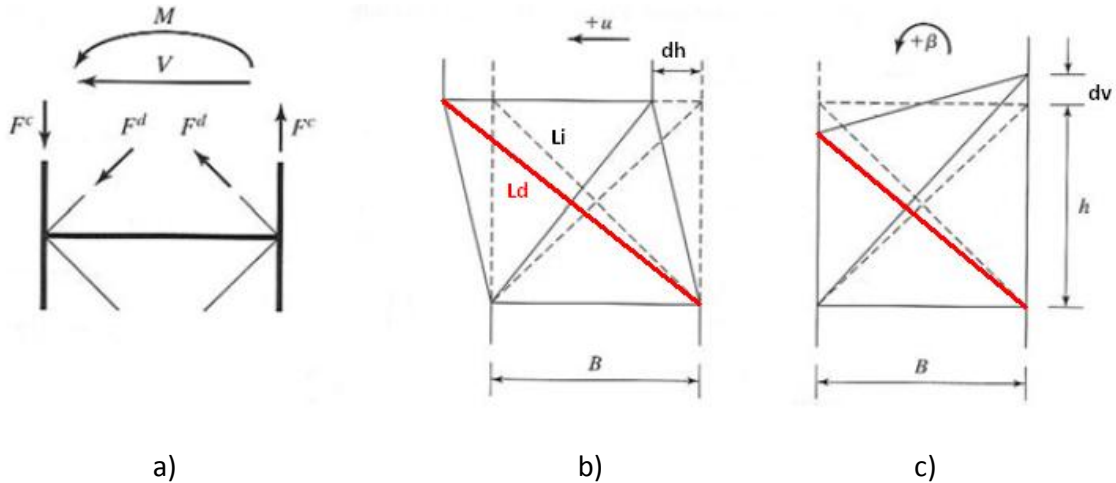


Figure 5.3 - Brace frame model: a) forces; b) lateral deformation; c) vertical deformation (adapted from Moon *et al.*, 2007)

Based on Figure 5.3 b), it is possible to derive an expression, based on geometrical properties, that relates the lateral storey displacement to the axial deformation of the compressed brace:

$$L_i = \sqrt{B^2 + h^2} \quad (18)$$

$$L_d = \sqrt{(B + d_h)^2 + h^2} \quad (19)$$

Where  $L_i$  is the initial length of the brace,  $L_d$  is the deformed length of the brace,  $B$  is the bay length,  $h$  is the storey height of and  $d_h$  is the storey lateral displacement.

Finally, the change in length ( $\Delta_b$ ) of the brace under analysis is given by:

$$\Delta_b = L_d - L_i \quad (20)$$

An analytical study was carried out to investigate the influence of the vertical component of the brace displacement associated with the storey's rotation in the overall deformation. The study consisted of a pushover analysis performed on a 3-storey steel braced RC frame.

The lateral displacements of the frame at the 1<sup>st</sup> storey were obtained from the pushover analysis. The axial deformation of the tensile brace was calculated using Expressions (18), (19) and (20) neglecting the vertical displacement. The axial brace displacements were also evaluated by accounting for both horizontal and vertical displacements.

The brace axial deformations calculated according to the two different assumptions are shown in Figure 5.4.

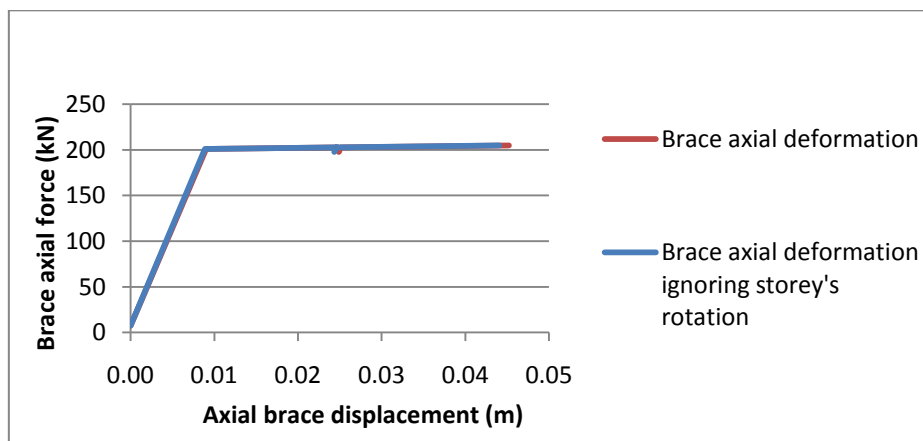


Figure 5.4 - Influence of frame rotation in braces behaviour

It can be seen from the results that despite the two curves being not coincident, the fact is that by neglecting the effects of the vertical displacement of the RC frame due to the overturning moment, the error is minimum. For the sake of simplicity, in this work will be considered only the horizontal deformation to calculate the displacement at which yielding occurs.

We are now in a position to develop a simple expression that enables the calculation of the frame displacement at yielding.

Since:

$$\Delta_y = \sqrt{L_d^2 - h^2} - B \quad (21)$$

With:

$$L_d = L_i + \Delta_{yb} \quad (22)$$

Based on the calculated values it is possible to identify pairs of forces and lateral displacements associated to each of the braces selected. The most important parameter is the storey drift of the frame associated with the yielding of the steel brace. By knowing this displacement of the MDOF structure and the mass present at each floor, the displacement of the equivalent SDOF can be easily calculated by employing Expression (15) developed in Section 4.5.6.

### **5.3.2. Ultimate Displacement ( $\Delta_u$ )**

The design displacement of the SDOF substitute structure depends both on the limit state displacement leading to failure of the most critical member of the MDOF structure, and on the assumed displacement shape of the structure [Priestley *et al.* 2007].

In Chapters 2 and 4 of this thesis, special attention was given to the behaviour of hybrid structures. It was concluded that the two main systems (RC and steel braces) act in parallel. This means that the capacity of the system can be approximated by adding the capacities of each individual system. Moreover, and because the objective in adding the bracing system is to increase the lateral strength and stiffness of the structure, it is expected that the collapse of the hybrid system is governed by failure of one or several members of the RC frame.

Because the axial load plays an important role in the lateral deformation capacity of the RC columns, it is necessary to estimate the axial load installed in the RC columns at the collapse limit state. In other words, by knowing the maximum axial load that each of the selected braces imposes on the columns, it is possible to calculate the lateral deformation capacity of these members and therefore the ultimate displacements of both the MDOF equivalent SDOF systems.

To find the maximum axial load in the columns at the first storey it is conservatively assumed that all the braces in the structure reached yield. This assumption may not always correspond to reality, but for the time being, it is considered to be a reasonable approximation.

### **5.3.2.1. Parameters for the Calculation of the Ultimate Displacement**

By conservatively assuming that at the ultimate stage all the braces reached yield in all bays and over the height of the structure, it is possible to calculate the maximum increment of axial compression that the columns can observe. This is done by adding all the vertical components resulting from the brace axial capacities (except that of the compressive brace of the 1<sup>st</sup> storey which transmits the load directly to the foundation).

At this point, it is possible to estimate the maximum axial force that one given column can experience at collapse. For that purpose one needs to add the axial force in the RC columns at collapse, found from a non-linear static analysis of the bare RC frame to the summation of all the vertical components of the braces over the height of the frame. To better understand this process, let's take the following example:

From a pushover analysis of a 2-storey frame with one bay 6m span and 3m of storey height results an axial load in the RC column at maximum displacement of 400kN. If the braces selected have a capacity in compression of 20kN and a tensile capacity of 150kN, the vertical components per floor are 8.9kN and 67kN, respectively. Then, the axial load in the column will be  $400 + 2 * 67 + 8.9 = 542.9\text{kN}$ . Note that the compressive brace in the first floor is connected directly to the foundation and, hence, it is not added to the column.

Finally, with the RC column properties and the estimate of the axial load, it is possible to determine the maximum deformation capacity of the member. In this work the software RESPONSE-2000 [Response-2000] was used for this purpose.

### **5.3.2.2. Column Deformation Capacity**

Response-2000 is a program developed at the University of Toronto in Canada by Bentz and Collins [Response-2000]. The program enables the user to analyze both reinforced concrete sections and elements taking into account axial, flexure and shear actions. The program also takes into account the P- $\Delta$  effects, shears capacity and yield penetration.

In this work, the objective is to find the maximum deformation capacity of the RC columns subjected to different axial loads. As illustrated in Figure 5.5, total column lateral displacement measured at the top of each column can be assumed to result from the summation of deformations due to: a) flexure, ( $\Delta_{\text{flexure}}$ ); b) longitudinal bar slip at column ends, ( $\Delta_{\text{slip}}$ ); and c) shear, ( $\Delta_{\text{shear}}$ ).

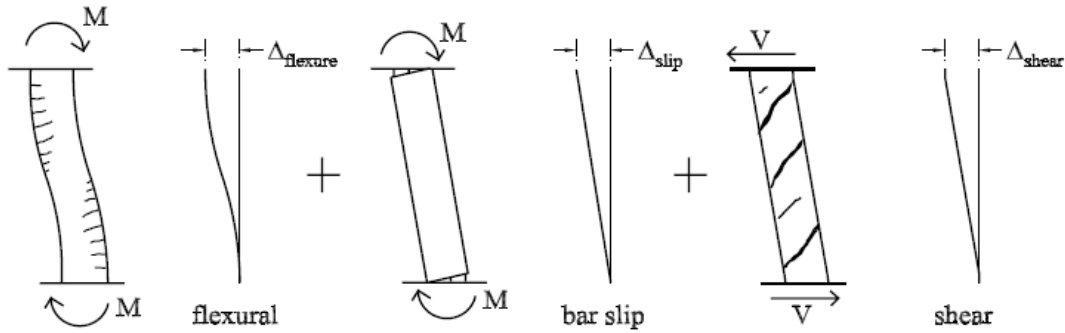


Figure 5.5 - Contribution of displacement components to total lateral displacement (adapted from Sozen *et al.*, 2004)

Initially, the program calls for the column section geometry and materials properties. The second step consists of the definition of the element length and the boundary conditions. Regarding the boundary conditions, it is necessary to define the location of the contraflexure point in the column. To evaluate this parameter, the moments at the top and bottom of the 1<sup>st</sup> storey column were obtained from pushover analyses performed on a 3-storey frame (unbraced and braced). The moments are presented in Figure 5.6 a) and b):

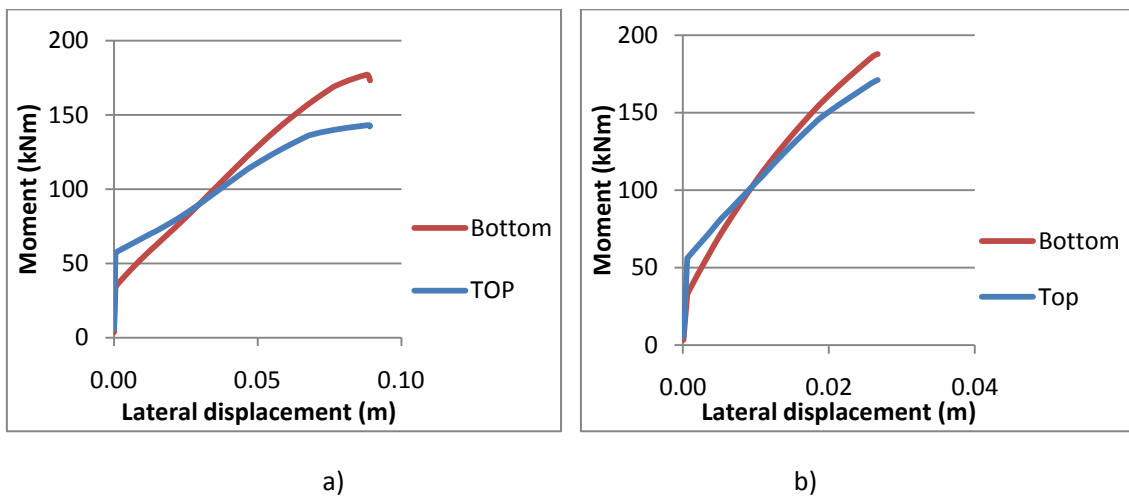


Figure 5.6 - Evolution of moments: a) bare frame, b) braced frame

The plots indicate that in the initial steps of the pushover, the moment at the top section of the column is higher than the moment at the base. However, as the analysis proceeds into the non-linear range, the moments at the bottom increase and reach values that are higher than those obtained at the top section.

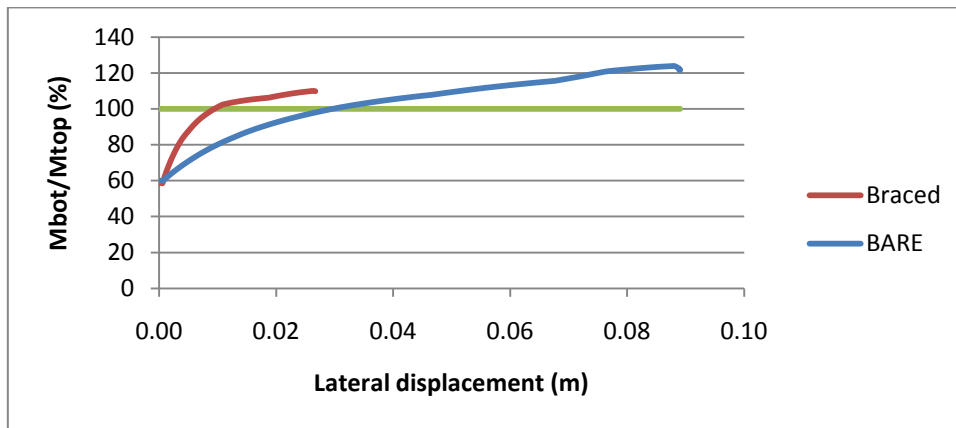


Figure 5.7 - Moments evolution in RC columns with and without bracing system

Based on these observations it becomes clear that it is not possible to define an exact value for the contra-flexure point. Therefore, it was decided that a good approximation could be to define the contra-flexure point at the mid-span of the member. By doing this, the maximum deformation capacity of the critical RC column is conservatively estimated.

To exemplify what was described above, a generic column was subjected to different values of axial load and was pushed up to failure. Moreover, for the same conditions, one column was assumed to have equal moments at the top and at the base and in the other column the moment at the top was half of the moment at the base. The deformation capacity of each column for different levels of axial load is plotted in Figure 5.8.

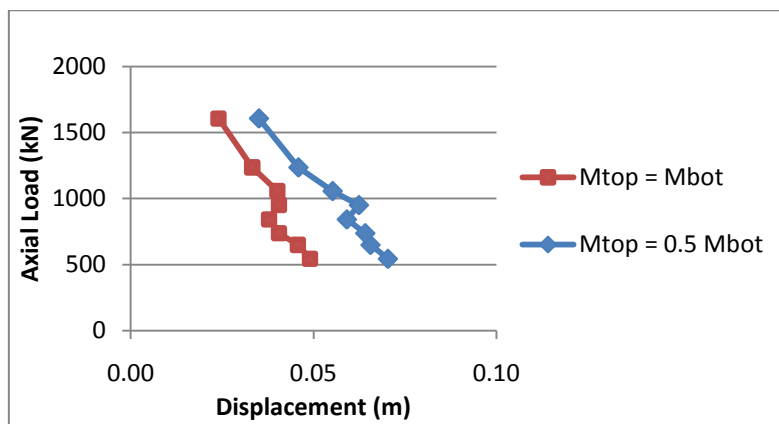


Figure 5.8 - Comparison of an RC column capacity considering different contra-flexure lengths

The results presented in the figure confirm two important ideas. The first is the fact that, generically, as the axial load increases, the deformation capacity of the column decreases. The small deviation obtained for an axial load of about 1000kN is justified by the fact that for this particular section, the flexural capacity is optimized for values of axial load close to this value. This is demonstrated in the M-N interaction plot obtained from the Response-2000 program present in Figure 5.9.

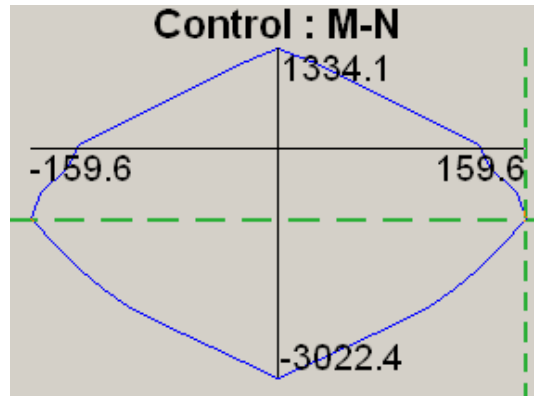


Figure 5.9 - M-N interaction plot (adapted from [RESPONSE-2000])

The second idea is the demonstration that as the contra-flexure point deviates from the mid-span of the element, the displacement capacity of the column increases for the same level of axial load.

### 5.3.3. Lateral Strength ( $V_y$ )

After defining the ultimate displacement it is possible to calculate an estimate of the lateral strength of the hybrid system. Once again, depending on the adopted braces, the fraction of base shear resulting from the addition of the steel braces can be calculated as the summation of the horizontal components of the braces in tension and in compression located at the 1<sup>st</sup> storey.

In order to find the lateral capacity of the original RC structure one just needs look at the pushover results and to find the base shear corresponding to the ultimate displacement found in the previous section. The total lateral strength ( $V_y$ ) of the hybrid structure is then calculated by the summation of both components.

### 5.3.4. Equivalent Viscous Damping (EVD)

The equivalent viscous damping (EVD) is a function of the expected hysteretic behaviour and of the ductility of the non-linear system given by  $\mu = \Delta_d / \Delta_y$ , where  $\Delta_d$  refers to the design displacement, and  $\Delta_y$  to the yield displacement.

Over the past years several proposals have been made for EVD-ductility relationships. In the present work, the expressions proposed by Priestley *et al.* (2007) will be adopted.

It must be pointed out that there is not a specific expression for steel braced RC frames. However, the expressions available for concrete frame buildings and for steel frame building are very similar.

- Concrete frame buildings

$$\xi_{eq} = 0.05 + 0.565 \times \left( \frac{\mu-1}{\mu \times \pi} \right) \quad (23)$$

- Steel frame buildings

$$\xi_{eq} = 0.05 + 0.577 \times \left( \frac{\mu-1}{\mu \times \pi} \right) \quad (24)$$

In the present work, and for the sake of simplicity, the expression for concrete frames will be adopted. It is expected that for hybrid structures the value of EVD should fall in the interval defined by the two expressions. Yet, the adoption of the Expression (23) should be accurate enough and is expected to produce conservative values.

### 5.3.5. Earthquake Demand

As in any seismic design processes, it is necessary to define the seismic hazard of the site in which the building is going to be located. In DDBD, the seismic demand is usually defined by an inelastic displacement spectrum. In this proposal, since the goal is to make use of the CSM, it is necessary to generate an acceleration-displacement response spectrum (ADRS). This can be done by plotting the response spectral accelerations (y-axis) against the corresponding spectral displacements (x-axis).

## 5.4. RETROFITTING SOLUTION

After the definition of the required parameters for the application of the method, it is now possible, for any of the steel brace system considered, to evaluate the maximum lateral displacement capacity of the retrofitting solution. Figure 5.10 illustrates the variation of the target displacement with the lateral strength for a hypothetical RC structure and 8 different brace cross-sections.

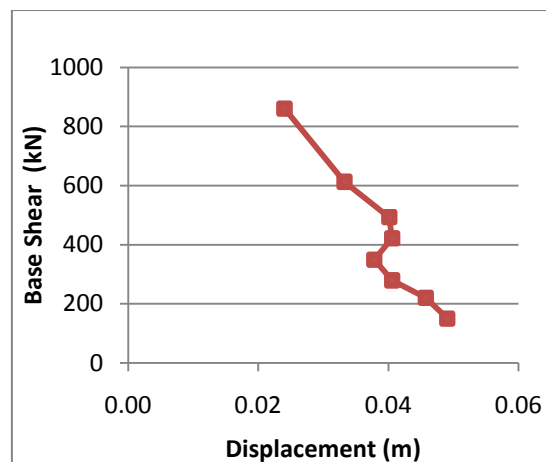


Figure 5.10 - Illustration of a base shear-target displacement plot for different brace properties



In order to evaluate if any of the adopted solutions satisfy the seismic requirements, it is necessary to calculate the ductility and consequently the equivalent viscous damping associated to the system, so that the elastic spectra can be transformed into an inelastic spectra.

After defining both the capacity and the demand curves, the CSM methodology can be applied by superimposing the two curves. It must be pointed out that, in order to superimpose the curves, it is necessary to transform the lateral strength of the structure into spectral accelerations. This can be easily done by dividing the lateral strength obtained by the equivalent mass of the equivalent SDOF structure.

Figure 5.11 represents an example of the application of two different X-bracing systems in the same RC frame, superimposed with the correspondent inelastic spectra. It is possible to observe that in case a), the inelastic spectra cannot be reduced further since it is already reduced for the maximum ductility capacity that the structure can achieve. This means that, since the capacity curve cannot intersect the spectra, it is expected an unsatisfactory seismic behaviour. On the other hand, for case b), the capacity curve will intersect the spectra in a point somewhere between the ultimate limit state (blue dot) and the origin. This means that, in order to evaluate the performance point (i.e., the intersection point), the inelastic spectra should be amplified. However, the performance will correspond to a deformation level that is lower than the deformation capacity of the hybrid structure, indicating therefore the presence of a satisfactory seismic behaviour.

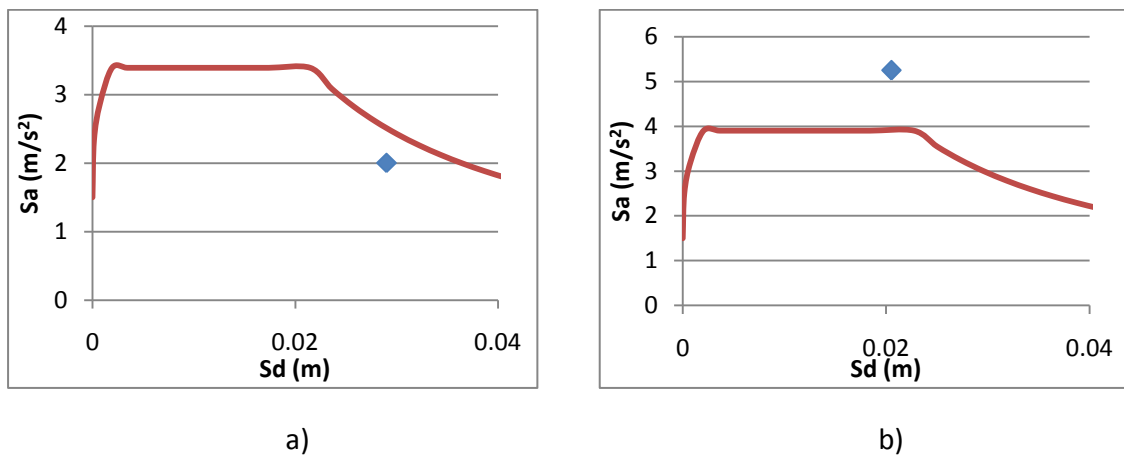


Figure 5.11 - Evaluation of the seismic behaviour for two different solutions: a) unsatisfactory seismic behaviour; b) satisfactory behaviour

This graphical solution is very practical because the engineer can compare the final behaviour of the different solutions adopted in the initial stage of the process and select the one that satisfies better the retrofitting purpose.

## **5.5. ALTERNATIVE PROCESS**

The method described in the previous sections has the advantage that is a non-iterative process and that the final solutions can be compared at the end of the procedure. However, the calculation of the ultimate displacement capacity of the RC columns needs to be carried out as many times as different braces are selected in the initial phase. Based on the DDBD methodology, this issue can be avoided, or at least minimised.

The process is basically the same, however only one brace is selected at the initial stage. At the step when the performance point and the lateral capacity of the structure are calculated, it is possible to follow the DDBD process and, by inputting the design displacement in the inelastic displacement spectrum one can find the corresponding secant period and therefore calculate the required lateral strength. If the required base shear is higher than the lateral capacity of the hybrid system, then the process should start again assuming stronger braces, until the required lateral strength is lower than the available capacity estimated for the hybrid system.

## **5.6. CONCLUDING REMARKS**

In this chapter a detailed explanation of the proposed method for seismic design of hybrid systems was presented. The method is based on the Capacity Spectrum Method which is typically used for assessment purposes.

It is worth noting that one of the main goals was to keep the model as simple as possible, and for this purpose, some approximations have been assumed.

In order to evaluate the maximum lateral deformation capacity of the structure, it was assumed that all the braces over the height of the structures reached their maximum capacity. As explained before, for some cases this assumption may be too conservative. In fact, it is possible to update this estimate during the design process by considering the lateral deformed shape based on the expressions derived in Chapter 4. This can be done by calculating the inter-storey drifts in all stories as a function of the current estimate of the ultimate displacement. Based on this calculation, the forces installed on the braces can be determined and hence a more accurate estimate of the axial load installed in the RC columns can be obtained. The process should be repeated until convergence is achieved. The iterative procedure is time-consuming compared with the level of optimization obtained. However, for high-rise buildings, this process is recommended in order to avoid a very conservative and non-efficient solution.

Another simplification was assumed in the calculation of the lateral strength provided by the bracing system. This calculation is based on the summation of the buckling and yield capacities of the braces in compression and in tension, respectively. In a real scenario, after reaching these forces, the force in the compressive brace tends to decrease after

buckling occurs and the force in the tensile brace tends to increase due to strain-hardening effects. Once again this estimated can be improved in the same way described above. However, the reduction in the compressive brace is relatively insignificant and it compensates the strength increase of the tensile brace that has been ignored in the calculations.

In the next chapter the proposed method will be applied to a RC frame.

## 6. VALIDATION OF THE PROPOSED METHOD

*"It is better to be approximately right than precisely wrong"*

Warren Buffett

### 6.1. INTRODUCTION

In the present chapter, the proposed method will be applied to a typical RC building requiring retrofitting. The results obtained herein have two main goals: the first is to clarify the steps of the design method proposed in the previous chapter; the second goal is to verify if the method leads to retrofitted structures with adequate seismic performance.

### 6.2. STRUCTURE CHARACTERIZATION AND SEISMIC VULNERABILITY

The building considered is a 3-storey, 5-bays RC structure with 4m spacing between frames. The structure represents a building with insufficient seismic resistance in which the elements were solely designed for gravity loads according to Eurocodes 1 [CEN, 2001] and 2 [CEN, 2004]. The dead load considered was  $9\text{kN/m}^2$  whilst the imposed load was assumed as  $5\text{kN/m}^2$ . The elevation view of one of the RC moment frames is shown in Figure 6.1. The cross-sections adopted for the beams and columns are illustrated in Figure 6.2.

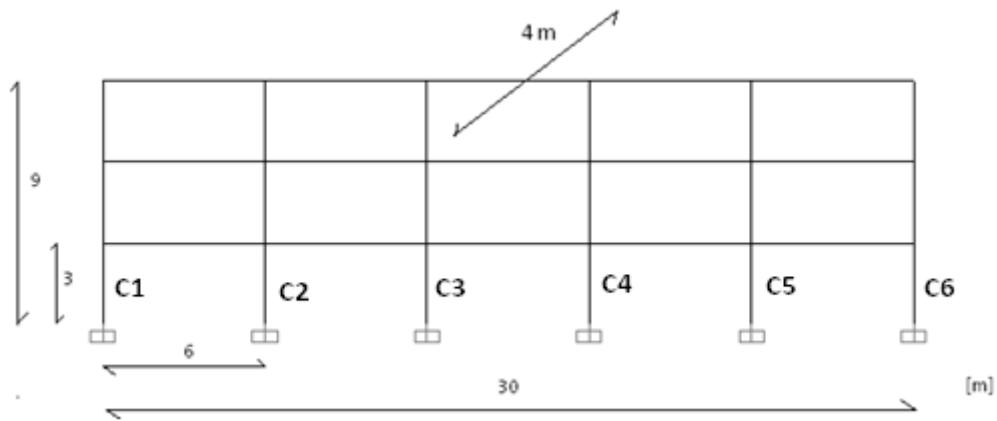


Figure 6.1 – RC frame

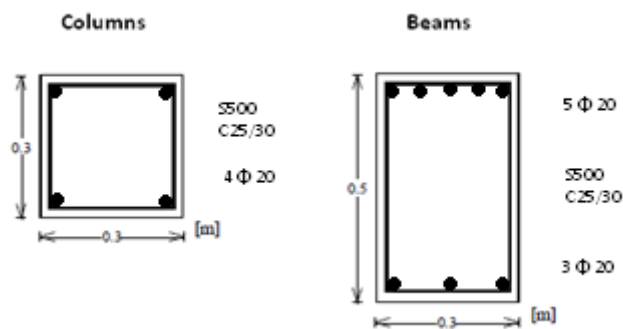


Figure 6.2 – Beam and column cross-sections

In order to assess the seismic performance of the original RC structure, it is fundamental to know the seismic vulnerability of the site in which the structure is located. For this study it was assumed that the structure is located in Lisbon. In fact, Portugal has a medium/high seismic risk and, moreover, there is a large building stock of RC buildings that were constructed in the second half of the last century, characterized by elements with limited deformation capacity and therefore prone to require retrofitting.

Eurocode 8 defines two types of seismic actions. For the purpose of this study only seismic action type 1 will be considered. Moreover, it will be assumed that the structure is founded on a soil of type B according to EC8. Based on these considerations, the reference Peak ground acceleration was taken as  $1.5\text{m/s}^2$ .

### 6.3. SEISMIC ASSESSMENT

The assessment of the original RC structure was carried out by applying the Capacity Spectrum Method (CSM). As already described before, this method consists of the nonlinear-static (or pushover) analysis of the structure followed by the conversion of the pushover curve into a capacity curve corresponding to the behaviour of an equivalent

SDOF system. In the same plot the earthquake demand is represented in the format of an inelastic acceleration-displacement response spectrum (ADRS).

The results from the pushover analysis performed on one of the RC frames of the structure are shown in Figure 6.4. In the final part of the capacity curve it is observed a significant reduction of strength corresponding to failure of some of the 1<sup>st</sup> storey RC columns of the frame.

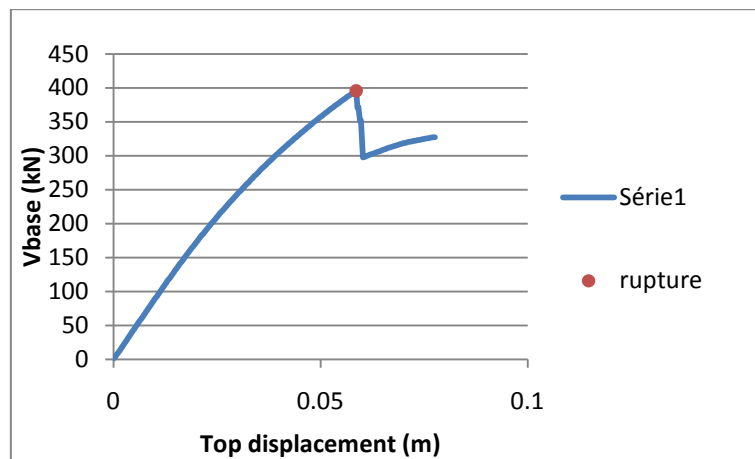


Figure 6.4 - Capacity curve of the MDOF

In order to apply the CSM, it is necessary to define a bilinear representation of the capacity curve. As shown in Figure 6.5, this was achieved by imposing equal areas above and below the capacity curve.

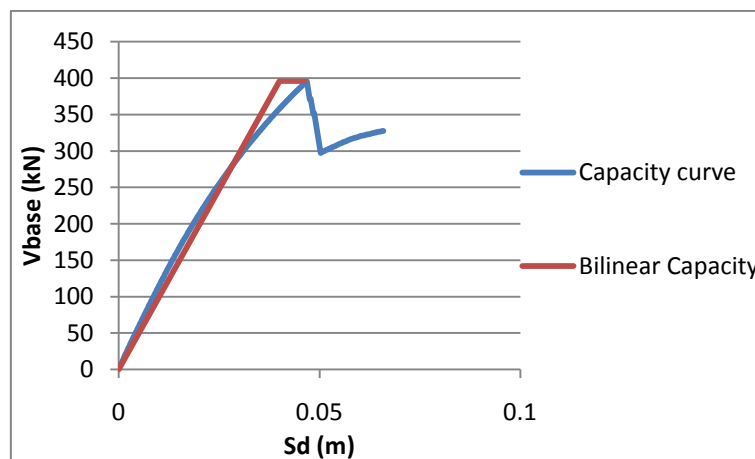


Figure 6.5 - Bilinear curve of the SDOF

Finally, in order to evaluate the seismic performance of the structure the equivalent viscous damping of the structure was calculated and the elastic acceleration displacement response spectrum (ADRS) was reduced.

As shown in Figure 6.6, the bilinear curve does not intersect the response spectrum for the corresponding EVD associated to the ductility capacity of the structure. This means that a performance point cannot be determined for the structure. This observation leads to the conclusion that the structure is not able to resist the design earthquake.

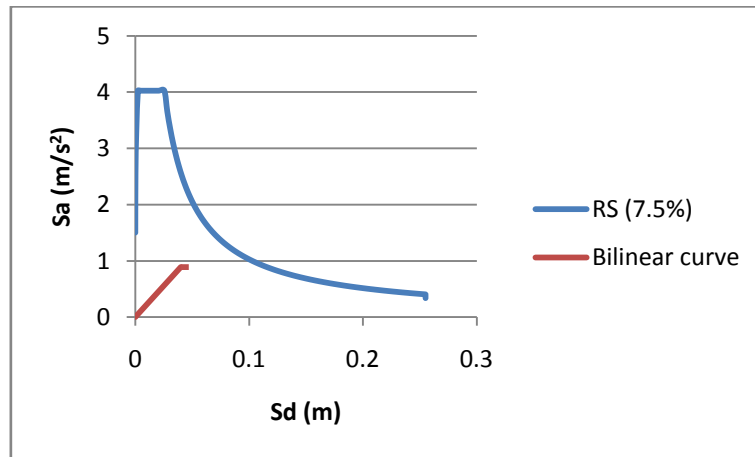


Figure 6.6 - Application of the CSM procedure

### 6.4. RETROFITTING DESIGN

From the pushover analysis carried out in the previous section, it was possible to determine the values of total base shear and axial loads installed in all columns for all steps. In Figure 6.7 it is possible to observe that the variation of the axial load due to the contribution of the overturning moment is more visible in the external columns (C1 and C6). In fact, in the internal columns (C2 to C5) the variation of axial force is almost negligible.

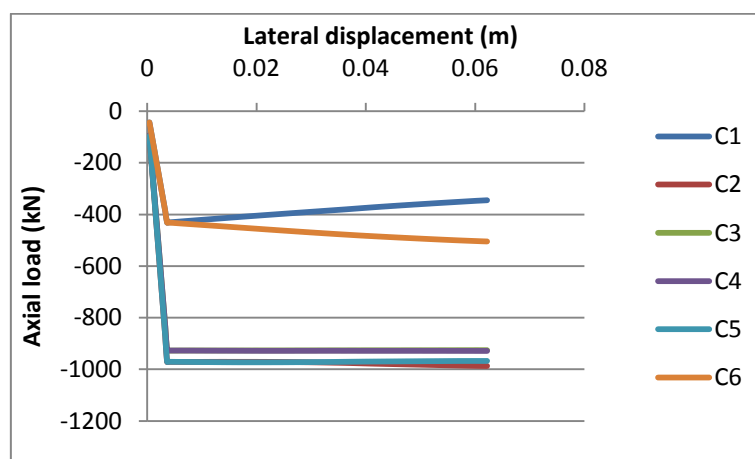


Figure 6.7 - History of axial loads in the pushover analyze

Moreover, since the RC section of the columns is known, it is possible to calculate the moment-axial load interaction diagram (Figure 6.8), and based on the values of axial load in the columns calculated before, it is possible to define a range of acceptable increments of axial load in the columns. At this stage is important to remind the reader that it is preferable to locate the bracing system in the inner bays of the frame in order to prevent overloading of the external RC columns due to overturning moments. It is also important to make sure that the increment of axial load does not exceed the maximum axial load found for the RC frame so that tensile forces at the foundations are avoided.

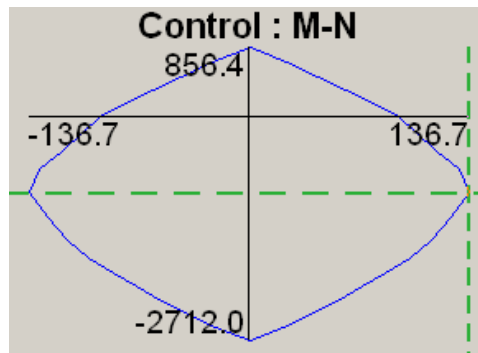


Figure 6.8 - M-N interaction diagram (adapted from [RESPONSE-2000])

From the above results, a group of possible circular hollow steel brace sections is proposed in Table 6.1.

Table 6.1 - Basic properties of selected steel braces

Brace ID	Outside diameter	Thickness	Sectional area	Moment of inertia	Slenderness	Compressive Capacity	Tensile Capacity	Total Brace Forces Components	
	D (mm)	T (mm)	A (cm <sup>2</sup> )	I (cm <sup>4</sup> )	$\lambda$	Nb,Rd (kN)	Ppl,Rd (kN)	Base Shear	Axial load
Brace 1	76.1	3.2	7.33	48.8	3	21.4	201.6	199.6	288.9
Brace 2	88.9	3.6	9.65	87.9	2.6	38.6	265.4	272.0	389.6
Brace 3	114.3	3.2	11.2	172	2	75.4	308.0	343.2	479.6
Brace 4	139.7	3.2	13.7	320	1.6	140.4	376.8	462.8	629.6
Brace 5	139.7	5	21.2	481	1.7	211.0	583.0	710.6	968.7

The table provides values of base shear corresponding to the addition of the horizontal component due to the development of the compressive and tensile capacities of the braces located in one single bay. The axial load values given in the last column of Table 6.1 correspond to the axial load increment at the base of each of the six columns introduced by the steel braces. The final axial load is then defined by the summation of the vertical components of the braces in all floors in one bay (except the compressive brace of the 1<sup>st</sup> floor that load directly to the foundation), assuming that all braces reach the maximum strength.



The global yield displacement of the frame can be determined based on the brace properties and on the geometry of the RC frame (Table 6.2).

Table 6.2 – Global yield displacement of the frame for different braces

Brace ID	Brace Elongation at Yielding	1st Story Displacement at Yielding	SDOF Displacement
	$\Delta l_y$ (m)	$\Delta y_1$ (m)	$\Delta y$ (m)
Brace 1	0.0092	0.0103	0.0168
Brace 2	0.0092	0.0103	0.0168
Brace 3	0.0092	0.0103	0.0168
Brace 4	0.0092	0.0103	0.0168
Brace 5	0.0092	0.0103	0.0168

In order to find the most efficient and economical solution, three different layout solutions are to be tested. A schematic representation for each solution is illustrated in Figures 6.9 to 6.11. In the first solution only the first bay is braced and consequently only columns C3 and 4 (will be affected. The second solution is the one affecting more columns, namely columns C2, C3, C4 and C5. The third solution consists of a larger number of braced bays. In this solution, only the second and fifth columns will be affected in terms of axial loads. This is due to the fact that the axial loads induced to columns C3 and C4 by the braces located on the middle bay are cancelled out by the forces induced by the braces on the adjacent bays.

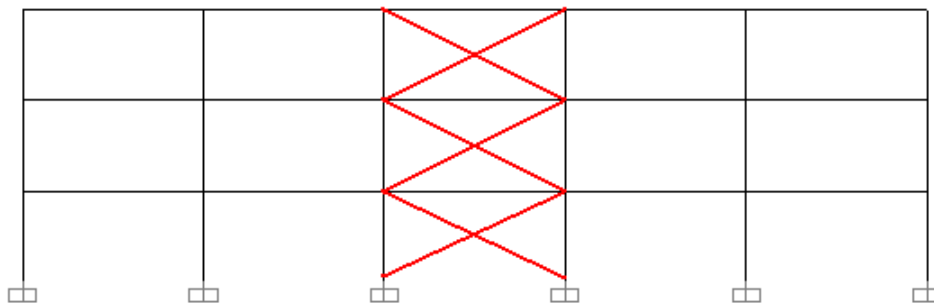


Figure 6.9 - Solution 1

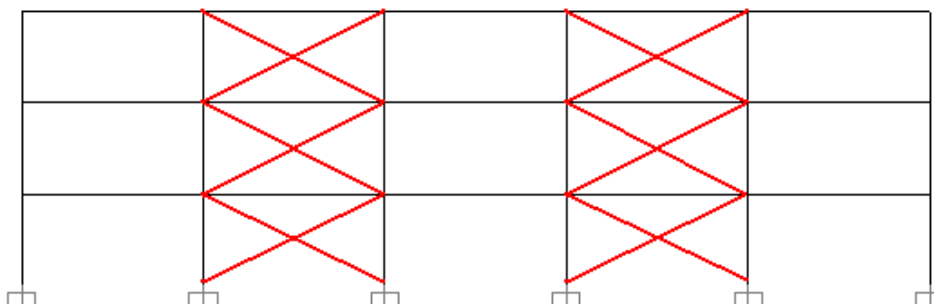


Figure 6.10 - Solution 2

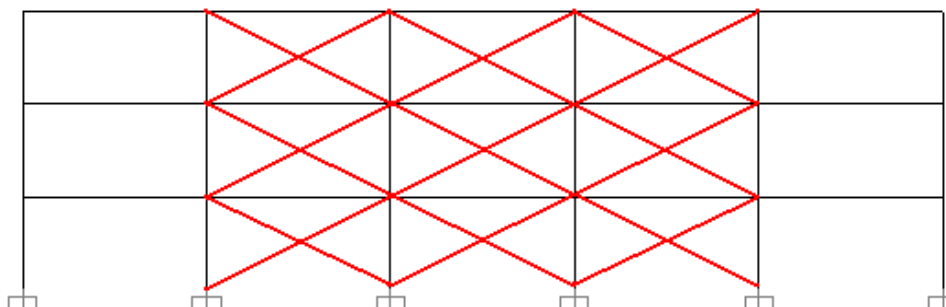


Figure 6.11 - Solution 3

At this stage it is possible to quantify the variation of axial load in the RC columns for the three different solutions, and for each of the brace cross-sections adopted. A summary of the maximum and minimum values of axial force is presented in Tables 6.3 and 6.4, respectively. It is worth noting that the negative values in the tables correspond to compressive axial forces.

Table 6.3 - Maximum compressive axial load in the RC column for different brace properties

Brace ID	Maximum Axial Load for Different Columns and Braces					
	Column 1	Column 2	Column 3	Column 4	Column 5	Column 6
bare frame	-352.3	-977.1	-929.8	-930.5	-968.5	-498.7
Brace 1	-352.3	-1266.0	-1218.8	-1219.4	-1257.4	-498.7
Brace 2	-352.3	-1366.7	-1319.5	-1320.1	-1358.1	-498.7
Brace 3	-352.3	-1456.7	-1409.4	-1410.1	-1448.1	-498.7
Brace 4	-352.3	-1606.7	-1559.4	-1560.1	-1598.0	-498.7
Brace 5	-352.3	-1945.8	-1898.5	-1899.2	-1937.1	-498.7

Table 6.4 - Minimum compressive axial load in the RC column for different brace properties

Brace ID	Maximum Axial Load for Different Columns and Braces					
	Column 1	Column 2	Column 3	Column 4	Column 5	Column 6
bare frame	-352.3	-977.1	-929.8	-930.5	-968.5	-498.7
Brace 1	-352.3	-688.2	-640.9	-641.6	-679.5	-498.7
Brace 2	-352.3	-587.5	-540.2	-540.9	-578.8	-498.7
Brace 3	-352.3	-497.5	-450.2	-450.9	-488.8	-498.7
Brace 4	-352.3	-347.5	-300.2	-300.9	-338.9	-498.7
Brace 5	-352.3	-8.4	38.9	38.2	0.2	-498.7

Note that the values corresponding to columns C1 and C6 do not change. This is due to the fact that, for the assumed solutions, the steel braces are not linked to the external columns. It must be pointed out that tensile axial forces develop in the internal columns

for the “Brace 5” cross-section. However, the magnitude of the axial load is very small. Note that these values were calculated assuming that all braces over the height of the building were at maximum capacity. As discussed in the previous chapter this is a conservative assumption, especially in cases where strong braces are applied.

With the estimates of axial load in every RC column, we are now in a position to calculate the lateral deformation capacity of each column and for each of the three solutions. The values obtained so far could be easily calculated with a common spreadsheet. However, for step, a more sophisticated program is required. The column deformation capacity was calculated with the RESPONSE-2000 software. In Tables 6.5, 6.6 and 6.7, the values in red indicate the deformation capacity of the columns that observed an increment of axial load due to the application of steel braces. It is clear that the deformation capacity of those columns reduced with the increase of axial load.

Table 6.5 - Maximum deformation capacity for each RC column in solution 1

Brace ID	Maximum Columns Displacement for Different Braces					
	Column 1	Column 2	Column 3	Column 4	Column 5	Column 6
Brace 1	0.0257	0.0237	0.0183	0.0183	0.0237	0.045
Brace 2	0.0257	0.0237	0.0165	0.0165	0.0237	0.045
Brace 3	0.0257	0.0237	0.0158	0.0158	0.0237	0.045
Brace 4	0.0257	0.0237	0.0142	0.0142	0.0237	0.045
Brace 5	0.0257	0.0237	0.0127	0.0127	0.0237	0.045

Table 6.6 - Maximum deformation capacity for each RC column in solution 2

Brace ID	Maximum Columns Displacement for Different Braces					
	Column 1	Column 2	Column 3	Column 4	Column 5	Column 6
Brace 1	0.0257	0.0178	0.0183	0.0183	0.0178	0.045
Brace 2	0.0257	0.0162	0.0165	0.0165	0.0162	0.045
Brace 3	0.0257	0.0151	0.0158	0.0158	0.0151	0.045
Brace 4	0.0257	0.0141	0.0142	0.0142	0.0141	0.045
Brace 5	0.0257	0.0126	0.0127	0.0127	0.0126	0.045

Table 6.7 - Maximum deformation capacity for each RC column in solution 3

Brace ID	Maximum Columns Displacement for Different Braces					
	Column 1	Column 2	Column 3	Column 4	Column 5	Column 6
Brace 1	0.0257	0.0178	0.0237	0.0237	0.0178	0.045
Brace 2	0.0257	0.0162	0.0237	0.0237	0.0162	0.045
Brace 3	0.0257	0.0151	0.0237	0.0237	0.0151	0.045
Brace 4	0.0257	0.0141	0.0237	0.0237	0.0141	0.045
Brace 5	0.0257	0.0126	0.0237	0.0237	0.0126	0.045

The design displacement of the frame can be defined by imposing the first storey to be equal to the minimum values obtained in each line of the previous tables. By imposing this condition, the maximum lateral deformation of the structure is controlled such that the maximum deformation of the most critical RC column is not exceeded.

Following this approach one can calculate the maximum displacement capacity of the equivalent SDOF structure by using the new expression for displacement profiles proposed in Chapter 4. Furthermore, the total base shear capacity of the building can be estimated by adding the contribution of the bracing system for each case to the value of the lateral capacity of the bare RC frame provided by the pushover analysis corresponding to the maximum displacement that the new retrofitted structure is expected to observe.

Table 6.8 provides a summary of the yield displacements ( $\Delta y$ ), design displacements ( $\Delta u$ ) and lateral strengths ( $V_y$ ) of the equivalent SDOF structure for all the different solutions and brace cross-sections.

Table 6.8 - DBD parameters for all solutions studied

Brace ID	Solution 1			Solution 2			Solution 3		
	$\Delta Y$ (m)	$\Delta u$ (m)	$V_y$ (kN)	$\Delta Y$ (m)	$\Delta u$ (m)	$V_y$ (kN)	$\Delta Y$ (m)	$\Delta u$ (m)	$V_y$ (kN)
Brace 1	0.0168	0.0298	549.4	0.0168	0.0290	742.8	0.0168	0.0290	942.4
Brace 2	0.0168	0.0269	600.6	0.0168	0.0264	867.4	0.0168	0.0264	1139.4
Brace 3	0.0168	0.0257	662.7	0.0168	0.0246	993.9	0.0168	0.0246	1337.1
Brace 4	0.0168	0.0231	759.4	0.0168	0.0230	1219.4	0.0168	0.0230	1682.2
Brace 5	0.0168	0.0207	985.5	0.0168	0.0205	1693.1	0.0168	0.0205	2403.7

The above values, namely the design displacement ( $\Delta u$ ) and the lateral strength ( $V_y$ ), can be better interpreted in a graphical manner (Figure 6.12).

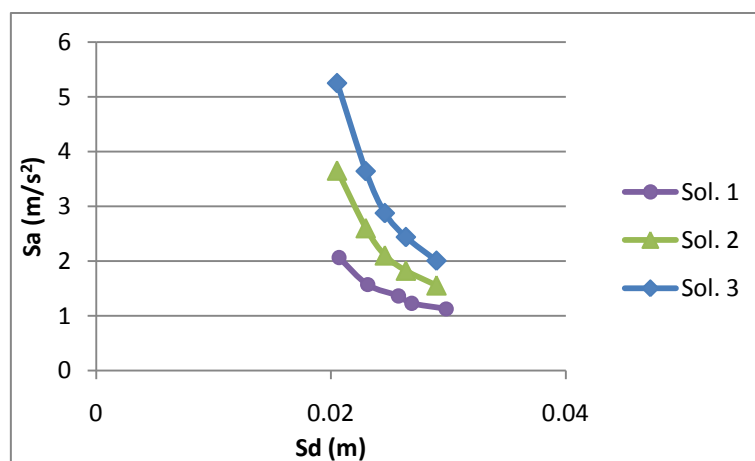


Figure 6.12 - Comparison of the design displacements for all studied solutions

The evaluation of the seismic performance requires the calculation of the equivalent viscous damping (EVD) associated to each solution. Based on the yield and design

displacements represented in the previous table, the ductility and consequently the EVD can be determined in order to reduce the elastic spectrum to an inelastic spectrum. As expected, the values do not change significantly with the solution adopted since the yield displacement does not vary much for the steel braces selected, and the design displacement does not change significantly with the different solutions. However, a reduction on both the ductility and the EVD is perceptible as the brace strength increases. The values obtained for the ductility and equivalent viscous damping are presented in Table 6.9.

Table 6.9 - Values of ductility and equivalent viscous damping for all studies solutions

Brace ID	Solution 1		Solution 2		Solution 3	
	$\mu$	$\zeta_{eq}$ (%)	$\mu$	$\zeta_{eq}$ (%)	$\mu$	$\zeta_{eq}$ (%)
Brace 1	1.8	12.9	1.7	12.6	1.7	12.6
Brace 2	1.6	11.7	1.6	11.5	1.6	11.5
Brace 3	1.5	11.2	1.5	10.7	1.5	10.7
Brace 4	1.4	9.9	1.4	9.8	1.4	9.8
Brace 5	1.2	8.4	1.2	8.3	1.2	8.3

In order to evaluate if any of the solutions satisfy the seismic requirements, the performance points are superimposed to the corresponding inelastic response spectra (Figures 6.13 to Figure 6.15). The solutions representing a good seismic behaviour can be as the cases in which the performance points are in the outside area of the inelastic response spectra.

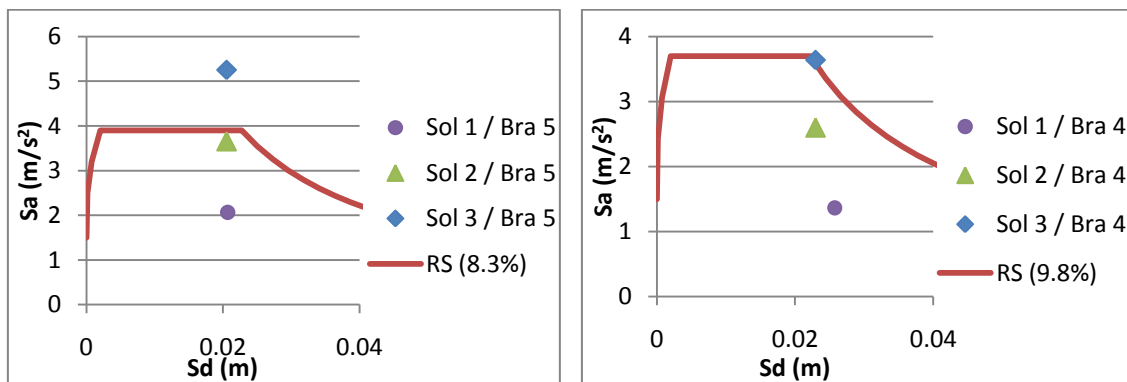


Figure 6.13 - Superposition of response spectra with the performance points of braces 5 and 4

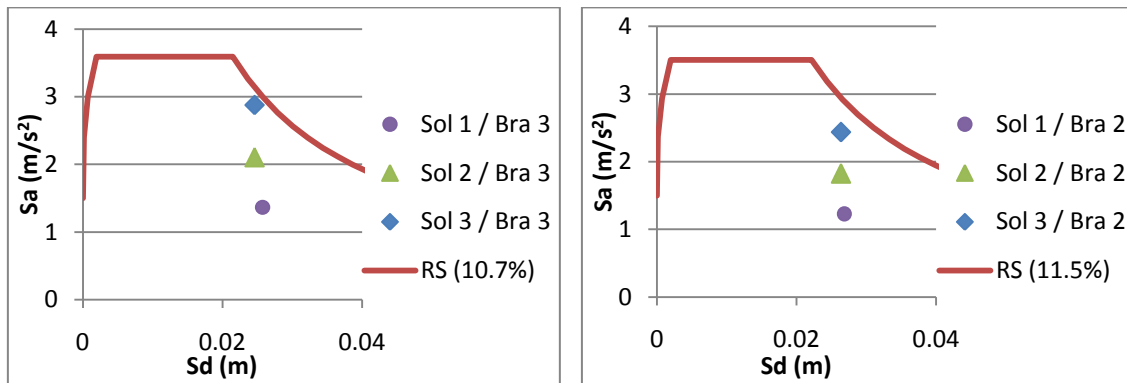


Figure 6.14 - Superposition of response spectra with the performance points of braces 3 and 2

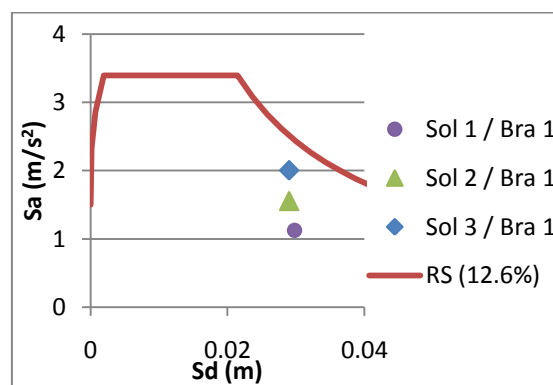


Figure 6.15 - Superposition of response spectra with the performance points of brace 1

From the previous figures it is possible to verify that only the retrofitting cases with “solution 3” and with braces 4 and 5 satisfy the requirements of the seismic demand.

From the possible solutions, the use of “braces 4” seems to be more economical but it is close to the limit of an acceptable seismic performance. On the other hand, if the objective is to develop a solution where little damage occurs then solution 3 with braces 5 appears to be more advisable.

## 6.5. VERIFICATION OF THE OBTAINED RESULTS

By calculating the fundamental periods of vibration of both the RC frame and the retrofitted solution consisting of “solution 3” with braces 4 (Table 6.10) it is possible to compare the dynamic characteristics of the bare RC frame and the retrofitted frame. It can be seen that by adding the braces the fundamental period of the retrofitted frame reduced by more than half in comparison with the corresponding period of the original RC frame. This important change of the period is largely due to the significant increase in terms of stiffness resulting from the introduction of the braces.

Table 6.10 - Fundamental period of vibration of the original and retrofitted structure

	Structure	
	Unbraced	Braced
T (s)	0.9	0.37

A pushover analysis of the retrofitted frame (Solution 3 with braces 4) was performed in order to investigate if the proposed design method produced a reliable structural solution. The results from the pushover analysis along with the representation of the performance point are presented in Figure 6.16.

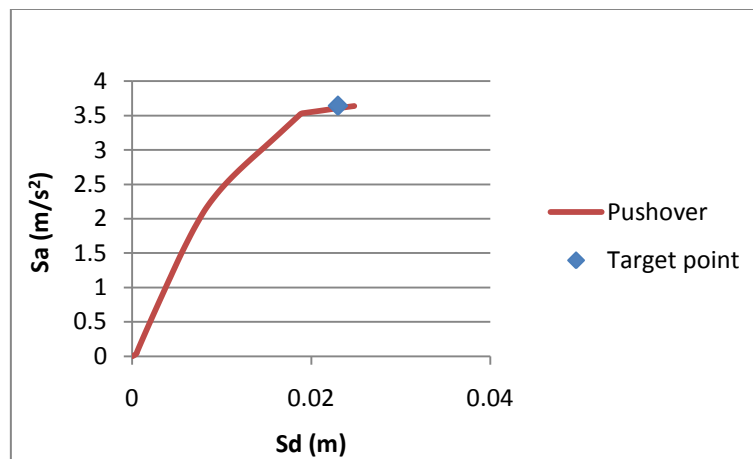


Figure 6.16 - Comparison of the calculated target point with the capacity curve of the braced structure

The results confirm that the performance point estimated using the proposed method is consistent with the global behaviour of the structure observed in the pushover analysis.

The small difference in the results, especially regarding the displacement, can be justified by the fact that it was assumed that all the steel braces were responding at full capacity. This implies that the level of axial load adopted for the calculation of the maximum deformation capacity of the RC column was overestimated. However, as it was mentioned previously, this simplification produces conservative results and, in order to keep the method simple, it was decided not to improve the estimate of axial load installed in the columns.

Regarding the lateral strength, the difference in the obtained results is irrelevant. This observation demonstrates that, by assuming in the calculation that the lateral strength obtained from the steel braces assuming the braces responding at full capacity, produces an accurate estimate of the lateral strength. In fact, the reduction of compressive force of the braces after buckling is very small compared with the total base shear. Moreover, by the strain-hardening developing on the tensile braces was neglected in the calculation of the lateral strength.

Finally, in order to assess if the assumption of relating the global yield displacement of the structure with the yielding of the tensile brace, a bilinear representation of the capacity curve was considered (Figure 6.17).

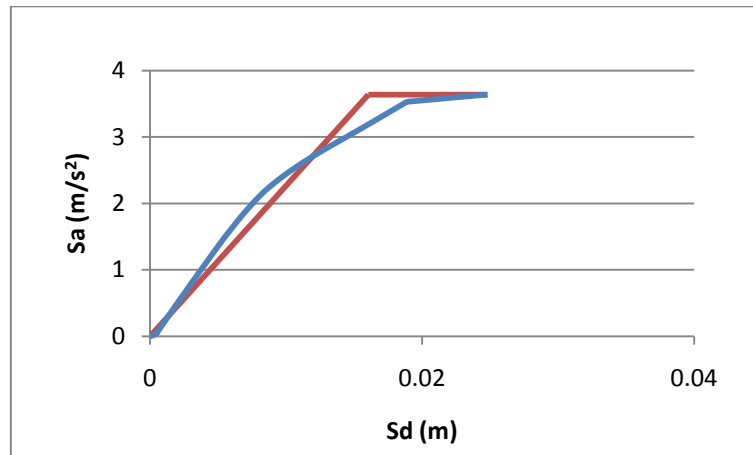


Figure 6.17 - Representation of the Capacity curve with the corresponding bilinear representation

Based on the bilinear representation, a new ductility capacity was estimated and a value of 1.54 was obtained. Comparing this value with the value assumed in the application of the method (1.40), it appears that the assumption considered was acceptable.

## 6.6. CONCLUDING REMARKS

In this chapter the application of the proposed method was explained through an example. The structural solution that was achieved and the performance assessment that was carried out demonstrated that the design method can be easily applied and that reliable retrofitting solutions for RC frames with steel braces can be obtained.

In the design process, it was used a method based on the CSM instead of the application of the method based on DDBD. The main disadvantage of the applied method is the fact that it is necessary to calculate several columns capacities during the process. However, despite this inconvenience, all the process can be automatic, and this fact can save more time. On the other hand, by using a graphical interpretation, the designer user can easily compare all the solutions considered and make a better judgement on the most adequate solution to adopt.



## 7. CONCLUSION

*"The day you stop moving and you say "this far enough," you will be dead"*

Augustine of Hippo (354 – 430)

### 7.1. FINAL REMARKS

This dissertation focused on the seismic retrofitting of RC frames with steel braces. Previous analytical and experimental studies indicated that the application of steel braces in RC frames may significantly improve the performance of RC buildings with inadequate seismic behaviour. In some applications this technique may be more advantageous in comparison with other retrofitting systems.

One of the main factors that limit the application of this retrofitting technique is the limited design guidance provided by the current seismic codes. In the present work the behaviour of these hybrid structures have been analyzed in detail. The knowledge acquired, combined with the recent developments in seismic design, namely the Direct Displacement-Based Design method proposed by Priestley *et al.* (2007), resulted in the proposal of a design approach for the retrofitting of regular RC frames with steel braces. The proposed method is simple, intuitive and easy to use in practical applications. In order to simplify the process, some approximations have been done without jeopardizing the required accuracy inherent to the structural design.

It must be emphasized that, due to the time required to perform non-linear dynamic analysis, and in order to obtain solid study, the vast study on the displacement profiles planned during the work was reduced to only one RC frame with two different braces. Thus, despite the proposed method being generic, at this moment its use is limited to low-rise structures due to the lack of displacement profiles for taller buildings.

Another issue that can be expected regarding high-rise buildings is related with the predictable development of high levels of axial load in the columns at the lower storeys. To avoid this possible problem, the proposed retrofitting technique can be combined with other types of interventions available for strengthening of RC elements (e.g., the use of FRP). On the other hand, since the seismic loads are concentrated at the base of the building and decrease over the height, the retrofitting solution can be optimized by changing the brace strength based on the expected seismic demand.

## **7.2. FUTURE DEVELOPMENTS**

In order to extend the applicability of the method to other structures, it is important to investigate if the determined displacement profiles can also be applied to taller building. To this end, non-linear dynamic analysis of steel braced RC frames with varying height should be carried out.

It would be also of interest to investigate the change of the displacement profiles when the brace strength is changed over the height of the structure. It is expected that a more rational distribution of the braces will lead to a more efficient and economical solution.

Finally it must be outlined that the equivalent viscous damping calculated in this work was based on expressions proposed for RC frames. It is expected that the obtained values are a good approximation with the real values. However a deeper study should investigate and, if required, develop new expressions for steel braced RC frames.

## REFERENCES

Abou-Elfath, H., [1998] "Rehabilitation of Nonductile Reinforced Concrete Buildings using Steel Systems", PhD thesis, McMaster University, Ontario, Canada.

Abou-Elfath, H., Ghobarah, A. [2000] "Behaviour of reinforced concrete frames rehabilitated with concentric steel bracing", *Can. J. Civ. Eng.* 27: 433-444.

Antonucci, R., Balducci, F., Cappanera, F., Castellano, M. G. [2009] "Structure prefabbricate con contraventi dissipativi: l'esempio del nuovo polo didattico della Facoltà di Ingegneria dell'Università Politecnica delle Marche di Ancona", *Progettazione Sismica*, Numero 01. (in Italian).

Applied Technology Council, "ATC-40: Seismic evaluation and retrofit of concrete buildings – Volume 1".

Asgarian, B., Shokrgozar, H. R. [2009] "BRBF response modification factor", *Journal of Constructional Steel Research* 65 (2009) 290-298.

Aydin, E., Boduroglu, M. H. [2008] "Optimal placement of steel diagonal braces for upgrading the seismic capacity of existing structures and its comparison with optimal dampers", *Journal of Constructional Steel Research* 64 72-86.

Badoux, M. [1987] "Seismic retrofitting of reinforced concrete frame structures with steel bracing systems", Ph.D. Thesis. Texas: the University of Texas at Austin.

Badoux, M., Jirsa, J. O. [1990] "Steel Bracing of RC Frames for Seismic Retrofitting", *Journal of Structural Engineering*, Vol.116, No. 1.

Black, G., Wenger, W., Popov, E. [1980] "Inelastic Buckling of Steel Struts Under Cyclic Load Reversals", Report NO. UCB/EERC-80/40, College of Engineering, University of California, Berkeley, California, USA.

Bouwkamp, J., Pinto, A. V., Molina, F. J., Varum, H. [2000] "Cyclic tests on RC frame retrofitted with K-bracing and shear-link dissipator", EUR Report No. 20136 EN, ELSA, JRC-Ispira, EC, Italy.

Broderick, B. M., Goggins, J. M., Elghazouli, A. Y. [2005] "Cyclic performance of steel and composite bracing members", *Journal of Constructional Steel Research* 61 493-514.

Calabrese, A., Almeida, J.P., Pinho, R. [2010] "Numerical issues in distributed inelasticity modelling of RC frame elements for seismic analysis", *Journal of Earthquake Engineering*, Volume 14 Supplement 1, pp. 38-68.

Collins, M. P., Mitchell, D. [1997] "Prestressed Concrete Structures", Response Publications, Canada.

Della Corte, G., Mazzolani, F. M. [2008] "Theoretical Developments and Numerical Verification of a Displacement-Based Design Procedure for Steel Braced Structures", The 14<sup>th</sup> World Conference on Earthquake Engineering, Beijing, China.

Di Sarno, L., Manfredi, G. [2009] "Design approach for the seismic strengthening of an existing RC building with buckling restrained braces", STESSA 2009.

Di Sarno, L., Manfredi, G. [2009] "Experimental tests on full scale RC frames retrofitted with buckling restrained braces", STESSA 2009.

CEN [2005] "EN 1998-1, Eurocode 8: Design provisions for earthquake resistance of structures Part 1: General rules, seismic actions and rules for buildings".

CEN [2001] "prEN 1991-1-1, Eurocode 1: Actions on structures: Densities, self-weight and imposed loads for buildings".

CEN [2004] "EN 1992-1-1, Eurocode 2: Design of concrete structures: General rules and rules for buildings".

CEN [2003] "ENV 1993-1-1, Eurocode 3: Design of steel structures: General rules and rules for buildings".

Fardis, M. N. [1998] "Seismic assessment and retrofit of RC structures". Proceedings of the Eleventh European Conference on Earthquake Engineering - Invited Lectures, Paris, France, pp. 53-64.

Freeman, S.A. [1998] "The Capacity Spectrum Method as a Tool for Seismic Design", 11<sup>th</sup> European Conference on Earthquake Engineering, Paris, A.A.Balkema, Rotterdam.

Freeman, S. A. [2004] "Review of the Development of the Capacity Spectrum Method", *Journal of Earthquake Technology*, Paper No.438, Vol. 41, No.1, pp.1-13.

Freeman, S. A. , Nicoletti, J. P., Tyrell, J. V. [1975] "Evaluations of Existing Buildings for Seismic Risk - A Case Study of Puget Sound Naval Shipyard, Bremerton, Washington", Proceedings of U.S. National Conference on Earthquake Engineering, Berkeley, U.S.A., pp. 113-122.

Gan, W. [1996] "Earthquake Response of Steel Braces and Braced Steel Frames", Report No. EERL 96-06, California Institute of Technology, Pasadena, California.

Ghobarah, A., Abou Elfath, H. [2001] "Rehabilitation of a reinforced concrete frame using eccentric steel bracing", *Engineering Structures* 23, 745-755.

Godínez-Domínguez, E. A., Tena-Colunga, A. [2010] "Nonlinear behaviour of code-design reinforced concrete concentric braced frames under lateral loading", *Engineering Structures* 32, 944-963.

Jordan, R. K. [1990] "Evaluation of strengthening schemes for reinforced concrete moment-resisting frame structures subjected to seismic loads", PhD dissertation, University of Texas.

Kumar, M., Castro, J. M., Elghazouli, A. Y. and Stafford, P. J. [2010] "Influence of mean period of ground motion on the dynamic response of single and multi degree of freedom systems", *Earthquake Engineering and Structural Dynamics*. Accepted for publication.

Lee, K., Bruneau, M. [2005] "Energy Dissipation of Compression Members in Concentric Braced Frames: Review of Experimental Data", *Journal of Structural Engineering*, Vol. 131, No. 4.

Longo, A., Montuori, R., Piluso, V. [2008] "Failure Mode Control of X-Braced Frames Under Seismic Actions", *Journal of Earthquake Engineering* 12:728-759.

Maheri, M. R., Akbari, R. [2003] "Seismic behaviour factor, R, for steel X-braced and knee-braced RC buildings", *Engineering Structures* 25 (2003) 1505-1513.

Maheri, M. R., Hadjipour, A. [2003] "Experimental investigation and design of steel brace connection to RC frame", *Engineering Structures* 25 (2003) 1707-1714.

Maheri, M. R., Kousari, R., Razazan, M. [2003] "Pushover tests on steel X-braced and knee-braced RC frames", *Engineering Structures* 25, 1697-1705.

Maheri, M. R., Sahebi, A. [1997] "Use of steel bracing in reinforced concrete frames", *Engineering Structures*, Vol. 19, No. 12, pp. 1018-1024.

Maheri, M. R., Ghaffarzadeh, H. [2008] "Connection overstrength in steel-braced RC frames", *Engineering Structures* 30, 1938-1948.

Mander, J. B., Priestley, M. J. N., Park, R. [1988] "Theoretical Stress-Strain Model for Confined Concrete", *Journal of Structural Engineering*, Vol.114, No. 8.

Mazzolani, F. M. [2008] " Innovative metal systems for seismic upgrading of RC structures", *Journal of Constructional Steel Research* 64, 882-895.

Mazzolani, F. M. [2009] "Adeguamento sismico di edifici in c.a. progettati per soli carichi verticali mediante controventi metallici", *Progettazione Sismica*, Numero 01. (in Italian).

Miranda, E., Ruiz-García, J. [2002] "Evaluation of approximate methods to estimate maximum inelastic displacement demands", *Earthquake Engineering and Structural Dynamics*, 31:539-560.

Moehle, J. P., [2000] "State of Research on Seismic Retrofit of Concrete Building Structures in the US", *US-Japan Symposium and Workshop on Seismic Retrofit of Concrete structures-State of Research and Practice*.

Moon, K., Connor, J., Fernandez, J. [2007] "Diagrid Structural Systems for Tall Buildings: Characteristics and Methodology for Preliminary Design", *Structural Design Tall Spec. Build.* 16, 205–230.

Nateghi, F. [1995] "Seismic strengthening of eight-storey RC apartment building using steel braces", *Engineering Structures*, Vol.17 No. 6, pp.455-461.

PEER [2006] "OpenSees: Open System for Earthquake Engineering Simulation", *Pacific Earthquake Engineering Research Center, University of California, Berkeley, CA*.

Paulay, T., Priestley, M. J. N. [1992] "Seismic Design of Reinforced Concrete and Masonry Buildings" *John Wiley & sons, Inc.*

PEER [2009] "Pacific Earthquake Engineering Research Center: NGA Database".

PEER [2009] "Pacific Earthquake Engineering Research Center".

Pettinga, J. D., Priestley, M. J. N. [2005] "Dynamic Behaviour of Reinforced Concrete Frames Design with Direct Displacement-Based Design, ROSE Research Report No. 2005/02, IUSS Press, Pavia, 154pp.

Pincheira, J. A., Jirsa, J. O. [1995] "Seismic Response of RC Frames Retrofitted with Steel Braces or Walls", *Journal of Structural Engineering / August 1995 / 1225-1235*.

Pinho, R. [2000] "Selective Retrofitting of RC Structures in Seismic Areas", *PhD thesis, Imperial College, London, UK*.

Priestley, M. J. N. [2003] "Myths and Fallacies in Earthquake Engineering, Revisited: The Mallet Milne Lecture", *IUSS Press, Pavia, Italy*.

Priestley, M.J.N. and Calvi, G.M. [1997] "Assessment of existing buildings", *CEB Bulletin 236 - Seismic Design of Reinforced Concrete Structures, CEB Task Group 3.2, Comité Euro-International du Béton, Lausanne, Switzerland, pp. 159-204*.

Priestley, M. J. N., Calvi, G. M., Kowalsky, M. J. [2007] "Displacement-Based Seismic Design of Structures", *IUSS Press, Pavia, Italy*.

Queirós N. [2009] "Análise e Dimensionamento Sísmico de Estruturas Híbridas Aço-Betão" *Tese de Mestrado em Engenharia Civil, Faculdade de Engenharia da Universidade do Porto, Porto, Portugal (in Portuguese)*.

Rathje, E.M., Faraj, F., Russel, S. and Bray, J.D. [2004]. "Empirical Relationships for Frequency Content Parameters of Earthquake Ground Motions". *Earthquake Spectra*, 20: 119-144.

Ravi Kumar, G., Satish Kumar, S. R., Kalyanaram, V. [2007] "Behaviour of frames with Non-Buckling bracing under earthquake loading", *Journal of Constructional Steel Research* 63, 254-262.

Response-2000, "Reinforced Concrete Sectional Analysis using the Modified Compression Field Theory", version 1.0.5, University of Toronto.

SAP2000, "Linear and nonlinear static and dynamic analysis and design of three-dimensional structures", Version 9, Computer and Structures, Inc.

Schnepf, S., Stempniewski, L., Lungu, D. [2007] "Application of the capacity spectrum method for seismic evaluation of structures", *International Symposium on Strong Vrancea Earthquakes and Risk Mitigation*, Bucharest, Romania.

SeismoSoft [2009] "SeismoStruct: A computer program for static and dynamic nonlinear analysis of framed structures".

Sozen, H., Moehle, J. P. [2004] "Strength and Deformation Capacity of reinforced Concrete Columns with Limited Ductility", 13<sup>th</sup> World Conference on Earthquake Engineering, Vancouver, B.C., Canada.

Sugano, S. [1996] "State-of-the-Art in Techniques for Rehabilitation of Buildings", 11 WCEE, Acapulco, Mexico, Paper no. 2179, Elsevier.

Terán-Gilmore, A., Bertero, V. V., Youssef, N. F.G. [1996] "Seismic Rehabilitation of Infilled Non-Ductile Frame Buildings Using Post-Tensioned Steel Braces", *Earthquake Spectra* Volume 12, Issue 4, pp. 863-882.

Tremblay, R. [2002] "Inelastic seismic response of steel bracing members", *Journal of Constructional Steel Research* 58, 665-701.

Varum, H. [2003] "Seismic Assessment, Strengthening and Repair of Existing Buildings", PhD thesis, Universidade de Aveiro, Aveiro, Portugal.

Wyllie, L. [1983] "Seismic strengthening procedures for existing buildings", *Strengthening of Buildings Structures-Diagnosis and Theory*, International Association of Bridges and Structural Engineering Symp., Venice, Italy, 363-370.

Xie, Q. [2005] "State of the art of buckling-restrained braces in Asia", *Journal of Constructional Steel Research* 61, 727-748.

Yousef, M. A., Ghaffarzadeh, H., Nehdi, M. [2007] "Seismic performance of RC frames with concentric internal steel bracing" *Engineering Structures* 29 1561-1568.